Louisiana State University
LSU Digital Commons

LSU Master's Theses | Graduate School

2016

Comparison of Advanced Radiotherapy Techniques for Post-Mastectomy Breast Cancer Patients

David Elward Heins
Louisiana State University and Agricultural and Mechanical College

Follow this and additional works at: https://digitalcommons.lsu.edu/gradschool_theses

 Part of the Physical Sciences and Mathematics Commons

Recommended Citation

Heins, David Elward, "Comparison of Advanced Radiotherapy Techniques for Post-Mastectomy Breast Cancer Patients" (2016). *LSU Master's Theses*. 1882.
https://digitalcommons.lsu.edu/gradschool_theses/1882

This Thesis is brought to you for free and open access by the Graduate School at LSU Digital Commons. It has been accepted for inclusion in LSU Master's Theses by an authorized graduate school editor of LSU Digital Commons. For more information, please contact gradetd@lsu.edu.

COMPARISON OF ADVANCED RADIOTHERAPY TECHNIQUES FOR POST-MASTECTOMY BREAST CANCER PATIENTS

A Thesis

Submitted to the Graduate Faculty of the
Louisiana State University and
Agricultural and Mechanical College
in partial fulfillment of the
requirements for the degree of
Master of Science

in

The Department of Physics and Astronomy

by
David Elward Heins
B.S., Pittsburg State University, 2011
B.S., Pittsburg State University, 2013
August 2016

This work is dedicated to my wife, Andrea

and daughter, Anastasia,

for always supporting me.

Acknowledgements

I would like to thank my advisor, Dr. Rui Zhang, for guiding me and motivating me in my research endeavor. I would also like to recognize the rest of our research group, Dr. Jihyung Yoon, and Xiadong Zhao who were instrumental in assisting with measurements, reading TLDs, and generally providing input and support at our meetings. I would also like to thank the rest of my graduate committee, Drs. BeiBei Guo, Wayne Newhauser, and Rongying Jin. They were an amazing group that provided imperative input in moving our research forward and ultimately completing the project. I would like to give further recognition to Dr. BeiBei Guo for her tremendous help with the statistical analysis of our data. Great appreciation goes out to Drs. Kenneth Hogstrom and Bobby Carver and Mr. Kevin Erhart for their input, guidance, and technical support in helping me develop the BECT+VMAT treatment planning technique and sometimes challenging software utilization.

I would like to acknowledge several staff members at Mary Bird Perkins Cancer Center. I want to thank Dr. Mary Ella Sanders for taking time from her busy clinical day to approve numerous treatment plans. I want to recognize Mr. Connel Chu for all of his help ranging from using the machines to helping me overcome challenges using the treatment planning systems. I would also like to thank Mr. David Perrin for his help using the clinical machines and equipment. I want to thank Susan Hammond for helping with all the administrative tasks. I want to give special thanks to the talented and patient dosimetry team for helping me early into my project with treatment planning; Mr. Frank Apollo, Mr. Eddie Singleton, Mr. Chad Dunn, and Mr. Hamlet Spears.

Special thanks goes to my classmates and peers; Desmond Fernandez, Erin Chambers, and John Chapman. Your support, input in my project, and help keeping our schedules and timelines straight have been invaluable. I would like to thank the remainder LSU/MBPCC medical physics program faculty and staff for sharing their vast knowledge and experience that was instrumental in my success in the program.

Finally, I would also like to thank my wife Andrea Heins for her confidence, patience, and support for me during this challenging experience.

Table of Contents

List of Tables

List of Figures

Abstract

Purpose: To determine if bolus electron conformal therapy (BECT) combined with volumetric modulated arc therapy (VMAT) and flattening filter free volumetric modulated arc therapy (FFFVMAT (6x and 10x)) can maintain equal or better dose coverage than standard volumetric modulated arc therapy (VMAT) while reducing doses to organs at risk (OARs).

Methods: BECT+VMAT, FFFVMAT (6x and 10x), and VMAT treatment plans were produced for ten post-mastectomy radiotherapy (PMRT) patients previously treated at our clinic. The treatment plans were created on a commercially available treatment planning system (TPS) and all completed treatment plans were reviewed and approved by a radiation oncologist. The plans were evaluated based on planning target volume (PTV) coverage, tumor control probability (TCP), dose homogeneity index (DHI), conformity index (CI), dose to organs at risk (OARs), and second risks for OARs.

Results: All techniques produced clinically acceptable PMRT plans. Overall, BECT+VMAT plans exhibited significantly higher maximum dose compared to all VMAT techniques. BECT+VMAT and FFFVMAT10x had slightly improved TCP over FFFVMAT6x and VMAT ($p > 0.05$). However, all VMAT techniques showed statistically significant improvement in CI and DHI over BECT+VMAT. All techniques showed no statistical significant difference in mean lung dose. BECT+VMAT exhibited a reduced mean heart dose over VMAT ($p = 0.06$). FFFVMAT6x had significantly higher mean heart dose compared to VMAT. In addition, BECT+VMAT was able to reduce mean dose to the contralateral breast with statistical significance, compared to VMAT. Both FFFVMAT techniques had comparable but slightly reduced dose compared to VMAT with FFFVMAT6x showing statistical significance.

Conclusion: This work has shown that BECT+VMAT produces clinically acceptable plans while reducing OARs doses. Both FFFVMAT techniques are comparable to VMAT with FFFVMAT6x having slight improvements. In addition, FFFVMAT techniques exhibited reduced treatment times over VMAT. Even though all VMAT techniques produce more homogenous and conformal dose distributions, BECT+VMAT is a viable option for treating post-mastectomy patients. This work has demonstrated that

patients with increased risk of cardiovascular disease or radiation-induced cancer of the contralateral breast may benefit from BECT+VMAT. Also, patients with increased risk of radiation-induced cancer of the contralateral breast may benefit from FFFVMAT6x.

Chapter 1 Introduction

1.1 Background and Significance

Breast cancer is the second leading cause of cancer related deaths among women preceded only by lung cancer (Siegel *et al.,* 2015). Breast cancer is estimated to have the highest incidence rate of all cancers among women in the United States in the year 2015 (Siegel *et al.,* 2015). As shown in figure 1.1, it is estimated in 2015 that 29% (231,840) of new cancer cases will be breast cancer and 15% (40,290) of cancer related deaths among women will be attributed to breast cancer.

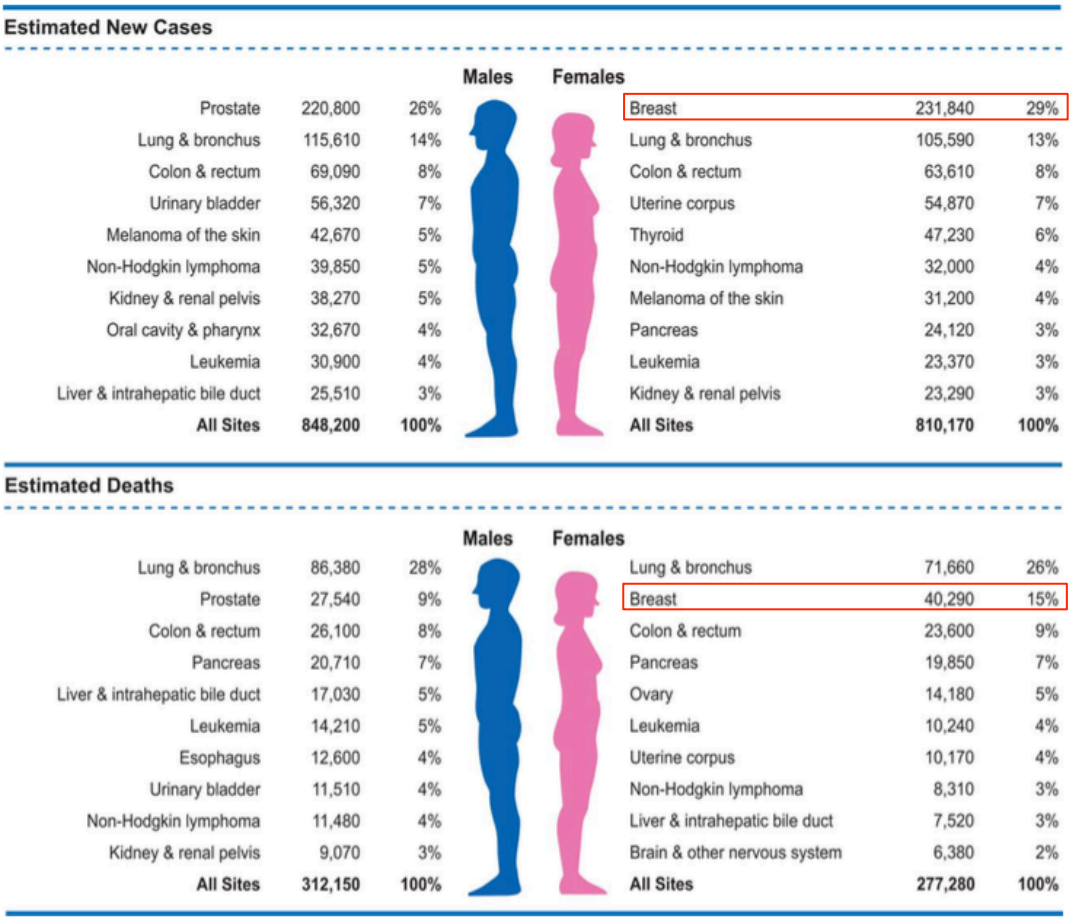

Figure 1.1 Leading Cancer types for estimated new cases and deaths for 2015. Source: Siegel *et al*., (2015)

In general there are three major techniques to treat breast cancer: surgery, chemotherapy, and radiation therapy. Surgery and radiation therapy treat local and regional disease while chemotherapy is a systemic treatment. Early stage disease can be treated with breast conserving surgery called a

lumpectomy or a mastectomy in conjunction with postoperative radiotherapy and systemic chemotherapy (Harris *et al.,* 1996, Bonadonna *et al.,* 1997, Wood *et al.,* 2005). Disease with a large tumor of greater than 5 cm or multicentric disease will usually require a mastectomy (Overgaard *et al.,* 1997).

There are three types of mastectomies. A simple mastectomy is the removal of the breast tissue alone. A modified radical mastectomy includes the removal of the breast tissue and axillary lymph nodes. A radical mastectomy is the same as a modified radical mastectomy with the additional removal of the underlying pectoralis major muscle. With advanced disease, in addition to the mastectomy, post-mastectomy radiotherapy (PMRT) is usually indicated (Harris *et al.,* 1996, Bonadonna *et al.,* 1997, Wood *et al.,* 2005).

1.2 Post-Mastectomy Radiotherapy (PMRT)

More advanced disease that has axillary lymph node involvement and positive surgical margins will usually require PMRT (Overgaard *et al*., 1997). PMRT can potentially prevent local recurrence that could be caused by microscopic disease left behind after surgery (EBCTCG, 2005). Several studies have shown that PMRT improves local control of primary tumor and increases overall long term survival of breast cancer patients (Overgaard *et al*., 1997, Peirce *et al*., 2002, EBCTCG, 2005, Marks *et al.,* 2010, Taddei *et al.,* 2013, Fischbach *et al*., 2013, Ma *et al*., 2013, Zhang *et al.,* 2015). Overgaard *et al.* (1997) shows the estimated ten year overall survival of 1708 women who were treated with concurrent radiotherapy and chemotherapy (852) and those treated with chemotherapy alone (856), the overall survival at 10 years is improved by nearly 10% with the use of radiotherapy. In addition, another study by the Early Breast Cancer Trialists' Collaborative Group (EBCTCG) estimated an approximate 5.4% reduction in breast cancer mortality among 8505 women who underwent mastectomy plus radiotherapy versus mastectomy alone (EBCTCG, 2005). Overgaard *et al.* (1997) determined that no specific subgroups of women benefited more from PMRT. There are several radiation delivery treatment technologies available. However, currently there is no "gold standard" for post-mastectomy chest wall irradiation (Peirce *et al*., 2002, Fischbach *et al*., 2013).

Post-mastectomy chest wall treatment fields typically include the chest wall, internal mammary chain lymph nodes (IMN), axillary lymph nodes (AX), and the supraclavicular lymph nodes (SC) (van der Laan *et al.,* 2010, Nichols, 2012, Hernandez, 2014). The Radiation Therapy Oncology Group (RTOG) further defines the area for treatment (RTOG, 2015). Figure 1.2 is a beams eye view of the treatment area for a typical post-mastectomy treatment area (Hernandez, 2014). The area covers the chest wall with the superior border covering the SC nodes, the medial border covers the IMN, the inferior border matches the apparent loss (no longer see the inferior border) of the contralateral breast, and the lateral border runs to the mid-axillary line. In addition, the anterior border of the treatment volume is the skin surface and the posterior border is the rib-pleural interface including the ribs and muscles (RTOG, 2015). It is important to increase the skin dose to adequate levels. For treatments using 6 MV photons a uniform tissue-equivalent material called bolus is used to increase the skin dose in the "build-up" region of the photon beam (Fischbach *et al*., 2013, Hernandez, 2014). A Bolus can be seen on the patient's surface in Figure 1.2.

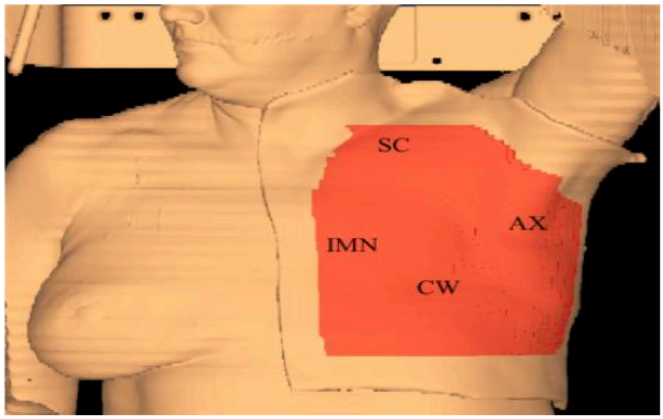

Figure 1.2 Beams eye view of typical post-mastectomy treatment field. SC: supraclavicular lymph nodes; AX: axillary lymph nodes; CW: chest wall; IMN: internal mammary chain lymph nodes. Source: Hernandez (2014)

1.3 PMRT Techniques

Historically PMRT has been delivered using a mixed-beam (MB) technique. One method utilizes tangential photon beams for the chest wall with an anterior electron beam for regional lymph nodes (Peirce *et al*., 2002, Ma *et al*., 2013). Another method uses anterior and posterior photon fields to treat the

supraclavicular and axillary lymph nodes with anterior and oblique electron fields to treat the chest wall (Overgaard *et al*., 1997, Nichols, 2012).

Beyond traditional treatment methods, there are advanced technologies for PMRT: Intensity Modulated Radiation Therapy (IMRT) has been shown to improve target dose homogeneity and conformity in addition to spare normal tissues over conventional methods (Rudat *et al*., 2014, Zhang *et al.,* 2015). At Mary Bird Perkins Cancer Center (MBPCC) in Baton Rouge Louisiana the primary methods for PMRT are Helical Tomotherapy and Standard Volumetric Modulated Arc Therapy (VMAT) (Nichols, 2012), two types of advanced IMRT. VMAT is a method of delivering IMRT in a continuous arc and has been shown to conform well and deliver quality treatments to the chest wall (Nichols, 2012, Zhang *et al.,* 2015). Zhang *et al.* (2015) has shown that VMAT plans exhibit an improvement over conventional IMRT plans in sparing healthy tissue for PMRT. Figure 1.3 shows isodose distributions from IMRT and VMAT plans for a left side post-mastectomy chest wall patient; VMAT delivered less low-dose to the heart, left lung, and less high-dose to the contralateral breast. Figure 1.4 shows the Dose Volume Histogram (DVH), for the same patient, giving a graphical representation of the reduced doses in the heart, left lung, and contralateral breast. In addition, VMAT is able to reduce the number of monitor units (MU) required, resulting in shorter treatment times and less whole body dose compared with IMRT (Zhang *et al.,* 2015).

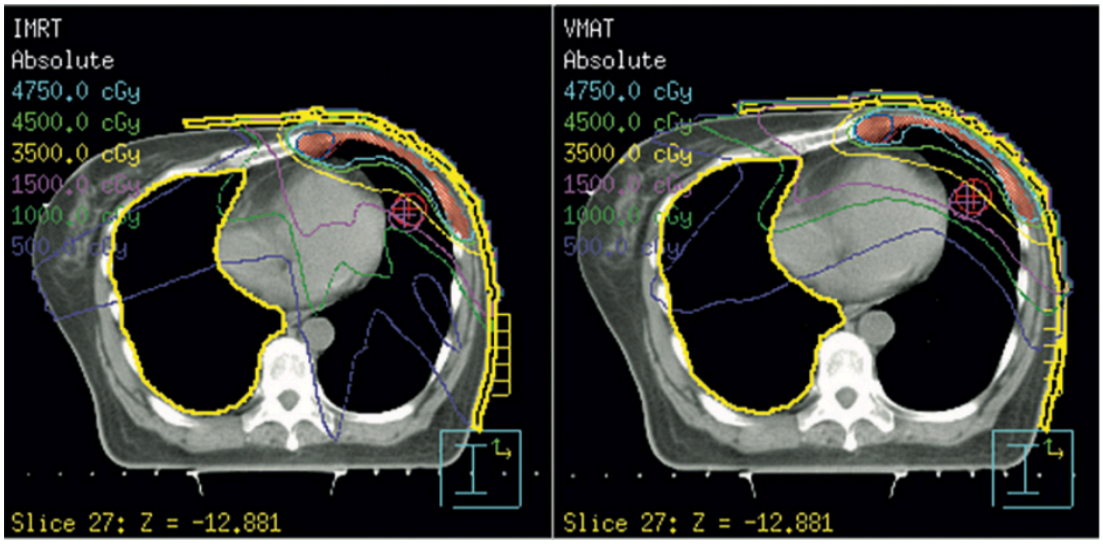

Figure 1.3 Isodose comparisons between IMRT and VMAT for PMRT. Source: Zhang *et al.,* (2015)

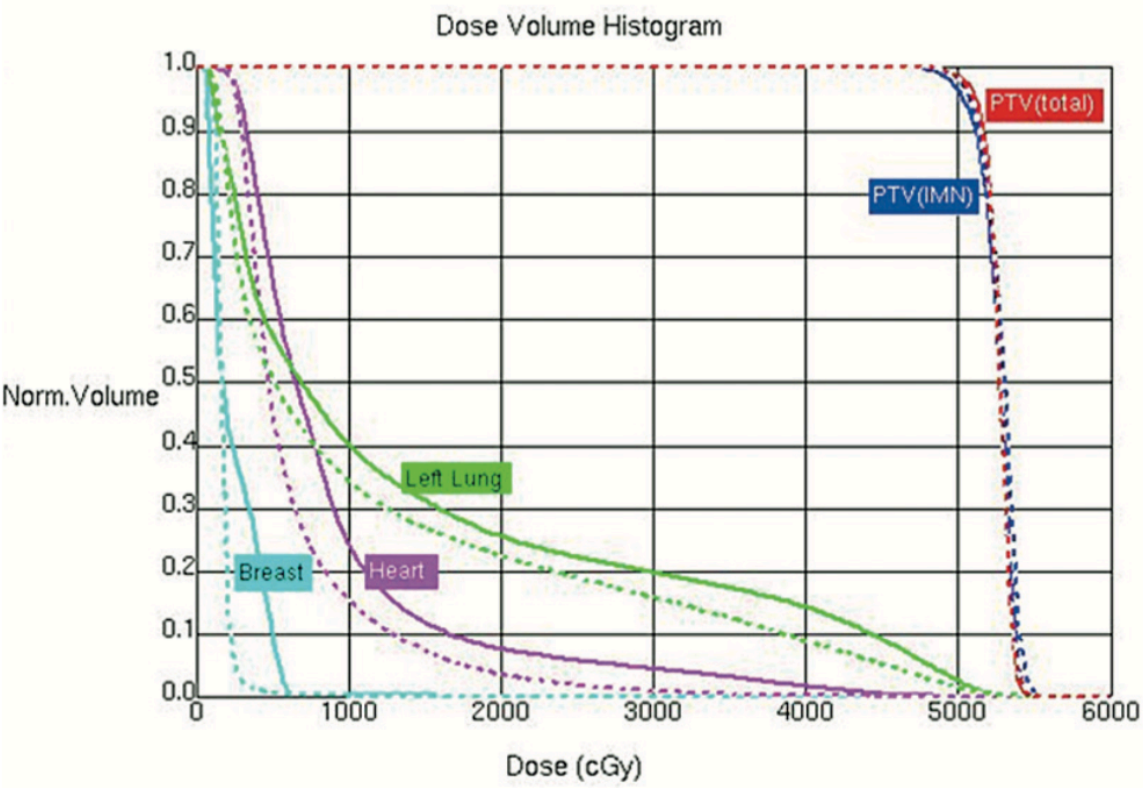

Figure 1.4 DVH comparison between IMRT and VMAT for PMRT plans shown in figure 1.3. IMRT displayed as solid line and VMAT as dashed line. Taken from Zhang *et al.,* (2015)

1.4 Flattening Filter Free VMAT (FFFVMAT)

Helical Tomotherapy (HT) and Cyberknife utilize unflattened photon beams (Georg *et al*., 2011) and many VMAT linear accelerators have the flattening filter free option. Historically, conventional photon beams are flattened using a flattening filter (a Gaussian shaped high-Z material used to spread out the forward peak of the unflattened beam) (Zwahlen *et al.,* 2012). This was done to achieve a flat, uniform beam that resulted in simplified calculations and easier treatment planning for IMRT treatments (Cashmore *et al*., 2008, Zwahlen *et al.,* 2012). In contrast, unflattened beams that do not use a flattening filter are forward peaked (Cashmore *et al*., 2008). It has been stated that for treatments requiring highly modulated photon fields the flattened beam is unnecessary since the goal is a non-uniform field (Mackie *et al.*, Georg *et al*., 2011) and it has been shown that flattened and unflattened optimized photon fluence maps are similar for IMRT and VMAT (Zwahlen *et al.,* 2012). Figure 1.5 compares the normalized measured percent depth dose (PDD) data for the flattened and unflattened 6 MV beam for one of the

linear accelerators at MBPCC. The two beams are very similar with only slight differences in the build-up region, depth of maximum dose (d_{max}), and less than five percent difference in the low dose tail of the curve. The d_{max} for the flattened beam is 1.67 cm and d_{max} for the unflattened beam is 1.78 cm, a 1.1 mm difference that is in agreement with other institutions (Georg *et al*., 2011).

Unflattened photon beams exhibit many benefits over traditional flattened beams. Cashmore *et al.* (2008) reported several dosimetric benefits of unflattened photon beams, including reduced penumbra, lower out-of-field dose, increased dose rate, and reduced head scatter (Cashmore *et al*., 2008). One of the major advantages of flattening filter free machines is the reported reduction in head scatter. Cashmore *et al.* (2008) showed a reduction in head scatter by up to 70%. This can reduce out-of-field dose and may be more pronounced for large field sizes such as those used for post-mastectomy chest wall treatments (Cashmore *et al*., 2008, Zwahlen *et al.,* 2012). Figure 1.6 shows reduced head scatter, normalized to a 10 x 10 cm^2 field, for large field sizes for 6 MV photon beam.

Figure 1.7 shows the normalized x-axis cross-plane profiles for the flattened and unflattened 6 MV beam for one of the linear accelerators at MBPCC. The figure shows a reduction in out-of-field relative dose. Also seen is the forward peak and the flattened peak of the unflattened and flattened beams, respectively. Another benefit of flattening filter free beams is an increase in delivery efficiency resulting in increased dose rates (Mackie *et al.*, Cashmore *et al*., 2008, Sorensen *et al*., 2011, Zwahlen *et al.,* 2012, Lang *et al*., 2013, Spruijt *et al*., 2013,). This can reduce the delivery time of treatments but is dependent on physical machine constraints such as Multi-Leaf Collimator (MLC) speed and gantry rotation speed (Lang *et al*., 2013). In addition, studies have shown that increased dose rates will have no influence over treatment outcomes (cell survival) compared to lower dose rates seen with flattened beams (Sorensen *et al*., 2011).

Flattening filter free beams have softer energy spectra. This is because the flattening filter will preferentially attenuate low energy photons causing beam hardening. The result of a softer beam is increased skin dose (Mackie *et al.*, Georg *et al*., 2011). Furthermore, removing the flattening filter could increase the dose accuracy of the treatment planning system (Cashmore *et al*., 2008, Georg *et al*., 2011).

It has also been shown that the dose conformity and dose homogeneity in the patient is similar for both flattened and unflattened photon beams (Zwahlen *et al.,* 2012, Spruijt *et al*., 2013).

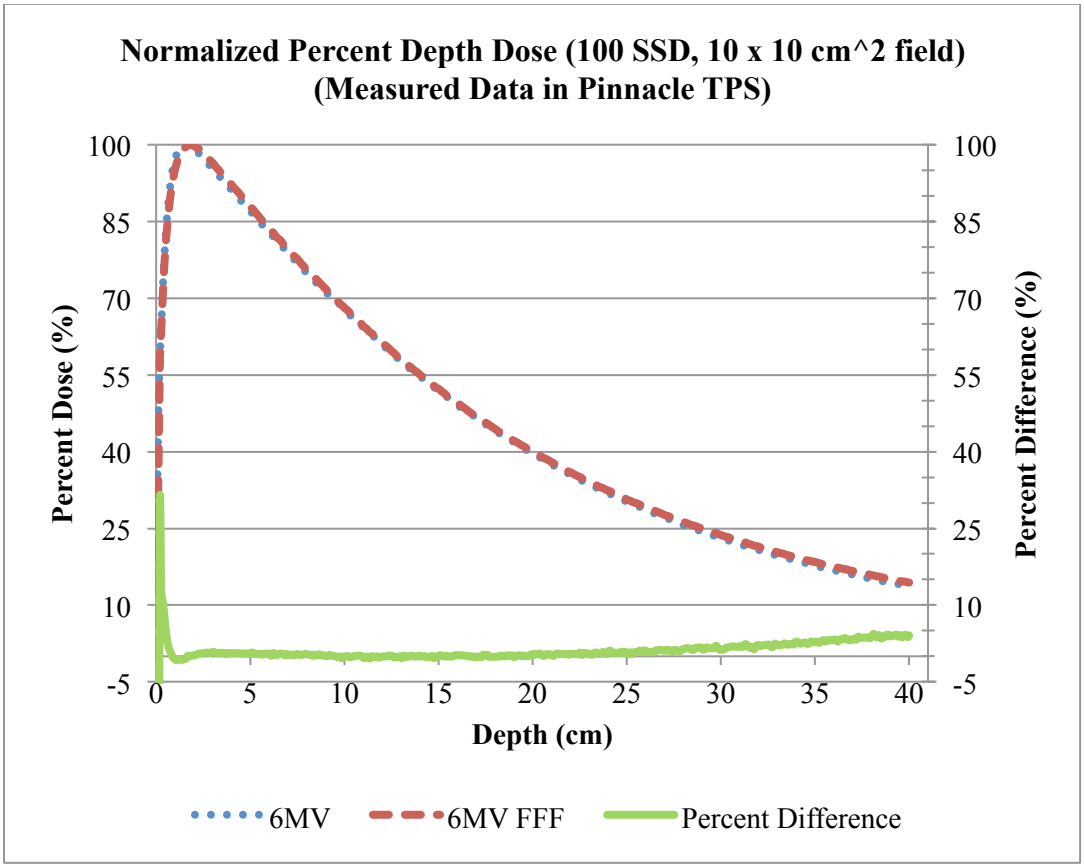

Figure 1.5 Normalized PDD data for 6 MV photon beam from one of the linear accelerators at Mary Bird Perkins Cancer Center Baton Rouge Louisiana.

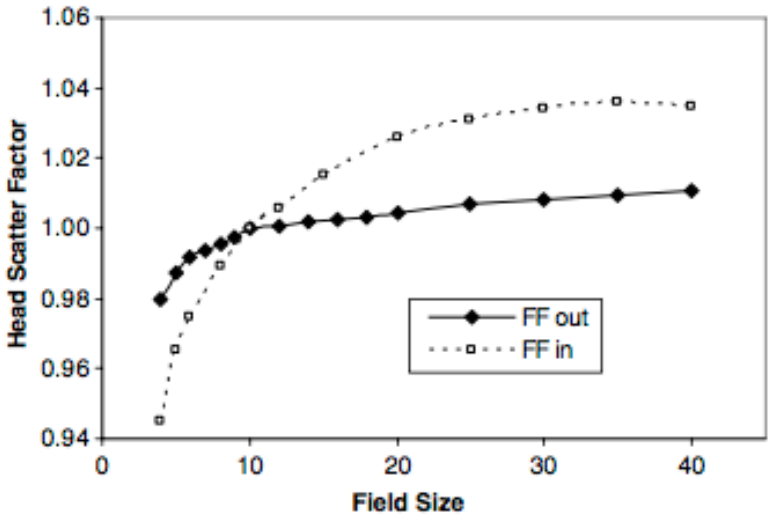

Figure 1.6 Head scatter factor as a function of field size for 6 MV photon beam (normalized to a 10 x 10 cm^2 field). Source: Cashmore *et al.,* (2008)

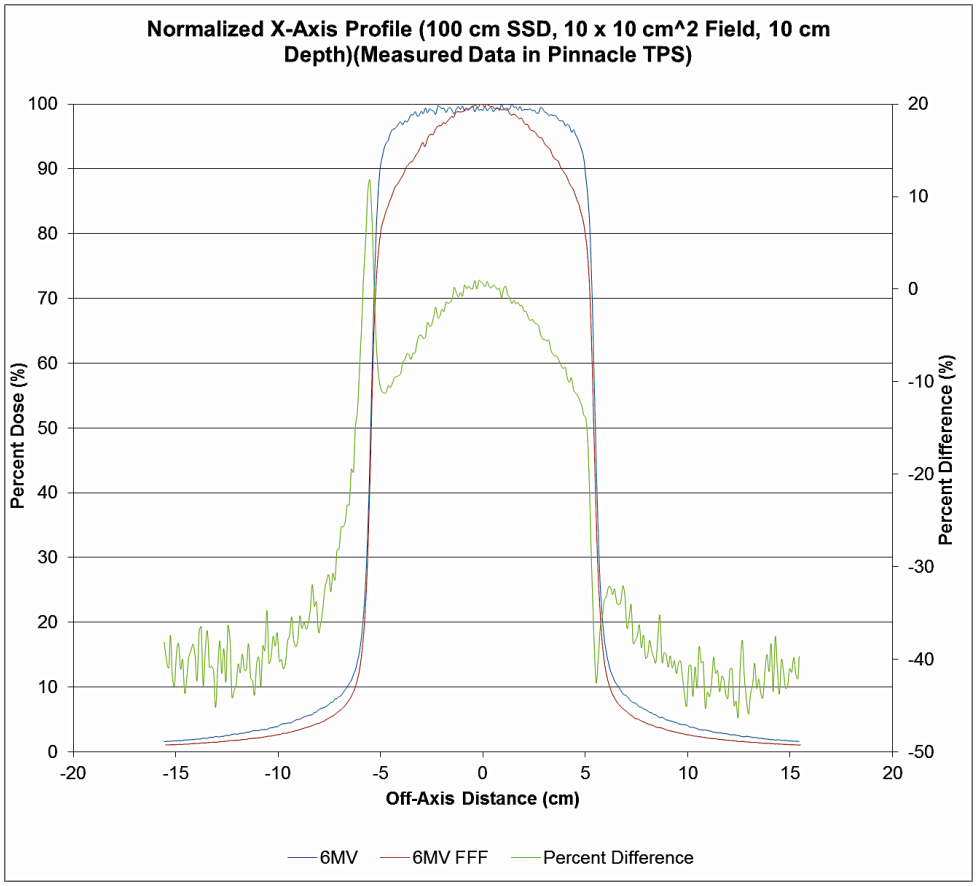

Figure 1.7 Normalized x-axis cross-plane profile for flattened and unflattened 6 MV photon beam from one of the linear accelerators at Mary Bird Perkins Cancer Center.

1.5 BECT+IMXT

Another method for treating post-mastectomy chest wall is mixed beam therapy consisting of bolus electron conformal therapy (BECT) combined with intensity modulated x-ray therapy (IMXT). High-energy electrons have a short range in tissue. This allows electron therapy to have rapid distal dose fall-off and therefore conforms to the distal edge of the target (Mu *et al*., 2004, Hogstrom *et al.,* 2008). These characteristics make electrons suitable for the treatment of the chest wall where the target volume is superficial and organs at risk (OARs) like the lungs and heart are close to the target (van der Laan *et al.,* 2010, Rosca, 2012). Advanced electron therapy uses energy modulation to further control the distal dose fall-off (Hogstrom *et al.,* 2008). One method of achieving energy modulation for electron beams is the use of wax bolus on the patient surface where the distal edge is machined to achieve an excellent fit to the patients chest wall and the proximal edge is machined with a variable surface to achieve 90% isodose

coverage while conforming to the planning target volume (PTV), sparing distal OARs (Hogstrom *et al.,* 2008, Rosca, 2012). In addition to providing a conformal dose distribution, BECT sometimes improves dose homogeneity by smoothing patient surface irregularities. BECT has been shown to be very effective at treating post-mastectomy patients (Perkins *et al*., 2001, Hogstrom *et al.,* 2008, Kavanaugh *et al*., 2013). A machineable wax bolus used in Bolus –ECT is shown in figure 1.8. Dose homogeneity can still be a problem and can be clinically unacceptable. However, optimizing IMXT over a BECT dose plan in mixed beam therapy can improve dose homogeneity to the PTV (Hogstrom *et al.,* 2008, Kavanaugh *et al*., 2013). Another important advantage to mixed beam therapy over IMXT alone is reduced normal tissue integral dose that has an important effect on reducing side effects of the treatment (Mu *et al*., 2004, van der Laan *et al.,* 2010, Rosca, 2012, Kavanaugh *et al*., 2013). Figure 1.9 compares IMXT and BECT alone to the mixed-beam treatment plan. It shows that the mixed-beam has more uniform dose to the PTV than BECT alone and less normal tissue integral dose than IMXT alone. Figure 1.10 reveals the reduced normal tissue integral dose that can be achieved with mixed-beam therapy of electrons and IMXT as compared to IMXT only.

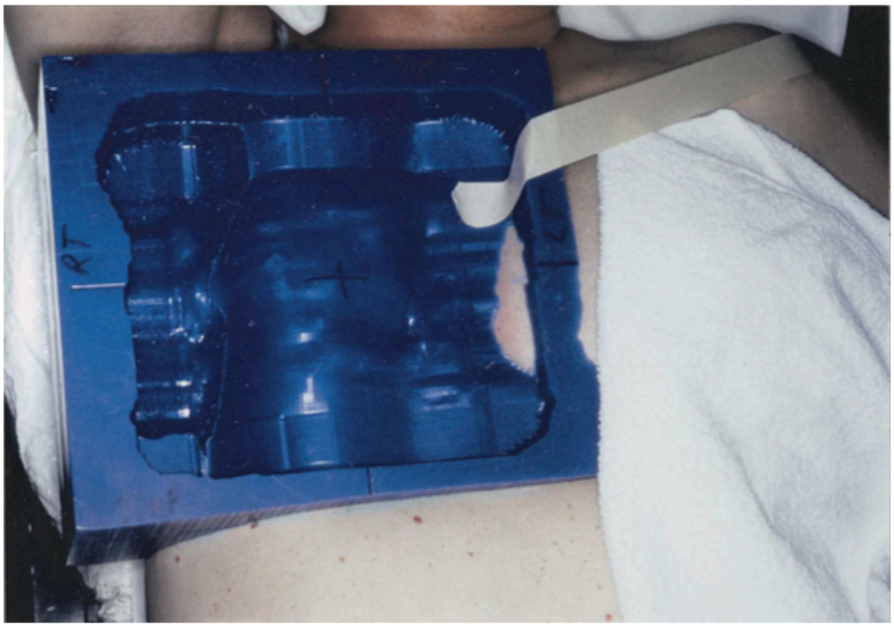

Figure 1.8 Machineable wax bolus on patient surface used in BECT. Source: Perkins *et al.,* (2001)

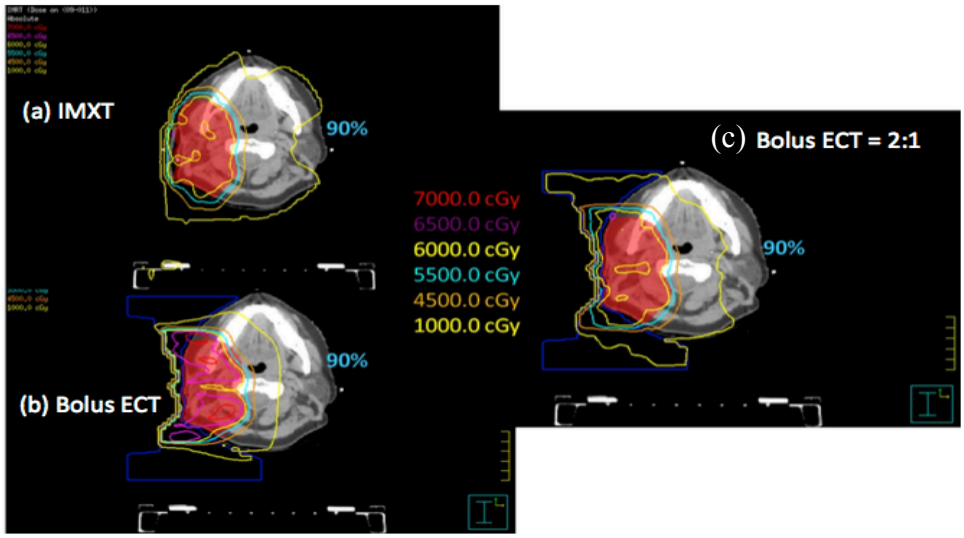

Figure 1.9 Treatment plan comparison of IMXT (a), BECT (b), and mixed beam therapy (c). Source: Kavanaugh (2013)

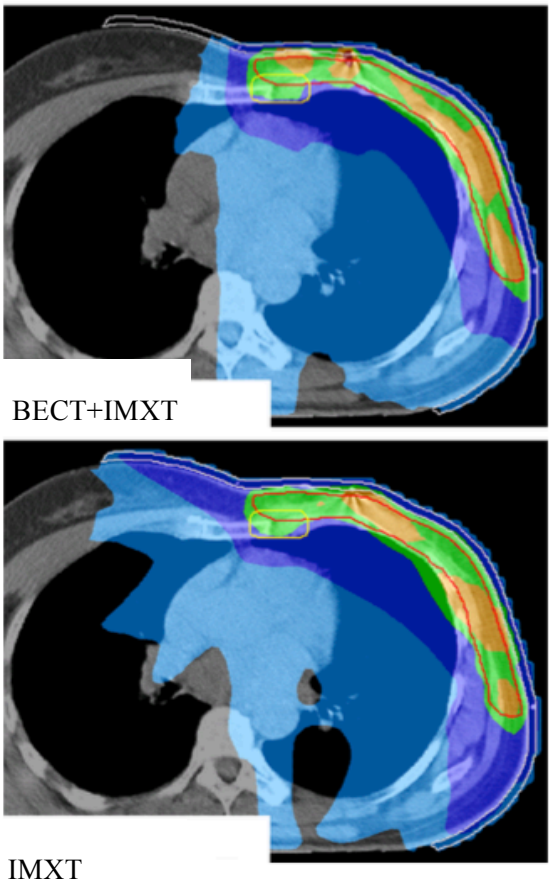

Figure 1.10 Treatment plan comparison of BECT+IMXT (above) and IMXT alone (below). Source: van der Laan *et al.,* (2010)

1.6 PMRT Complications

Side effects, including normal tissue complications such as second cancers, are serious concerns with all radiotherapy. It is especially important for young women to reduce contralateral breast dose to reduce the risk of secondary cancer associated with conventional post-mastectomy radiotherapy methods (van der Laan *et al.,* 2010, Spruijt *et al*., 2013, Zhang *et al.,* 2015). Research has shown breast irradiation is linked to increased side effects of the skin, heart, and lung (Levitt & Perez, 1987, Harris *et al*., 1996, Lichter, 1998, Almberg *et al*., 2011, Donovan *et al*., 2012, Rudat *et al*., 2014). Risk models such as the biological effects of ionizing radiation (BEIR) VII risk model, lifetime attributable risk (LAR), linear quadratic (LQ) model, and other normal tissue complication probability (NTCP) models and second cancer complication probability (SCCP) models are available to researchers and clinicians but care must be taken in using them and they should not be used for clinical decision making rather a tool for comparing techniques. (Peirce *et al*., 2002, Marks *et al.,* 2010, Donovan *et al*., 2012). Quantitative Analysis of Normal Tissue Effects in the Clinic (QUANTEC) guidelines are used to define the limiting dose to healthy tissue to reduce the likelihood of serious side effects (Marks *et al*., 2010). These tools are very useful when comparing different modalities for treating post-mastectomy patients.

1.7 Purpose of Study/Statement of Problem

With all of the knowledge and experience available today, there are still gaps in knowledge that need to be filled. Advanced methods are controversial as to whether they improve tumor control and reduce side effects. More treatment planning studies need to be conducted using flattening filter free beams with large field sizes such as those used in post-mastectomy radiotherapy (Cashmore *et al*., 2008, Spruijt *et al*., 2013). In addition, more comparative studies looking at treatment plan quality for flattening filter free beams are needed (Georg *et al*., 2011). Reports on conformal electron therapy planning are limited and need to be increased (van der Laan *et al.,* 2010). It has also been reported that current commercial TPS do not calculate out-of-field dose and skin dose accurately (Almberg *et al*., 2011, Donovan *et al*., 2012, Zwahlen *et al.,* 2012). Anthropomorphic phantom measurements are needed for verifying TPS calculation accuracies and for more robust side effect calculations (Almberg *et al*., 2011,

Donovan *et al*., 2012). Currently no studies have been conducted using FFFVMAT or BECT+VMAT for left-side PMRT. This study was conducted to determine if bolus electron conformal therapy (BECT) combined with volumetric modulated arc therapy (VMAT) and FFFVMAT (6x and 10x) can maintain equal or better dose coverage than VMAT while reducing doses to OARs.

1.8 Hypothesis and Specific Aims

For a sample of left-sided post-mastectomy breast cancer patients, BECT+VMAT and FFFVMAT (6x and 10x) can maintain equal or better dose coverage than VMAT while statistically significantly lowering ($p < 0.05$) predicted risks of side effects.

This hypothesis was tested by comparing calculated dosimetric and radiobiological endpoints for ten randomly selected patients who have undergone VMAT treatment for the left side of the chest wall. Comprehensive dose reconstructions, tumor control probability, normal tissue complication probability for the whole heart, myocardium, lungs, and the second cancer risks for contralateral breast and lungs were performed. These tests were accomplished through the following specific aims:

Aim 1: Compare treatment plans and predicted risks of side effects between BECT+VMAT and VMAT plans.

Aim 2: Compare treatment plans and predicted risks of side effects between FFFVMAT (6x and 10x) and VMAT plans.

Chapter 2 Methods

2.1 Patient Selection

This study retrospectively considered ten consecutively sampled left side post-mastectomy patients. Table 2.1 lists the patient selection criteria.

Table 2.1 Patient selection criteria

Patient and Treatment Factors	Inclusion Criteria	Exclusion Criteria
Age	20yrs<age<80yrs	Age<20yrs, Age>80yrs
Surgery	Mastectomy	Bi-lateral Mastectomy, Lumpectomy, Chemo Port
Disease	Localized to chest wall and regional lymphatics	Distant metastases
Treatment	VMAT, 1 or 2 arcs	Other

All patients received a left side modified radical mastectomy and were treated by the same radiation oncologist at MBPCC. All CT data sets were anonymized and assigned a unique research identifier ranging from CW1 to CW10. BECT+VMAT, VMAT (6x), and FFFVMAT (6x and 10x) treatment plans were produced on pre-contoured and clinically used computed tomography (CT) scans. CT scans had been acquired on a large bore GE LightSpeed 16 CT scanner (General Electric Medical Systems). For all ten patients, new VMAT and FFFVMAT (6x and 10x) treatment plans were produced. For nine of the patients, BECT+VMAT plans were produced. The tenth patient was not used for BECT+VMAT because the PTV extended to the rib-lung interface and was therefor deemed unsuitable for BECT+VMAT. The treatment planning for all modalities were produced on a commercially available TPS in the clinical dosimetry lab at MBPCC. All completed treatment plans were reviewed and approved by a single board certified radiation oncologist (Dr. M. Sanders). Furthermore, the Louisiana State University Internal Review Board approved this study.

2.2 Contours

All patients were previously scanned in the supine position with the free breathing CT data sets including all anatomy from the top of the head down to the lower abdomen. The PTV for each patient was previously contoured by the same radiation oncologist and was included in the anonymized data sets. The PTV included the chest wall, supraclavicular lymph nodes, axillary lymph nodes, and internal mammary chain lymph nodes, as shown in figure 1.2. Nine patient PTVs excluded RTOG specification for including ribs and intercostal tissue. In addition, patients had a 1 cm tissue-equivalent bolus placed on the surface of their chest wall. For this study the dose within the tissue-equivalent bolus was unnecessary so it was removed from the "PTV evaluate" contour used in optimizing and evaluating the plans.

Figure 2.1 shows the contours used in optimizing and evaluating the PTV in the treatment planning system. The green plus red is the original contour created by the radiation oncologist. The red contour is the modified "PTV evaluate" that does not include the 1 cm tissue-equivalent bolus. This contour was used in planning and optimizing all the VMAT techniques in this study. The red contour was also used for evaluating the PTV dose metrics for all techniques. The yellow contour is a 5 mm shell that is used to evaluate the skin dose within the PTV.

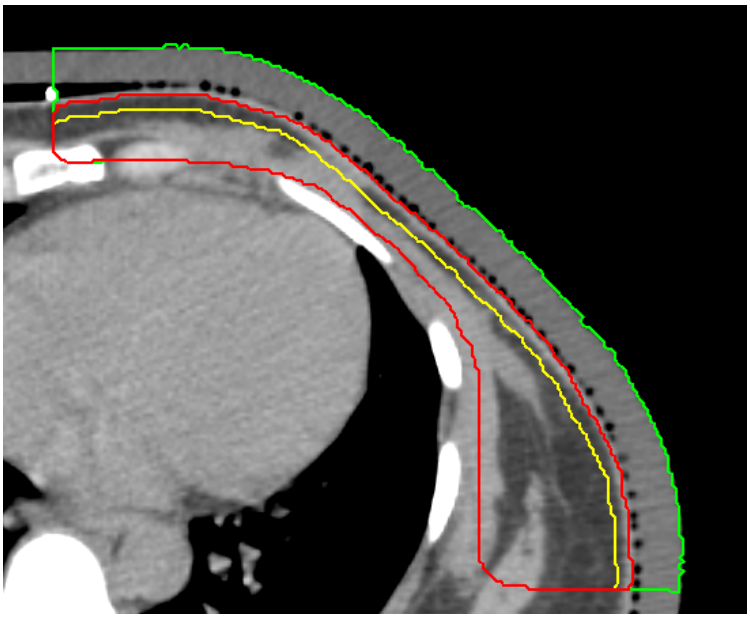

Figure 2.1 Planning target volumes for all VMAT techniques and BECT+VMAT (red), including the chest wall and 1 cm tissue-equivalent bolus (red + green), and 5 mm skin contour (yellow)

Figure 2.2 gives a three-dimensional representation of the PTVs used in planning and evaluating all techniques in this study. The image on the left shows the superclavicular PTV and electron chest wall PTV for the BECT+VMAT technique while the image on the right shows the PTV used for all the VMAT techniques as well as the VMAT component of the BECT technique.

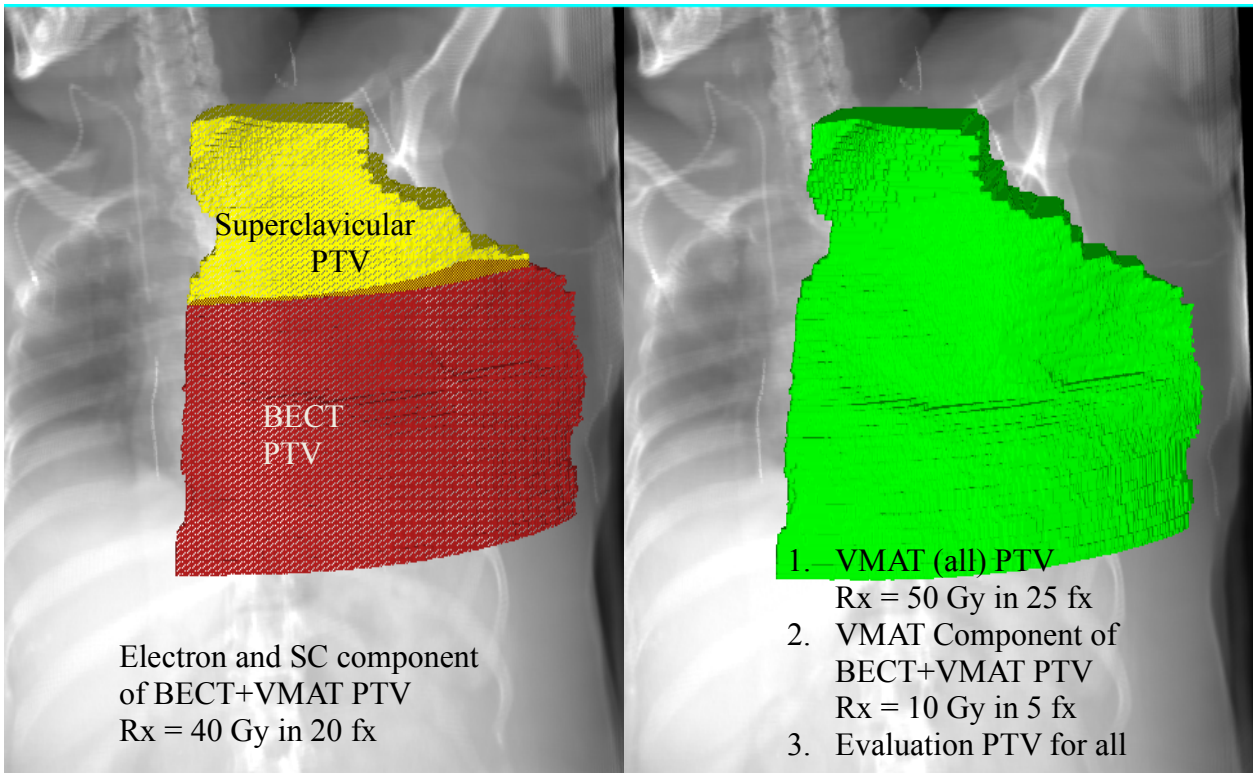

Figure 2.2 Planning target volumes with prescriptions for all VMAT techniques and BECT+VMAT.

The organs at risk (OARs) were also included in the CT data sets and were drawn by the planning radiation oncologist for all the patients. The OARs included lungs, whole heart, contralateral breast, esophagus, trachea, and spinal cord. New contours were added to the original CT data sets which included a 0.8 cm ring around the PTV, used to control hot or cold spots around the PTV, an external skin contour used in BECT+VMAT planning, the 5 mm thick shell for evaluating the skin dose inside the PTV, and unspecified tissue which included everything inside the external skin contour excluding the above mentioned OARs. In addition, the contour for the myocardium was created following the method of Zhang *et al.* (2013).

2.3 VMAT Treatment Planning

Both VMAT (6x) and FFFVMAT (6x and 10x) treatment plans were created in Phillips Pinnacle^3 v9.8 treatment planning software (TPS). All VMAT treatment plans used commissioned beam data from MBPCC Elekta Versa HD linear accelerator using a prescribed dose of 50.0 Gy in 25 fractions. All plans used 0 degree couch angle and 45 degree collimator angle. Every technique was planned using its maximum dose rate: VMAT (6x) used 600 Monitor Units (MU) per minute, FFFVMAT6x used 1200 MU per minute, and FFFVMAT10x used 2000 MU per minute. All dose calculations were conducted using a dose grid resolution of 4 mm^3. Each plan also utilized two partial arcs due to the complexity of the cases and close proximity to lungs, heart, and contralateral breast. Each arc covered approximately 220° with about 56 control points and 4° gantry spacing. The first arc was planned to be delivered counterclockwise with starting angles between 170-180° (floor to ceiling) and stopping angles between 304-320°. The second arc was planned to be delivered clockwise. Inverse planning for all VMAT techniques was done using the SmartArc optimization algorithm utilized by Pinnacle^3 v9.8 TPS.

The VMAT plans were optimized using a four-run technique. The first run consisted of 75 iterations of the SmartArc algorithm in addition to 25 iterations of the convolution dose algorithm with the primary focus on PTV coverage. All PTV optimization objectives were set to a weight of 100. The starting optimization objectives and constraints for all VMAT plans are shown in table 2.2. All of the following runs consisted of 35 iterations each of the SmartArc algorithm. For the second run the hotspots from the first run were contoured and an objective was added with max dose constraint set to 5200 cGy with a weight of 100. The hot spots were contoured by creating a contour from the 5350 cGy isodose line. For the third run the "PTV evaluate" region of interest (ROI) was uniformly contracted by 0.2 cm and labeled PTV min dose. This ROI was added to the optimizer and given a min dose objective of 5000 cGy with a weight of 100. In addition, hotspots from the second run were contoured and an objective was added with max dose constraint set to 5200 cGy with a weight of 100. For the fourth run the focus was set to reduce the dose to the heart, lung, and contralateral breast. At the beginning of the run the target doses were reduced by an amount that resulted in the objective value for that ROI to be around 0.005. The

objectives can be adjusted in real time as the optimizer is running. While the last run was being optimized the target doses of the aforementioned ROIs were adjusted to keep their objective value around 0.005.

For the FFFVMAT techniques, after the first run, the DVH did not meet the goals assigned in the optimizer. To fix this problem a "warm run" was done. Following each optimization the prescription was automatically changed from 100% normalization to the calculation point to monitor units per fraction. Resetting the prescription to 100% normalization to the calculation point and starting the optimizer from where it left off using 35 iterations would typically fix this. If the "PTV evaluate" still did not have the proper coverage, then a new ROI was created in the region of the "PTV evaluate" where the dose was too low. This ROI was then added to the optimizer and given a min dose of 5000 cGy with a weight of 100 and the optimizer was run for 35 iterations. After the "PTV evaluate" DVH had the proper dose coverage the four-run technique was continued.

Table 2.2 Starting VMAT optimization objectives and constraints

ROI	Type	Target Dose [cGy]	Volume [%]	Weight
PTV Evaluate	Min DVH	5000	98	100
PTV Evaluate	Max Dose	5200	-	100
Total Lung	Max DVH	1500	15	1
Total Lung	Max DVH	1000	35	1
Total Lung	Max DVH	500	60	1
Total Lung	Max Dose	4500	-	1
Heart	Max DVH	1500	15	1
Heart	Max DVH	1000	30	1
Heart	Max Dose	4000	-	1
Esophagus	Max Dose	2000	-	1
Airway	Max Dose	2000	-	1
Spinal Cord	Max Dose	1000	-	1
Contralateral Breast	Max Dose	1500	-	1
Ring	Max Dose	5000	-	25
Unspecified Tissue	Max Dose	2800	-	1

2.4 BECT+VMAT Treatment Planning

BECT+VMAT treatment plans were produced for nine of the ten patients using Phillips Pinnacle[3] v9.8 TPS. All BECT+VMAT treatment plans used commissioned beam data from MBPCC Elekta Infinity linear accelerator with Agility treatment head. BECT+VMAT is a mixed modality technique utilizing electrons, open field photon beams, and dual-arc VMAT using 6 MV photons. It uses a 4:1 ratio

where 20 of the 25 total fractions are an electron field to the chest wall and parallel opposed open anterior-posterior (AP) and open posterior-anterior (PA) photon beams to the superclavicular area. Generalizations of these two PTVs are shown in figure 2.2 in the left image. The final 5 of the 25 total fractions utilized a dual-arc VMAT technique, as described in section 2.3 of this chapter. The prescription dose of the electron and open photon fields were 40 Gy in 20 fractions and the dual-arc VMAT was prescribed to 10 Gy in 5 fractions. The VMAT PTV for this technique as well as the PTV used for final evaluation is shown in the right image of figure 2.2. Before creating these plans the original CT data sets needed modified.

Prior to creating these treatment plans the original CT data set field-of-view (FOV) needed to be increased. The original CT data sets were acquired using a 50 cm FOV on the CT scanner. When the machineable wax bolus contour was created it often extends outside the image space of this FOV. If this happens the contour could not be exported from the creation software. This required the FOV of the CT image set to be increased to approximately 70 cm. This was achieved by adding 20 cm margin to the left lateral and anterior portion of the CT image data set.

The same contours are used as in all the VMAT plans with the addition of carefully contouring out the tissue equivalent bolus material that is in place in the original CT images. This was not used for the electron portion of this technique. Once the contour is created the density was overridden to air, i.e. 0.001 gcm^{-3}.

To create the machineable wax bolus used in this technique, plan information including PTV and external skin contour structure files, beam orientation, beam modifiers, energy, and source to surface distance (SSD) were exported to the .decimal p.d (.decimal, Inc., Sanford, FL) software. The "PTV evaluate" ROI was split in order to create the "superclavicular PTV" and "BECT PTV" as shown in the left image of figure 2.2. Each patient was analyzed to properly identify the lowest optimal electron energy to give adequate coverage of the "BECT PTV". The goal was to have the 90% isodose line cover the distal edge of the "BECT PTV" using a single electron beam. The energies used were selected from 11 MeV, 13 MeV, 16 MeV, and 20 MeV with R_{90} values of 3.5 cm, 4 cm, 5 cm, and 6 cm, respectively.

Electron isocenter was placed on the central slice of the "BECT PTV", 5 cm anterior to the patient surface, resulting in a pre-bolus SSD of 105 cm allowing for adequate electron applicator clearance. The electron isocenter was also located laterally from the "BECT PTV" patient midline edge to approximately place the point in the center of the "BECT PTV". The gantry angle was chosen so the beam direction was perpendicular to patient surface on central axis (approximately 45°).

An electron field (cutout) was also created to conform the lateral edges of the electron beam to the "BECT PTV" plus margin. The following parameters were adjusted using the beams-eye-view (BEV) projection. A 1 cm margin was added around the "BECT PTV" to ensure the PTV was inside the penumbra and received 90% of the given dose. The couch was adjusted so the beam at the superior border had a straight edge, which slightly diverged from the "superclavicular PTV". This resulted in a non-zero couch angle. In addition, the cutout matched the superior border of the "BECT PTV" to reduce the penumbra from spilling into the "superclavicular PTV". The collimator was adjusted so the medial jaw was parallel to the "BECT PTV" medial edge. This adjustment maximized the distance between the "BECT PTV" outer edge and the electron field's (cutout) outer edge. The smallest electron applicator was selected that left a minimum (distance from outer edge of applicator edge to the electron's field edge) of 1-2 cm margin (applicator sizes were either 20x20 cm^2 or 25x25 cm^2). The dose was calculated using a dose grid resolution of 2 mm^3.

The finalized ROI structures and electron beam characteristics were exported from the TPS and transferred to the .decimal p.d planning computer using file transfer protocol (FTP). The plans were then imported into .decimal p.d planning software (v5.1.9) for bolus creation.

Bolus creation began by selecting the beam energy and the "BECT PTV" and external skin ROI structures. The bolus was created using a series of bolus operators and parameters that resulted in the best 90% isodose line coverage of the distal surface of the "BECT PTV". Typically the operation sequence was create followed by smooth using default parameters for both. Once the bolus design was finalized its shape was transferred back to the TPS.

The digital bolus contour was imported into a copy of the original treatment plan in the TPS labeled "Bolus-ECT". The density of the bolus contour was set to 0.92 g/cm^3 (Low *et al.,* 1995, Kavanaugh, 2013). The monitor units for the beam were set based on a calculation using the dose prescription, beam energy, applicator size, effecive rectangular field size, and SSD taken from the .decimal p.d planning software. MU's were calculated to give the prescribed dose to 95% of the given dose. The dose distribution was calculated using the Pencil Beam Redifinition Algorithm (PBRA) in the .decimal p.d planning software and the Pencil Beam Algorithm in the Pinnacle TPS.

Continuing the planning process required adding the AP/PA open photon fields to deliver dose to the "superclavicular PTV". First, the density of the bolus contour was turned off and the tissue equivalent bolus material was turned back on to calculate the photon components of the treatment plan. Modification of the bolus density results in the deletion of the ECT dose distribution, a necessary component of the treatment plan. Thus, the ECT dose distribution was recreated by copying the plan.Trial.binary file into a copy of the "Bolus-ECT' plan labeled "Bolus-ECT with IMXT" using identical dose grid parameters. From here the photon components of the treatment plan were created.

The AP/PA photon isocenter was placed on the inferior border of the superclavicular PTV at its medial border. The AP beam combined 6 MV photons and 15 MV photons so as to achieve adequate dose coverage to deep portions of the "superclavicular PTV". Due to the depth of the PTV a PA beam of 15 MV was also required. A multi-Leaf collimator was used to block the inferior border of the PTV to minimize or remove any hot spots (> 52 Gy) due to abutting the electron and photon beams. In addition there was a 1 cm margin around the superior and lateral borders of the PTV for proper dose coverage. The beams were weighted in such a way to maximize the 40 Gy prescription dose coverage while minimizing dose to tissue outside the superclavicular PTV. The beam angles were chosen to reduce dose to the esophagus and trachea and were approximately 345°. After the BECT PTV and superclavicular PTV were covered by their 40 Gy prescription the VMAT component of the plan was applied. The VMAT planning technique was identical to that described in section 2.3 with the exception it was optimized on top of the existing dose distributions.

2.5 Plan Acceptance Criteria

The following criteria were met for each treatment plan to be considered clinically acceptable and therefore representative of an actual plan administered to a patient.

1. Planning Target Volume (PTV) Coverage:

   The volume of the PTV receiving at least 95% of the prescribed dose is greater than or equal to 95% ($V_{D95\%} \geq 95\%$).

2. Organs At Risk (OARs) limitations:

   The volume of lungs receiving at least 20 Gy is less than 20% ($V_{D20Gy} < 20\%$). The volume of heart receiving at least 22.5 Gy is less than 20% ($V_{D22.5Gy} < 20\%$).

2.6 Treatment Plan Evaluation Metrics

2.6.1 Planning Target Volume (PTV)

The following dose-volume treatment plan metrics were evaluated for all treatment plans:

1. Dose Volume Histogram (DVH) for the PTV
2. Minimum, Maximum, and Mean doses with standard deviation for the PTV
3. The dose that 95% of the PTV volume receives ($D_{95\%}$)
4. Volume of the PTV that receives 95% of the prescription dose ($V_{D95\%}$)
5. Volume of the PTV that receives 107% of the prescription dose ($V_{D107\%}$)
6. Percent volume receiving 110% of prescribed dose within the treated volume ($TV\text{-}V_{110\%}$)
7. Dose Homogeneity Index (DHI)
8. Conformity Index (CI)

The DHI is

$$DHI = \frac{D_{max} - D_{min}}{D_{Rx}},$$

[2.1]

where D_{max} is the dose to 2% of the PTV, D_{min} is the dose to 98% of the PTV, and D_{RX} is the prescription dose (Wu *et al.,* 2003). A DHI value of zero is ideal and represents a homogenous dose to the entire PTV.

The CI is

$$CI = \frac{TV_{RI}}{TV} \times \frac{TV_{RI}}{V_{RI}},$$

[2.2]

where TV_{RI} is the target volume receiving the reference dose (47.5 Gy), TV is the PTV, and V_{RI} is the volume receiving reference isodose of 47.5 Gy (Van't Riet et al., 1997). A CI value of close to unity means the dose conformed excellently to the target volume.

TV-$V_{110\%}$ was calculated as described by Chen *et al.* (2010) and is the percent volume receiving 110% of the prescribed dose (55 Gy) within the treated volume (TV) where the treated volume is the volume enclosed by the prescribed dose (50 Gy). It has been shown that TV-$V_{110\%} > 5.13\%$ is an indicator of radiation induced skin toxicity that results in moist desquamation (Chen *et al.*, 2010).

2.6.2 Organs at Risk (OARs)

1. DVH for each OAR
2. Minimum, Maximum, and Mean doses with standard deviation for each OAR
3. Volume of lungs Receiving 5 Gy, 10 Gy, 20 Gy or more
4. Volume of Heart Receiving 5 Gy, 10 Gy, 22.5 Gy, 30 Gy or more
5. Volume of contralateral breast receiving 5 Gy or more

The OARs of most importance to this study were the lungs, heart, contralateral breast, skin, esophagus, spinal cord, and unspecified tissue. Radiation pneumonitis is of clinical concern for patients undergoing chest wall irradiation. The volume of lung receiving at least 20 Gy was less than or equal to 20% ($V_{20Gy} \leq 20\%$), as this has been shown to be the clinical threshold for pneumonitis (Ares *et al*., 2010, Hernandez, 2014). In addition, the volume of lung receiving at least 5 Gy was less than or equal to 42% ($V_{5Gy} \leq 42\%$), as any more is related to an increase in lung toxicity (Ares *et al*., 2010, Hernandez, 2014). Side effects to the heart are also concerning for chest wall irradiation. Doses to the heart above 30 Gy have been shown to increase cardiac mortality (Gagliardi *et al*., 1998, Hernandez, 2014). Also, a dose of 22.5 Gy to the heart has been correlated to increased rates of reduced myocardial perfusion (Ares *et al*., 2010, Hernandez, 2014).

2.7 Radiobiological Metric Comparison

2.7.1 Tumor Control Probability (TCP)

The most important task of radiation therapy is the ability to control the tumor. This project used the Webb and Brenner model to calculate the tumor control probability (TCP) (Brenner, 1993; Webb and Nahum, 1993). The model accounts for repopulation of the tumor cells. Unfortunately, α, β, and n values

are not reported for the chest wall. The next most appropriate values available for those variables are the ones used for whole breast and were used for this study following previous investigators (Nichols, 2012, Hernandez, 2014). Hernandez and Nichols determined the model for the overall TCP is the product of probabilities of tumor control in each PTV dose bin *i* of the differential DVH as

$$TCP = \prod_i TCP_i \,,$$

[2.3]

where TCP_i, the tumor control probability for each sub-volume *i* , or

$$TCP_i = e^{-N \cdot SF_i},$$

[2.4]

where N is the number of initial clonogenic cells in the tumor. N is

$$N = nV,$$

[2.5]

where *n* is the tumor cell density and is taken as $1.0X10^7$ cm^{-3} (Webb *et al.,* 1993) and V is the volume of the PTV. SF_i in equation [2.4] is the cell survival fraction and is predicted with the linear-quadratic model for cell survival and is given by

$$SF_i = e^{(-\alpha D_i - G\beta D_i^2)},$$

[2.6]

where the constant α is the rate of lethal cell damage and the constant β is the rate of sublethal cell damage. D_i is the dose per fraction to sub-volume *i*. G accounts for fractionation and the half-time for sublethal damage repair and is given by

$$G = \frac{1}{x},$$

[2.7]

where x is the number of fractions. The parameters used to calculate TCP are listed in table 2.3.

Table 2.3 Parameters used to calculate TCP.

Parameter	Value	Source
α	0.51 Gy^{-1}	(Hernandez, 2014, Nichols, 2012)
β	0.061 Gy^{-2}	
G	0.04	x = 25 fractions

2.7.2 Normal Tissue Complication Probability (NTCP)

Normal tissue complication probability of the lungs with radiation pneumonitis grade two or higher as an endpoint was calculated using the Lyman-Kutcher-Burman (LBK) model (Seppenwoolde *et al*., 2003, Nichols, 2012, Zhang *et al.,* 2013, Hernandez, 2014) according to

$$NTCP = \frac{1}{\sqrt{2\pi}} \int_{-\infty}^{t} e^{-\frac{x^2}{2}} dx,$$

[2.8]

where

$$t = \frac{EUD - TD_{50}}{m \cdot TD_{50}}.$$

[2.9]

TD_{50} is the total uniform dose given to the organ that results in 50% complication risk and m is the slope of the dose-response curve. The dose delivered to the lungs is inhomogeneous and the treatment plan differential DVH was reduced to an equivalent uniform dose (EUD) using equation [2.10] (Seppenwoolde *et al*., 2003, Hernandez, 2014). The EUD is the dose that will result in the same NTCP as the inhomogeneous dose, or

$$EUD = \left(\sum_i D_i^{\frac{1}{n}} \frac{v_i}{v_{tot}} \right)^n,$$

[2.10]

where D_i is the dose per fraction to sub-volume *i*, v_i is the volume irradiated with dose D_i, v_{tot} is the total lung volume, and n is the volume effect parameter. The parameters used to calculate NTCP for the lungs are listed in table 2.4.

Table 2.4 Parameters used to calculate NTCP, radiation pneumonitis for the lungs.

Parameter	Value	Source
m	0.37	(Seppenwoolde *et al.,* 2003, Hernandez, 2014)
n	0.99	
TD_{50}	30.8 Gy	

NTCP was also calculated for the whole heart and myocardium with cardiac mortality as the endpoint using the relative seriality model ((Kallman et al., 1992)). The relative seriality model considers the mixture of serial-arrange and parallel-arrange functional subunits of the heart and is

$$NTCP = \left\{1 - \prod_{i=1}^{n}(1 - P(D_i)^s)^{v_i}\right\}^{\frac{1}{s}},$$

[2.11]

where n is the total number of sub-volumes in the differential dose volume histogram, s is the relative seriality of the organ, defined as the ratio of serial functional subunits to the total functional subunits, and v_i is the fractional volume of the heart receiving dose D_i in sub-volume *i*. $P(D_i)$ is the probability of cell death when irradiated to a dose D_i and is

$$P(D_i) = 2^{-exp\left\{e\gamma\left(1-\frac{D_i}{TD_{50}}\right)\right\}},$$

[2.12]

where γ is the maximum relative slope of the dose-response curve and TD_{50} is the total uniform dose given to the organ that results in 50% complication risk. The parameters used to calculate NTCP for the whole heart and myocardium with a biological endpoint of cardiac mortality are given in table 2.5.

Table 2.5 Parameters used to calculate NTCP for the whole heart and myocardium with a biological endpoint of cardiac mortality

Structure	Parameter	Value	Source
Whole Heart	TD_{50}	52.3 Gy	(Gagliardi *et al.,* 2001), Hernandez, 2014)
	γ	1.28	
	s	1	
Myocardium	TD_{50}	52.2 Gy	
	γ	1.25	
	s	0.87	

2.7.3 Second Cancer Complication Probability (SCCP)

When patients require radiation therapy it is important for long-term survival to determine their risk for second cancers. In this study, second cancer complication probability (SCCP) of the contralateral breast and lung using the Schneider model (Schneider *et al*., 2005, Nichols, 2012, Hernandez, 2014) was calculated as

$$SCCP = In_{org} OED_{org},$$

[2.13]

where In_{org} is the organ specific absolute cancer incidence in percent per gray and represent lifetime risk assuming a residual life expectancy of 50 years. In_{org} was estimated using Japanese atomic bomb survival data (Hernandez, 2014). OED_{org} is the organ equivalent dose given in gray. It represents an evenly distributed dose to the organ to a corresponding inhomogeneous dose that causes the same radiation-induced cancer incidence. This study used the linear dose-response model given by equation [2.14] and the linear-exponential dose-response model given by equation [2.15] for the lung for the contralateral breast, based on the differential DVHs (Abo-Madyan *et al.,* 2014, Hernandez, 2014), or

$$OED_{org,linear} = \frac{1}{V_{org}} \sum_i (v_i \cdot D_i),$$

[2.14]

$$OED_{org,linear-exp} = \frac{1}{V_{org}} \sum_i (v_i \cdot D_i \cdot e^{-\alpha D_i}),$$

[2.15]

where v_i is the volume receiving dose D_i and is summed over all voxels of the organ of volume V_{org}. The parameter α is the organ specific cell sterilization parameter. Table 2.6 contains the parameters that were used to calculate SCCP for the contralateral breast and lungs.

Table 2.6 Parameters for calculating SCCP of the contralateral breast and lungs

Organ	α	In_{org}	Source
Breast	0.085 Gy^{-1}	0.78 %·Gy^{-1}	(Schneider *et al.,* 2005, Nichols, 2012, Hernandez, 2014)
Lungs	0.085 Gy^{-1}	1.68 %·Gy^{-1}	

2.8 Statistical Analysis

To test the hypothesis, the goals of specific aim 1 and 2 were to show that the prescribed dose coverage was not statistically significantly different for BECT+VMAT or FFFVMAT (6x and 10x) as compared to VMAT. Also, to show that the predicted risks of side effects were reduced by using BECT+VMAT or FFFVMAT (6x or 10x) with statistical significance as compared to VMAT. The mixed model approach (Guo *et al.*, 2015) was performed for all the PTV treatment plan metrics to show no statistically significant difference between all modalities. In addition, the mixed model approach was performed for all the OARs treatment plan metrics, NTCP, and SCCP for all modalities. Our study consisted to 4 techniques of unequal sample size. The mixed model approach was required because there is missing data for BECT+VMAT (nine patients) as compared to the VMAT techniques (ten patients). The data was dependent on using the same patients and changing the treatment technique. In addition, the statistical analysis was based on parametric procedures and thus assumed normal distribution of the data. The mixed model approach first tested for significance between all four techniques. If significance was determined then a pairwise comparison was conducted (Guo *et al.*, 2015).

2.9 Obtain Out-Of-Field Dose Values Using Anthropomorphic Phantom Measurements

Studies have shown that treatment planning systems tend to underestimate out-of-field and skin doses (Almberg *et al*., 2011, Spruijt *et al*., 2013, Taddei *et al.,* 2013, Jagetic & Newhauser, 2015). In this study anthropomorphic phantom measurements were conducted using thermoluminescent detectors (TLD) to correct for TPS calculation underestimates. An adult male phantom (CIRS, Model 701, Norfolk, Virginia) with a right breast attachment was used to simulate a left side mastectomy patient. The phantom was CT scanned and treatment plans were produced for VMAT, FFFVMAT (6x and 10x), and BECT+VMAT. In addition, a TLD location map was created to optimize TLD placement within the phantom.

Measurements were conducted using TLD100 powder placed into powder holding rods. Each modality was delivered and measured with the exception of the electron component of BECT+VMAT. The measured TLD values were used to correct the DVHs used to calculated NTCP and SCCP for OARs

based on the method described by Howell *et al.* (2010). For example, the TPS calculated dose values below 5% in the DVH for an OAR were increased by a factor of measured dose per calculated dose. This resulted in increased dose values for TPS calculated doses from 0 Gy to 2.5 Gy which improved the accuracy of NTCP and SCCP predictions. More details of out-of-field dose measurements will be provided in a separate study (Yoon *et al.,* in preparation).

2.10 Treatment Time and Total Number of Monitor Units (MU)

The time was measured for each treatment delivered to the CIRS phantom using a stopwatch for the VMAT and FFFVMAT plans. The treatment times were measured for 4 fractions (fx) for delivery of Arc 1 (beam on time), Arc 2 (beam on time), and total treatment time. Total treatment time includes delivery of both arcs in addition to the time in between arcs, time required to manually select and start the second arc. This time measurement was used to investigate reduced treatment time for FFFVMAT over VMAT. In addition, the total number of monitor units (MU) was recorded from the TPS for each technique.

Chapter 3 Results

3.1 Patient CW4

Patient CW4 has been chosen to be the representative patient for the cohort of patients used in this study. CW4 exhibits many, but not all, dosimetric and radiobiological findings close to the mean for the entire sample of patients. Patient CW4 was a 42 year old woman diagnosed with infiltrating ductal carcinoma of the left breast. The patient underwent post-mastectomy radiotherapy of the chest wall and regional lymph nodes following a modified radical mastectomy of the left breast at Mary Bird Perkins Cancer Center. The results for patient CW4 will be shown in the following manner:

1. Isodose distribution comparison
2. Dose volume histogram comparison
3. Dosimetric and radiobiological results for the planning target volume
4. Dosimetric and radiobiological results for the lungs, heart, contralateral breast, and skin

3.1.1 Isodose Distribution Comparison

Isodose distribution for patient CW4 for VMAT, FFFVMAT6x, FFFVMAT10x, and BECT+VMAT treatment plans in axial slice on VMAT beam isocenter are presented in figure 3.1. VMAT, FFFVMAT6x, FFFVMAT10x, and BECT+VMAT are shown in the top image, top middle image, bottom middle image, and bottom image, respectively. Table 3.1 lists the color coding used for isodose distributions in the following figures.

Table 3.1 Color coding for isodose distributions

Isodose Value [Gy]	Color
55.0	Yellow
52.5	Green
50.0	Blue
47.5	Cyan
35.0	Orange
25.0	Magenta
15.0	Dark Green
5.0	Red
2.5	Teal

All VMAT techniques met the plan evaluation criterion that 95% of the PTV volume received at least 95% of the prescribed dose (47.5 Gy). The BECT+VMAT plan was just under the requirement with 95% of the PTV volume receiving 94.8% of the prescribed dose (47.4 Gy). In addition, all techniques met the requirement that 20% of the lung volume received less than 20 Gy and 20% of the heart volume received less than 22.5 Gy. All of the VMAT techniques exhibited similar dose conformity and homogeneity. The BECT+VMAT plan showed less conformity and homogeneity than the VMAT plans. The BECT+VMAT plan showed reduced OARs doses with the largest reduction in dose to the contralateral breast and some reduction in the heart. In addition, FFFVMAT10x showed a slight reduction in dose to the contralateral breast compared to other VMAT techniques. The volume of the low dose regions (< 5 Gy) of the BECT+VMAT plan was reduced over all VMAT techniques. The BECT+VMAT plan showed the highest maximum dose as compared to any of the VMAT plans. This is especially apparent in the lateral portion of the PTV at the beam abutment region of the electron field and the open AP/PA photon fields. In addition, any region of the machineable wax bolus that has a steep or sharp edge caused hot and cold spots down stream in the patient. Smoothing the machineable wax bolus alleviated some of the hot spots but not all could be removed. This region showed hot spots on the order of 105% of the prescribed dose (52.5 Gy) and going up, in very small areas, as high as nearly 60 Gy.

3.1.2 DVH Comparison

Figure 3.2 – 3.4 shows the cumulative dose volume histograms for patient CW4 comparing all techniques. The figures include the DVH for the PTV, lungs, heart, and contralateral breast.

Important regions in the PTV dose volume histogram (DVH) are the “shoulder” and the “fall-off” region. The shoulder describes the area of the DVH where the dose begins to bend away from 100% of the PTV volume. The fall-off region describes vertical part of the PTV curve around the prescription dose from 100% of the PTV volume to 0% of the PTV volume. The ideal PTV DVH would have a horizontal line from 0 Gy to prescription dose (50 Gy) at 100% volume with no shoulder and the fall-off region would be a vertical line at prescription dose from 100% volume to 0% volume. On the other hand, the

ideal OAR DVH would have a vertical line at 0 Gy from 100% volume to 0% volume and then horizontal at 0% volume or simply a point at (0,0).

Figure 3.2 plots the DVHs for BECT+VMAT and VMAT for patient CW4. For VMAT the DVH curve for the PTV has a fairly narrow shoulder with sharp distal fall-off, representing a uniform dose distribution. In contrast, for BECT+VMAT the DVH curve for the PTV has a wider shoulder with less sharp distal fall-off, representing a less homogenous dose distribution and a higher maximum dose as stated earlier. However, the reviewing radiation oncologist deemed the BECT DVH curve for the PTV to be clinically acceptable.

The BECT+VMAT plan showed a marginal reduction in lung dose over VMAT. The low dose and high dose regions between the two plans were similar with the greatest improvement between 5 Gy and 30 Gy. VMAT showed higher doses for the heart where BECT+VMAT had reduced doses in the higher dose regions. The mean heart dose was reduced from 9.2 Gy for the VMAT plan to 6.7 Gy for the BECT+VMAT plan. In addition the BECT+VMAT was able to reduce low dose for the contralateral breast over VMAT.

Figure 3.3 shows the DVH for FFFVMAT6x and VMAT for this patient. The DVH curve for the PTV is nearly identical for both techniques, with both showing a narrow shoulder and sharp distal dose fall-off. The OARs show very similar curves for both techniques. FFFVMAT6x actually shows slight increases in dose for both the lungs and heart in the high dose regions. However, FFFVMAT6x does show a slight decrease in high dose for the contralateral breast. Figure 3.4 shows the DVH for FFFVMAT10x and VMAT for patient CW4. Again the DVH curve for the PTV is nearly identical for both techniques. Similar trends can be seen for the lungs and heart as seen for FFFVMAT6x. The lungs and heart have slight increase in dose in the higher dose regions. For FFFVMAT10x the contralateral breast dose is decreased along the entire dose range. Overall, both FFFVMAT (6x and 10x) techniques do not show improvements over the VMAT technique and in fact are slightly worse based on the treatment planning system calculations.

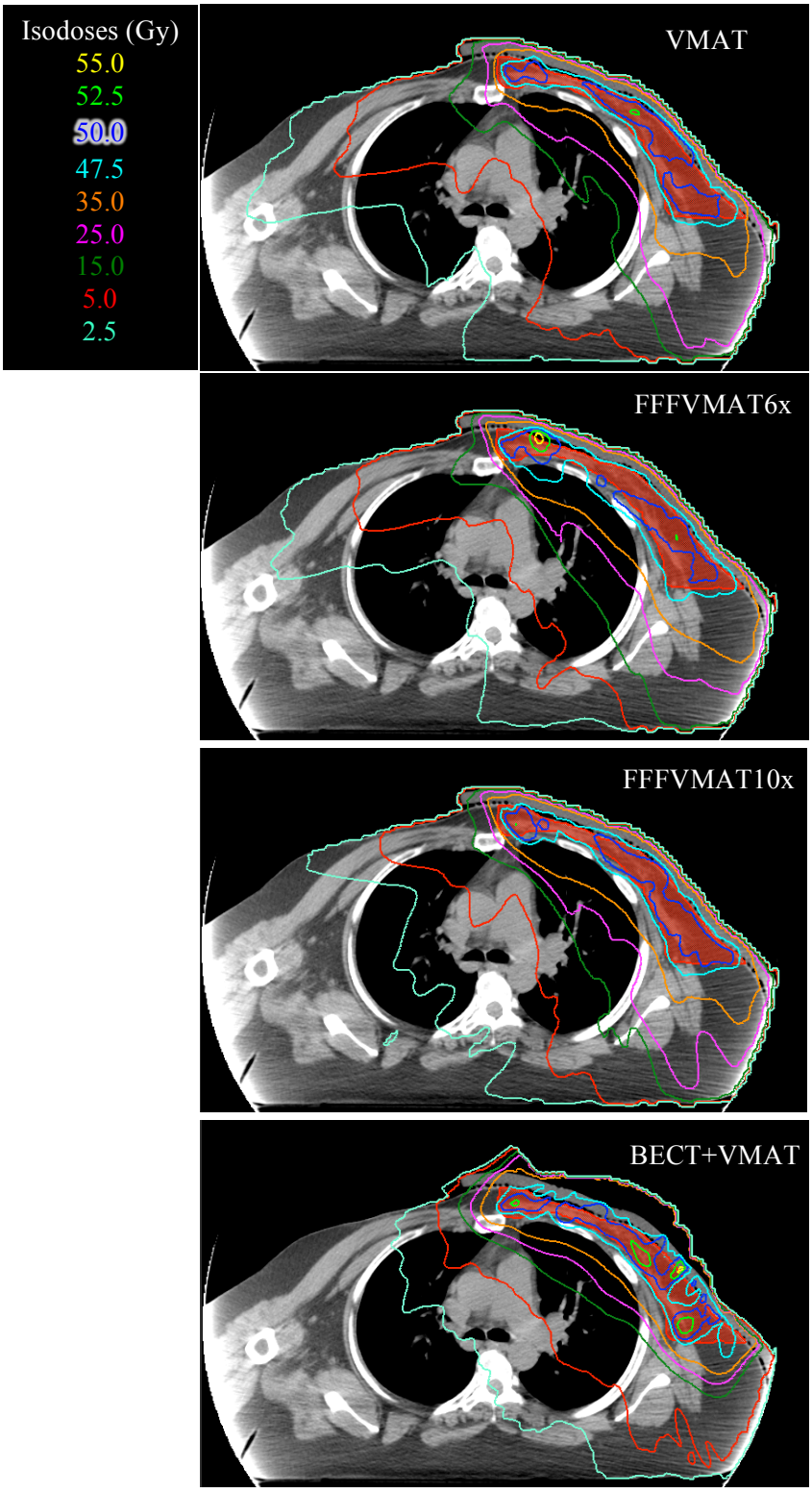

Figure 3.1 Isodose distribution for patient CW4 for VMAT (top), FFFVMAT6x (top middle), FFFVMAT10x (bottom middle), and BECT+VMAT (bottom) treatment plans in axial slice on VMAT beam isocenter.

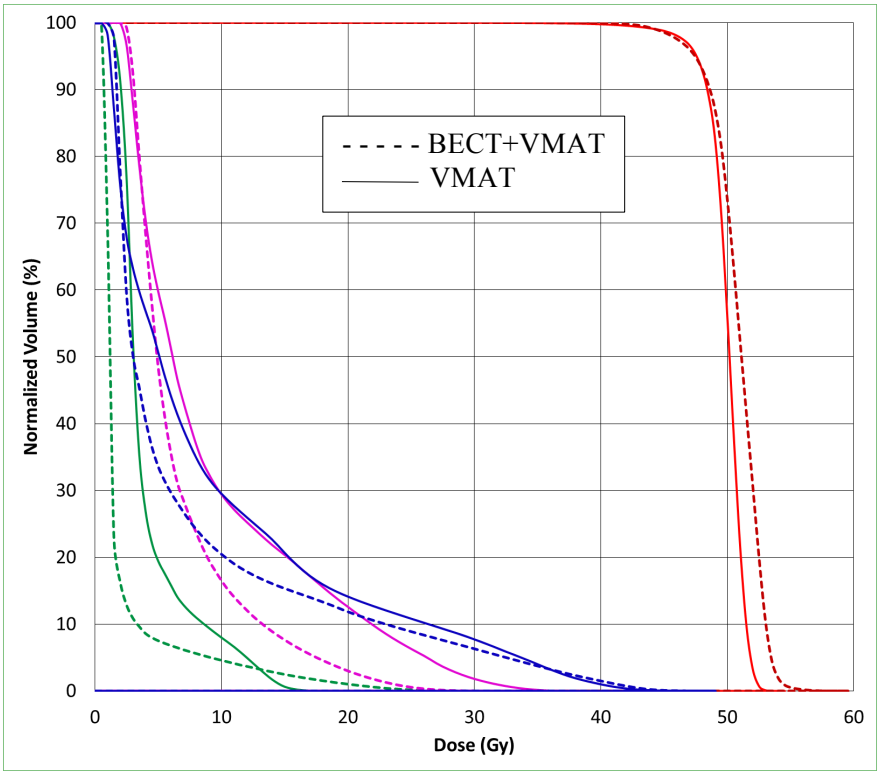

Figure 3.2 DVH for patient CW4 comparing PTV (red), lungs (blue), heart (magenta), and breast (green) for BECT+VMAT (dashed line) and VMAT (solid line).

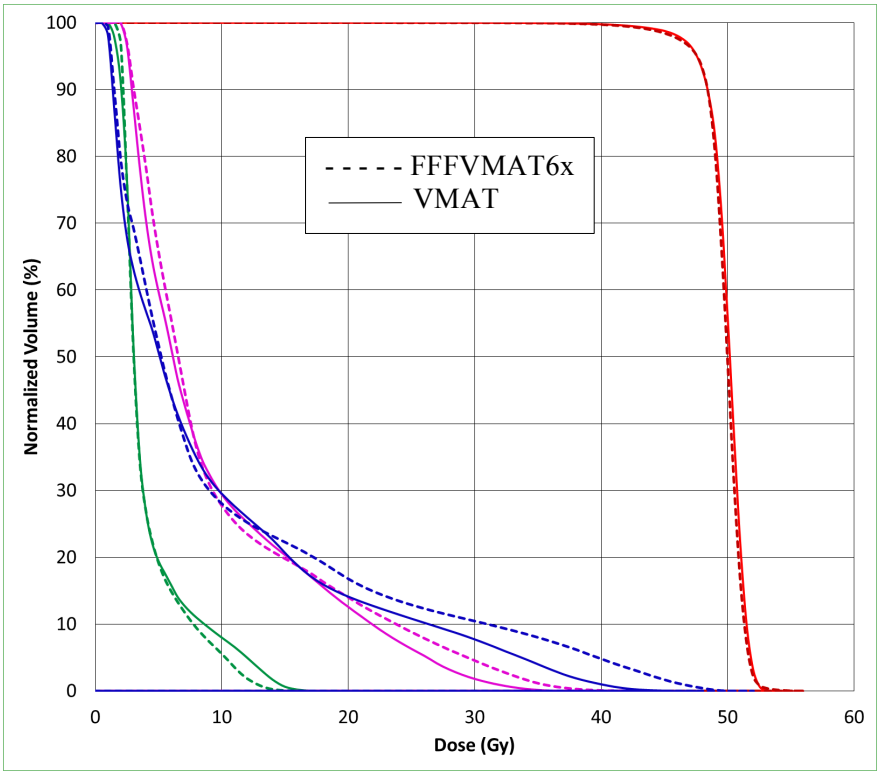

Figure 3.3 DVH for patient CW4 comparing PTV (red), lungs (blue), heart (magenta), and breast (green) for FFFVMAT6x (dashed line) and VMAT (solid line).

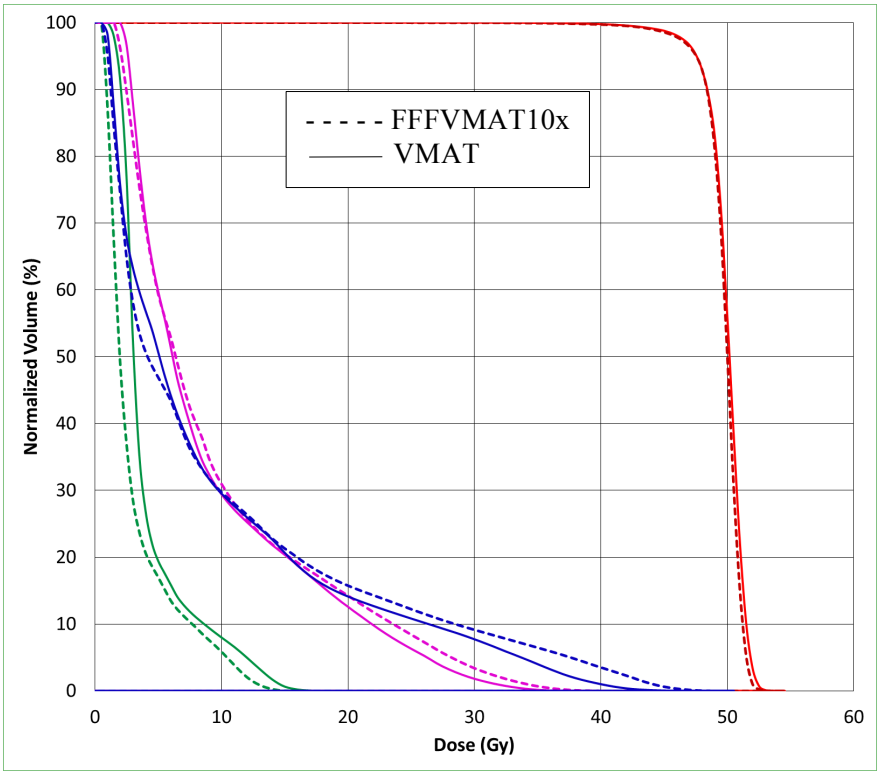

Figure 3.4 DVH for patient CW4 comparing PTV (red), lungs (blue), heart (magenta), and breast (green) for FFFVMAT10x (dashed line) and VMAT (solid line).

3.1.3 PTV

Table 3.2 gives the evaluation metrics for the PTV for patient CW4. All plans were normalized to have 95% of the PTV volume receive 95% of the prescription dose (47.5 Gy) therefore; nearly no difference was seen for $D_{95\%}$ and $V_{95\%}$. BECT+VMAT has larger hotspots and therefor has higher D_{max}, $D_{min,}$ and $V_{107\%}$ as compared to the VMAT plans. Maximum and minimum dose was recorded from the TPS. In addition, among the VMAT techniques FFFVMAT6x has higher D_{max} and $V_{107\%}$. The VMAT techniques had better conformity and homogeneity, essentially no difference among all three, than BECT+VMAT. All techniques were able to achieve greater than 99.5% tumor control probability.

Table 3.2 Evaluation metrics for the PTV for patient CW4

Plan	D_{mean} [Gy]	D_{max} [Gy]	D_{min} [Gy]	$D_{95\%}$ [Gy]	$V_{95\%}$ [%]	$V_{107\%}$ [%]	CI	DHI	TCP [%]
VMAT	49.9	54.3	24.2	47.6	95.3	0.02	0.72	0.12	99.60
FFFVMAT6x	49.8	56.0	23.8	47.6	95.2	0.26	0.67	0.13	99.50
FFFVMAT10x	49.8	54.4	24.5	47.6	95.2	0.02	0.68	0.13	99.60
BECT+VMAT	50.9	59.4	35.9	47.4	94.8	4.56	0.55	0.17	99.80

3.1.4 Lungs

Table 3.3 overviews the evaluation metrics for the lungs for patient CW4. BECT+VMAT had the lowest mean dose of 7.5 Gy and FFFVMAT6x had the highest mean dose of 10.2 Gy. Both VMAT and FFFVMAT10x had comparable mean dose around 9.3 Gy. In addition, FFFVMAT10x showed the highest maximum dose of 52.2 Gy. Maximum dose was recorded from the TPS. BECT+VMAT had the lowest V_{5Gy} and V_{10Gy} as compared to the VMAT techniques whose values were all nearly the same. The plan acceptance criterion that the volume of lungs receiving at least 20 Gy be less than 20% was met by all the techniques with BECT+VMAT having the lowest. Consequently, BECT+VMAT had the lowest NTCP of 2.17% as compared to VMAT, FFFVMAT6x, and FFFVMAT10x who's NTCP was 3.02%, 3.68%, and 3.26%, respectively. In addition, BECT+VMAT had the lowest SCCP of 13% as compared to the VMAT techniques, which were all above 15.73%. SCCP values shown were calculated using the linear dose-response model (see section 2.7.3).

Table 3.3 Evaluation metrics for the lungs for patient CW4

Plan	D_{mean} [Gy]	D_{max} [Gy]	V_{5Gy} [%]	V_{10Gy} [%]	V_{20Gy} [%]	NTCP [%]	SCCP [%]
VMAT	9.2	47.4	50.6	29.5	14.1	3.02	15.73
FFFVMAT6x	10.2	52.2	51.6	28.0	16.8	3.68	17.40
FFFVMAT10x	9.5	51.0	46.8	29.7	15.8	3.26	16.35
BECT+VMAT	7.5	49.3	33.5	20.5	11.8	2.17	13.00

3.1.5 Heart

Table 3.4 summarizes the evaluation metrics for the heart for patient CW4. BECT+VMAT showed the largest improvement in the mean dose with a reduction of nearly 3 Gy. The VMAT techniques had comparable mean heart dose of approximately 9.5 Gy and BECT+VMAT had a mean heart dose of 6.7 Gy. The maximum dose was comparable for all techniques with FFFVMAT6x exhibiting the highest. Maximum dose was recorded from the TPS. V_{5Gy} and V_{10Gy} was comparable for all VMAT techniques and significantly lower for BECT+VMAT. All techniques met the acceptance criteria that the volume of heart receiving at least 22.5 Gy be less than 20% with BECT+VMAT being the lowest at 1.5%. V_{30Gy}, associated with cardiac mortality, was 0.0% for BECT+VMAT, 1.8% for VMAT, and even higher for both FFFVMAT techniques. Whole Heart NTCP was lowest for BECT/IXMT followed

by VMAT, FFFVMAT10x, and FFFVMAT6x with values of 0.03%, 0.31%, 0.50%, and 0.61%, respectively. Myocardium NTCP followed the same trend with the lowest being BECT/ IXMT followed by VMAT, FFFVMAT10x, and FFFVMAT6x with values of 0.07%, 0.57%, 0.87%, and 1.11%, respectively.

Table 3.4 Evaluation metrics for the heart for patient CW4

Plan	D_{mean} [Gy]	D_{max} [Gy]	V_{5Gy} [%]	V_{10Gy} [%]	$V_{22.5Gy}$ [%]	V_{30Gy} [%]	Whole Heart NTCP [%]	Myocardium NTCP [%]
VMAT	9.2	38.4	59.8	29.4	9.2	1.8	0.31	0.57
FFFVMAT6x	9.7	45.2	65.6	27.7	11.3	4.5	0.61	1.11
FFFVMAT10x	9.5	41.4	59.4	31.0	11.2	3.4	0.50	0.87
BECT+VMAT	6.7	34.5	48.4	16.5	1.5	0.0	0.03	0.07

3.1.6 Contralateral Breast

Table 3.5 summarizes the evaluation metrics for the contralateral breast for patient CW4. The mean dose for the right breast was reduced by over 2 Gy using BECT+VMAT as compared to VMAT. There was less of a difference with FFFVMAT10x with only a 1 Gy reduction in dose. Both VMAT and FFFVMAT6x had very similar mean dose to the contralateral breast. In contrast, the maximum dose was exhibited by the BECT+VMAT plan, which is nearly twice as high as any of the VMAT techniques. Maximum dose was recorded from the TPS. The volume of the contralateral breast receiving at least 5 Gy was significantly reduced by BECT+VMAT over any VMAT technique. SCCP was lowest for BECT/IXMT followed by FFFVMAT10x, FFFVMAT6x, and VMAT with values of 1.87%, 2.41%, 3.10%, and 3.24%, respectively. SCCP values shown were calculated using the linear dose-response model (see section 2.7.3).

Table 3.5 Evaluation metrics for the contralateral breast for patient CW4

Plan	D_{mean} [Gy]	D_{max} [Gy]	V_{5Gy} [%]	SCCP [%]
VMAT	4.2	19.7	19.4	3.24
FFFVMAT6x	4.0	18.4	19.1	3.10
FFFVMAT10x	3.1	15.7	17.0	2.41
BECT+VMAT	2.1	30.1	7.5	1.87

3.1.7 Skin

Table 3.6 summarizes the evaluation metrics for the skin for patient CW4. The mean dose for all techniques was comparable and very close to the prescription dose (50 Gy). In addition, the minimum dose for all techniques was similar. The maximum dose was highest for BECT+VMAT with a value of 58.1 Gy. Among the VMAT techniques the highest dose was seen with FFFVMAT6x followed by VMAT and FFFVMAT10x with values of 56.0 Gy, 54.6 Gy, and 53.4 Gy, respectively. All techniques for this plan had TV-$V_{110\%}$ less than 5.13% so the patient does not show an increased risk of moist desquamation.

Table 3.6 Evaluation metrics for the skin (5 mm shell) for patient CW4

Plan	D_{mean} [Gy]	D_{max} [Gy]	D_{min} [Gy]	TV-$V_{110\%}$ [%]
VMAT	49.8	54.6	35.3	0.00
FFFVMAT6x	49.5	56.0	36.4	0.12
FFFVMAT10x	49.2	53.4	38.6	0.00
BECT+VMAT	50.5	58.1	36.6	0.50

3.2 Overview of Results for the Sample of Patients

The following sections give an overview of the results for the entire sample of patients for this study. The data will be discussed in terms of mean values for each metric along with any statistical significance. For all ten patients, VMAT and FFFVMAT (6x and 10x) plans were produced. Only nine of the patients were used for BECT+VMAT. The tenth patient was not used for BECT+VMAT because the PTV extended all the way to the rib-lung. Due to an uneven number of patients for each technique, statistical analysis was determined using a mixed model approach with a significance level of $p = 0.05$ (Guo *et al.,* 2015). Statistical comparison was conducted as VMAT vs. FFFVMAT6x, VMAT vs. FFFVMAT10x, and VMAT vs. BECT+VMAT.

3.2.1 PTV

Tables 3.7 - 3.10 list the dosimetric and radiobiological metrics used to evaluate the PTV for VMAT, FFFVMAT6x, FFFVMAT10x, and BECT+VMAT treatment plans. The maximum dose for all VMAT plans was comparable with no statistical significance ($p > 0.05$). Due to the hotspots in the

BECT+VMAT, the maximum dose to the PTV was significantly higher ($p < 0.001$) than VMAT. The minimum dose for all VMAT plans was comparable with no statistical significance ($p > 0.05$). The overall PTV dose was higher for BECT+VMAT plans so the minimum dose was statistically significantly higher ($p = 0.015$) than VMAT plans. All plans were normalized to have 95% of the PTV volume receive 95% of the prescription dose (47.5 Gy) therefore; no statistically significant difference was expected or seen for $\overline{D}_{95\%}$ and $\overline{V}_{95\%}$ between all techniques. No significant difference was shown for $\overline{V}_{107\%}$ for any VMAT technique. However, BECT+VMAT had 13.7% of the PTV volume receive over 107% of the prescription dose ($p < 0.001$). The VMAT techniques showed good conformity of the dose to the PTV with no significant difference seen between them ($p > 0.05$). BECT+VMAT was less conformal than VMAT ($p = 0.001$). Dose homogeneity was similar for all VMAT techniques with no statistically significant difference ($p > 0.05$). Again, BECT+VMAT exhibited less dose homogeneity than VMAT ($p < 0.001$). Mean tumor control probability was 98.6±1.6% for VMAT, 98.7±1.4% for FFFVMAT6x, 99.5±0.7% for FFFVMAT10x, and 99.7±0.1% for BECT+VMAT with no statistical difference between each technique and VMAT ($p > 0.05$).

3.2.2 Lungs

Tables 3.11 – 3.14 list the dosimetric and radiobiological metrics used to evaluate the lungs for VMAT, FFFVMAT6x, FFFVMAT10x, and BECT+VMAT treatment plans. No difference is seen for the mean dose for each technique compared to VMAT. All techniques had statistically significant higher maximum lung dose as compared to VMAT ($p < 0.05$). The volume of lungs receiving at least 5 Gy was significantly higher for both FFFVMAT (6x and 10x) techniques compared to VMAT. However, BECT+VMAT showed nearly 10% reduction in volume of lungs receiving at least 5 Gy ($p = 0.001$). The volume of lungs receiving at least 10 Gy was statistically insignificant for any technique over VMAT. The high dose region of lungs, volume of lungs receiving at least 20 Gy, was significantly higher for all techniques compared to VMAT ($p < 0.05$) but still under the 20% requirement of the plan acceptance criteria. No statistically significant difference was seen for any technique over VMAT for $\overline{NTCP}$ and $\overline{SCCP}$ for the lungs.

3.2.3 Heart

Tables 3.15 – 3.18 list the dosimetric and radiobiological metrics used to evaluate the heart for VMAT, FFFVMAT6x, FFFVMAT10x, and BECT+VMAT treatment plans. BECT+VMAT showed a 1.3 Gy reduction in mean dose to the heart compared to VMAT with values of 7.7±1.4 Gy and 9.0±1.5 Gy, respectively. However, no statistically significant difference was determined between the two ($p = 0.063$). In addition, FFFVMAT6x had a significantly higher mean lung dose over VMAT ($p = 0.017$) while no significant difference was seen between FFFVMAT10x and VMAT ($p = 0.062$). There was no statistically significant difference between any technique and VMAT for the maximum heart dose. The volume of heart receiving at least 5 Gy was significantly lower, over 10%, for BECT+VMAT over VMAT ($p = 0.032$). There was no significant difference between any FFFVMAT technique compared to VMAT for the volume of heart receiving at least 5 Gy ($p > 0.05$). Furthermore, no statistically significant difference was seen between any technique and VMAT for the volume of heart receiving at least 10 Gy. It was shown that both FFFVMAT6x and FFFVMAT10x had increased volume of heart receiving at least 22.5 Gy over VMAT. The volume of heart receiving at least 22.5 Gy was decreased for BECT+VMAT. It was also shown that both FFFVMAT6x and FFFVMAT10x had increased volume of heart receiving at least 30 Gy over VMAT and the volume of heart receiving at least 30 Gy was decreased for BECT+VMAT. The patient averaged predicted risk of cardiac mortality ($\overline{NTCP}$) for the whole heart was statistically significantly higher for FFFVMAT6x ($p = 0.013$) and was statistically significantly lower for BECT+VMAT ($p = 0.047$). The whole heart $\overline{NTCP}$ was determined to be 0.72±0.56% for VMAT, 0.94±0.58% for FFFVMAT6x ($p = 0.013$), 0.92±0.55% for FFFVMAT10x ($p = 0.114$), and 0.28±0.28% for BECT+VMAT ($p = 0.047$). Furthermore, the patient averaged predicted risk of cardiac mortality ($\overline{NTCP}$) for the myocardium was statistically significantly higher for FFFVMAT6x ($p = 0.011$) and no statistically significant difference was determined for either FFFVMAT10x ($p = 0.099$) or BECT+VMAT ($p = 0.054$) over VMAT. The myocardium $\overline{NTCP}$ was determined to be 1.14±0.91% for VMAT, 1.49±1.00% for FFFVMAT6x ($p = 0.011$), 1.45±0.96% for FFFVMAT10x ($p = 0.099$), and 0.43±0.42% for BECT+VMAT ($p = 0.054$).

3.2.4 Contralateral Breast

Tables 3.19 and 3.20 list the dosimetric and radiobiological metrics used to evaluate the contralateral breast for VMAT, FFFVMAT6x, FFFVMAT10x, and BECT+VMAT treatment plans. No statistically significance was seen between FFFVMAT10x and VMAT for the mean dose to the contralateral breast ($p = 0.781$). There was a statistically significant decrease in mean dose to the contralateral breast between FFFVMAT6x and VMAT ($p = 0.025$) as well as with BECT+VMAT and VMAT ($p < 0.001$). The mean dose was reduced by 1.8 Gy for BECT+VMAT over VMAT. There was no statistically significant difference seen for the maximum dose to the contralateral breast between any technique and VMAT. In addition, the volume of contralateral breast receiving at least 5 Gy was statistically significantly reduced for FFFVMAT6x and VMAT ($p = 0.032$) as well as with BECT+VMAT and VMAT ($p = 0.001$) with values of 22.6±12.4% for VMAT, 15.4±8.5% for FFFVMAT6x, and 4.3±2.7% for BECT+VMAT. No significant difference was seen between VMAT and FFFVMAT10x ($p = 0.925$). The same trend was observed for the patient averaged SCCP for the contralateral breast with statistically significant reduction for FFFVMAT6x and VMAT ($p = 0.026$) as well as with BECT+VMAT and VMAT ($p < 0.001$) with values of 3.03±0.88% for VMAT, 2.55±0.63% for FFFVMAT6x, and 1.50±0.50% for BECT+VMAT. No significant difference was seen between VMAT and FFFVMAT10x ($p = 0.737$).

3.2.5 Skin

Tables 3.21 and 3.22 list the dose volume metrics used to evaluate the skin (5 mm shell) for each patient. No statistically significant difference for the mean skin dose was seen between any FFFVMAT plans compared to VMAT ($p > 0.05$). The hotspots seen in the BECT+VMAT plans show a statistically significant increase in mean skin dose over VMAT ($p < 0.001$). There was no statistically significant difference in the maximum skin dose between FFFVMAT6x and VMAT ($p = 0.724$). However, a statistically significant reduction in the maximum skin dose was seen with FFFVMAT10x ($p = 0.039$). A statistically significant increase in maximum skin dose with BECT+VMAT as compared to VMAT ($p < 0.001$) was seen with values of 53.3±0.7 Gy for VMAT and 59.3±2.1 Gy for BECT+VMAT. There was

no statistically significant difference in minimum skin dose for any technique compared to VMAT. No statistically significant difference was shown for $\overline{TV-V}_{110\%}$ between the VMAT techniques. Again, BECT+VMAT had higher $\overline{TV-V}_{110\%}$ than VMAT ($p < 0.001$). Fortunately, All techniques for this patient had $\overline{TV-V}_{110\%}$ less than 5.13% so the patient does not show an increased risk of moist desquamation of the skin.

3.2.6 Treatment Time and Total Number of Monitor Units

Table 3.23 lists the treatment times for VMAT, FFFVMAT6x, and FFFVMAT10x treatment plans. No statistical significance was observed between FFFVMAT6x and VMAT or between FFFVMAT10x and VMAT for deliveries of Arc 1. FFFVMAT6x ($p < 0.001$) and FFFVMAT10x ($p < 0.001$) showed a statistically significant reduction in delivery time of Arc 2 over VMAT with mean times of 49±1 seconds for FFFVMAT6x, 47±1 seconds for FFFVMAT10x, and 61±1 seconds for VMAT. In addition, FFFVMAT6x ($p = 0.001$) and FFFVMAT10x ($p = 0.004$) showed a statistically significant reduction in mean delivery of total treatment time over VMAT with times of 2 min 20 seconds ±1 seconds for FFFVMAT6x, 2 min 18 seconds ±7 seconds for FFFVMAT10x, and 2 min 36 seconds ±5 seconds for VMAT.

Table 3.24 lists the total number of monitor units (MU) reported by the TPS for VMAT, FFFVMAT6x, and FFFVMAT10x treatment plans. The monitor units were recorded for Arc 1, Arc 2, and total number of monitor units. Total number of monitor units is the sum of both arcs. Increased monitor units represent a more modulated beam delivery and results in a more complex treatment plan. Both FFFVMAT6x ($p < 0.001$) and FFFVMAT10x ($p < 0.001$) had a statistically significant increase in mean monitor units for Arc 1 and Arc 2 compared to VMAT. In addition, Both FFFVMAT6x ($p < 0.001$) and FFFVMAT10x ($p < 0.001$) had a statistically significant increase in mean total MU compared to VMAT with values of 468±33.7 MU for VMAT, 648.5±60.7 MU for FFFVMAT6x, and 727.7±58.7 for FFFVMAT10x.

Table 3.7 Selected PTV evaluation metrics for VMAT, FFFVMAT6x, FFFVMAT10x, and BECT+VMAT. Abbreviations: D_{max} = maximum dose; D_{min} = minimum dose; FFFVMAT6x p-value = VMAT vs. FFFVMAT6x; FFFVMAT10x p-value = VMAT vs. FFFVMAT10x; BECT+VMAT p-value = VMAT vs. BECT+VMAT.

Patient	D_{max} [Gy]				D_{min} [Gy]			
	VMAT	FFFVMAT6x	FFFVMAT10x	BECT+VMAT	VMAT	FFFVMAT6x	FFFVMAT10x	BECT+VMAT
1	54.3	53.0	52.7	65.0	11.7	12.0	11.7	15.6
2	53.2	52.7	52.9	59.0	18.5	20.7	22.8	29.7
3	53.3	52.9	53.1	60.2	22.8	26.4	26.3	31.5
4	54.3	56.0	54.4	59.4	24.2	23.8	24.5	35.9
5	54.3	53.2	53.5	62.8	16.7	22.6	23.2	21.9
6	53.1	54.2	52.7	62.7	29.7	28.5	30.3	29.2
7	53.0	52.4	53.6	60.3	28.1	29.2	28.8	23.4
8	52.7	52.9	52.8	60.6	22.1	22.0	21.8	25.0
9	52.9	52.6	53.6	60.2	13.9	11.3	13.8	25.8
10	52.8	53.2	52.9	-	18.6	16.7	16.5	-
Mean	53.4	53.3	53.2	61.1	20.6	21.3	22.0	26.4
σ	0.7	1.1	0.5	1.9	5.8	6.3	6.2	6.0
p-value	FFFVMAT6x	FFFVMAT10x	BECT+VMAT		FFFVMAT6x	FFFVMAT10x	BECT+VMAT	
	0.787	0.433	<0.001		0.418	0.134	0.015	

Table 3.8 Selected PTV evaluation metrics for VMAT, FFFVMAT6x, FFFVMAT10x, and BECT+VMAT. Abbreviations: $D_{95\%}$ = dose that 95% of the volume receives; $V_{95\%}$ = volume that receives 95% of the prescription dose; NS = no statistical significance.

Patient	$D_{95\%}$ [Gy]				$V_{95\%}$ [%]			
	VMAT	FFFVMAT6x	FFFVMAT10x	BECT+VMAT	VMAT	FFFVMAT6x	FFFVMAT10x	BECT+VMAT
1	47.4	47.4	47.5	47.4	94.9	94.8	95.1	94.8
2	47.6	47.5	47.4	47.4	95.3	95.0	94.4	94.7
3	47.4	47.6	47.5	47.6	94.7	95.3	95.1	95.2
4	47.6	47.6	47.6	47.4	95.3	95.2	95.2	94.8
5	47.4	47.6	47.6	47.4	94.6	95.2	95.3	94.9
6	47.5	47.4	47.5	47.5	94.8	94.8	95.0	95.0
7	47.6	47.6	47.4	47.4	95.2	95.2	94.5	94.8
8	47.5	47.4	47.5	47.5	95.1	94.8	94.8	94.9
9	47.5	47.5	47.6	47.5	95.0	95.0	95.3	95.0
10	47.6	47.6	47.4	-	95.2	95.2	94.8	-
Mean	47.5	47.5	47.5	47.5	95.0	95.1	94.9	94.9
σ	0.1	0.1	0.1	0.1	0.2	0.2	0.3	0.1
p-value	FFFVMAT6x	FFFVMAT10x	BECT+VMAT		FFFVMAT6x	FFFVMAT10x	BECT+VMAT	
	NS	NS	NS		NS	NS	NS	

Table 3.9 Selected PTV evaluation metrics for VMAT, FFFVMAT6x, FFFVMAT10x, and BECT+VMAT. Abbreviations: $V_{107\%}$ = volume that receives 107% of the prescription dose; CI = conformity index.

Patient	$V_{107\%}$ [%]				CI [Ideal=1]			
	VMAT	FFFVMAT6x	FFFVMAT10x	BECT+VMAT	VMAT	FFFVMAT6x	FFFVMAT10x	BECT+VMAT
1	0.16	0.00	0.00	11.10	0.68	0.71	0.71	0.65
2	0.00	0.00	0.00	30.45	0.73	0.71	0.76	0.51
3	0.00	0.00	0.00	12.74	0.65	0.64	0.66	0.57
4	0.02	0.26	0.02	4.56	0.72	0.67	0.68	0.55
5	0.05	0.00	0.00	13.20	0.67	0.68	0.73	0.73
6	0.00	0.01	0.00	18.00	0.67	0.68	0.70	0.55
7	0.00	0.00	0.00	11.68	0.77	0.73	0.75	0.63
8	0.00	0.00	0.00	7.09	0.68	0.63	0.65	0.53
9	0.00	0.00	0.00	14.54	0.69	0.67	0.67	0.62
10	0.00	0.00	0.00	-	0.82	0.78	0.81	-
Mean	0.02	0.03	0.00	13.71	0.71	0.69	0.71	0.59
σ	0.1	0.1	0.0	7.4	0.05	0.04	0.05	0.07
p-value	FFFVMAT6x	FFFVMAT10x	BECT+VMAT		FFFVMAT6x	FFFVMAT10x	BECT+VMAT	
	1.000	0.193	<0.001		0.071	0.708	0.001	

Table 3.10 Selected PTV evaluation metrics for VMAT, FFFVMAT6x, FFFVMAT10x, and BECT+VMAT. Abbreviations: DHI = dose homogeneity index; TCP = tumor control probability.

Patient	DHI [Ideal=0]				TCP [%]			
	VMAT	FFFVMAT6x	FFFVMAT10x	BECT+VMAT	VMAT	FFFVMAT6x	FFFVMAT10x	BECT+VMAT
1	0.16	0.13	0.14	0.23	97.6	97.6	99.7	99.6
2	0.13	0.13	0.10	0.21	97.5	97.5	99.8	99.8
3	0.13	0.13	0.12	0.24	99.8	99.8	99.8	99.9
4	0.12	0.13	0.13	0.17	99.6	99.5	99.6	99.8
5	0.15	0.12	0.12	0.22	94.8	99.6	99.7	99.5
6	0.13	0.13	0.12	0.23	99.7	99.8	99.8	99.6
7	0.10	0.11	0.12	0.20	99.7	99.7	99.7	99.8
8	0.12	0.13	0.11	0.20	99.8	99.8	99.8	99.9
9	0.10	0.12	0.12	0.22	99.4	98.2	99.3	99.7
10	0.13	0.16	0.15	-	98.3	95.6	97.7	-
Mean	0.12	0.13	0.12	0.21	98.6	98.7	99.5	99.7
σ	0.02	0.01	0.02	0.02	1.6	1.4	0.7	0.1
p-value	FFFVMAT6x	FFFVMAT10x	BECT+VMAT		FFFVMAT6x	FFFVMAT10x	BECT+VMAT	
	0.751	0.545	<0.001		0.883	0.144	0.060	

Table 3.11 Selected lung evaluation metrics for VMAT, FFFVMAT6x, FFFVMAT10x, and BECT+VMAT. Abbreviations: D_{mean} = mean dose; D_{max} = maximum dose; NS = no statistical significance; FFFVMAT6x p-value = VMAT vs. FFFVMAT6x; FFFVMAT10x p-value = VMAT vs. FFFVMAT10x; BECT+VMAT p-value = VMAT vs. BECT+VMAT.

Patient	D_{mean} [Gy]				D_{max} [Gy]			
	VMAT	FFFVMAT6x	FFFVMAT10x	BECT+VMAT	VMAT	FFFVMAT6x	FFFVMAT10x	BECT+VMAT
1	8.7	9.0	9.3	8.3	49.9	52.5	49.5	51.2
2	8.5	9.0	8.8	6.6	48.5	50.5	49.0	50.5
3	8.8	10.2	10.3	8.6	51.2	50.7	52.2	52.6
4	9.2	10.2	9.5	7.5	47.4	52.2	51.0	49.3
5	8.4	9.6	9.2	8.3	49.6	52.6	51.7	53.6
6	9.9	10.8	10.5	9.3	51.2	52.6	51.3	54.7
7	8.6	9.0	9.1	9.5	47.0	47.8	49.5	54.3
8	8.0	8.3	8.7	9.4	50.0	51.3	50.4	53.2
9	8.0	8.2	8.5	8.6	46.3	49.9	49.7	51.2
10	8.9	9.0	9.9	-	51.0	52.0	51.5	-
Mean	8.7	9.3	9.4	8.5	49.2	51.2	50.6	52.3
σ	0.6	0.9	0.7	0.9	1.8	1.5	1.1	1.8
p-value	FFFVMAT6x	FFFVMAT10x	BECT+VMAT		FFFVMAT6x	FFFVMAT10x	BECT+VMAT	
	NS	NS	NS		0.003	0.014	0.001	

Table 3.12 Selected lung evaluation metrics for VMAT, FFFVMAT6x, FFFVMAT10x, and BECT+VMAT. Abbreviations: V_{5Gy} = volume that receives at least 5 Gy; V_{10Gy} = volume that receives at least 10 Gy; NS = no statistical significance.

Patient	V_{5Gy} [%]				V_{10Gy} [%]			
	VMAT	FFFVMAT6x	FFFVMAT10x	BECT+VMAT	VMAT	FFFVMAT6x	FFFVMAT10x	BECT+VMAT
1	41.4	48.1	45.1	32.4	23.5	23.2	23.8	23.3
2	41.3	42.2	43.9	30.4	22.7	23.1	22.9	19.4
3	41.7	51.7	57.3	38.3	22.9	27.8	26.6	23.3
4	50.6	51.6	46.8	33.5	29.5	28.0	29.7	20.5
5	41.3	42.1	43.3	36.5	22.7	25.8	24.8	22.5
6	54.7	58.5	59.9	34.9	26.7	32.0	29.9	23.2
7	47.7	51.9	55.1	38.2	25.3	27.1	27.3	25.1
8	39.1	42.6	41.6	32.2	22.1	22.5	23.1	26.3
9	37.4	34.9	38.7	31.3	23.4	23.5	23.5	23.1
10	39.9	39.1	45.2	-	25.7	24.7	28.1	-
Mean	43.5	46.3	47.7	34.2	24.5	25.8	26.0	22.9
σ	5.6	7.2	7.2	2.9	2.3	3.0	2.7	2.1
p-value	FFFVMAT6x	FFFVMAT10x	BECT+VMAT		FFFVMAT6x	FFFVMAT10x	BECT+VMAT	
	0.042	0.027	0.001		NS	NS	NS	

Table 3.13 Selected lung evaluation metrics for VMAT, FFFVMAT6x, FFFVMAT10x, and BECT+VMAT. Abbreviations: V_{20Gy} = volume that receives at least 20 Gy; NTCP = normal tissue complication probability; NS = no statistical significance.

Patient	V_{20Gy} [%]				NTCP [%]			
	VMAT	FFFVMAT6x	FFFVMAT10x	BECT+VMAT	VMAT	FFFVMAT6x	FFFVMAT10x	BECT+VMAT
1	13.4	12.6	13.6	15.6	2.73	2.87	3.03	2.58
2	13.5	14.0	13.6	11.6	2.66	2.94	2.79	1.80
3	13.1	15.1	15.1	15.0	2.81	3.65	3.70	2.71
4	14.1	16.8	15.8	11.8	3.02	3.68	3.26	2.17
5	13.3	15.0	14.7	14.8	2.59	3.32	3.10	2.56
6	14.3	15.0	14.7	16.7	3.43	4.10	3.87	3.15
7	11.0	11.5	11.6	17.2	2.65	2.87	2.95	3.28
8	12.4	12.6	14.2	19.7	2.38	2.52	2.75	3.20
9	12.1	13.0	13.0	17.0	2.38	2.51	2.63	2.80
10	15.0	15.5	16.2	-	2.91	2.98	3.47	-
Mean	13.2	14.1	14.3	15.5	2.76	3.14	3.16	2.69
σ	1.2	1.6	1.4	2.6	0.3	0.5	0.4	0.5
p-value	FFFVMAT6x	FFFVMAT10x	BECT+VMAT		FFFVMAT6x	FFFVMAT10x	BECT+VMAT	
	0.020	0.001	0.023		NS	NS	NS	

Table 3.14 Selected lung evaluation metrics for VMAT, FFFVMAT6x, FFFVMAT10x, and BECT+VMAT. Abbreviations: SCCP = second cancer complication probability; NS = no statistical significance.

Patient	SCCP [%]			
	VMAT	FFFVMAT6x	FFFVMAT10x	BECT+VMAT
1	14.92	15.29	15.74	14.39
2	14.65	15.47	15.03	11.51
3	15.11	17.35	17.45	14.80
4	15.73	17.40	16.35	13.00
5	14.43	16.50	15.93	14.31
6	16.81	18.37	17.85	16.03
7	14.64	15.31	15.55	16.39
8	13.75	14.19	14.93	16.16
9	13.74	14.16	14.55	15.05
10	15.39	15.57	16.89	-
Mean	14.92	15.96	16.03	14.63
σ	0.9	1.4	1.1	1.6
p-value	FFFVMAT6x	FFFVMAT10x	BECT+VMAT	
	NS	NS	NS	

Table 3.15 Selected heart evaluation metrics for VMAT, FFFVMAT6x, FFFVMAT10x, and BECT+VMAT. Abbreviations: D_{mean} = mean dose; D_{max} = maximum dose; NS = no statistical significance; FFFVMAT6x p-value = VMAT vs. FFFVMAT6x; FFFVMAT10x p-value = VMAT vs. FFFVMAT10x; BECT+VMAT p-value = VMAT vs. BECT+VMAT.

Patient	D_{mean} [Gy]				D_{max} [Gy]			
	VMAT	FFFVMAT6x	FFFVMAT10x	BECT+VMAT	VMAT	FFFVMAT6x	FFFVMAT10x	BECT+VMAT
1	9.0	10.5	10.6	8.1	43.0	45.0	44.3	39.5
2	10.2	11.2	10.8	6.2	41.3	44.6	45.2	36.9
3	7.0	9.4	9.6	7.9	40.2	43.4	43.9	40.5
4	9.2	9.7	9.5	6.7	38.4	45.2	41.4	34.5
5	10.0	12.0	11.8	6.6	47.5	48.6	48.0	36.9
6	10.9	12.6	10.5	10.1	49.1	49.8	45.8	44.3
7	9.4	9.6	9.0	9.6	43.6	43.0	45.3	46.9
8	9.3	9.3	10.0	6.7	43.4	44.7	45.8	43.9
9	9.2	9.3	9.2	6.9	39.0	43.2	44.7	40.3
10	5.8	5.3	5.7	-	31.7	38.3	39.3	-
Mean	9.0	9.9	9.7	7.7	41.7	44.6	44.4	40.4
σ	1.5	2.0	1.6	1.4	4.9	3.2	2.4	4.0
p-value	FFFVMAT6x	FFFVMAT10x	BECT+VMAT		FFFVMAT6x	FFFVMAT10x	BECT+VMAT	
	0.017	0.062	0.063		NS	NS	NS	

Table 3.16 Selected heart evaluation metrics for VMAT, FFFVMAT6x, FFFVMAT10x, and BECT+VMAT. Abbreviations: V_{5Gy} = volume that receives at least 5 Gy; V_{10Gy} = volume that receives at least 10 Gy; NS = no statistical significance.

Patient	V_{5Gy} [%]				V_{10Gy} [%]			
	VMAT	FFFVMAT6x	FFFVMAT10x	BECT+VMAT	VMAT	FFFVMAT6x	FFFVMAT10x	BECT+VMAT
1	56.4	72.5	72.1	50.1	25.8	31.3	30.5	27.0
2	82.8	86.0	79.6	40.2	25.1	28.2	29.8	16.0
3	43.3	69.6	69.9	54.3	15.6	23.9	30.2	26.1
4	59.8	65.6	59.4	48.4	29.4	27.7	31.0	16.5
5	64.9	79.4	75.6	49.9	24.9	33.6	35.2	17.3
6	85.2	93.4	80.8	69.8	29.2	45.7	30.7	32.0
7	68.6	65.2	63.5	68.2	26.7	29.0	24.5	27.7
8	67.6	65.7	69.9	41.1	26.6	26.8	27.1	19.5
9	73.3	64.0	60.1	45.0	24.1	22.5	23.2	17.7
10	51.1	42.3	44.8	-	10.7	7.7	10.9	-
Mean	65.3	70.4	67.6	51.9	23.8	27.6	27.3	22.2
σ	13.2	14.0	10.9	10.7	6.0	9.5	6.7	6.0
p-value	FFFVMAT6x	FFFVMAT10x	BECT+VMAT		FFFVMAT6x	FFFVMAT10x	BECT+VMAT	
	0.197	0.564	0.032		NS	NS	NS	

Table 3.17 Selected heart evaluation metrics for VMAT, FFFVMAT6x, FFFVMAT10x, and BECT+VMAT. Abbreviations: $V_{22.5Gy}$ = volume that receives at least 22.5 Gy; V_{30Gy} = volume that receives at least 30 Gy.

Patient	$V_{22.5Gy}$ [%]				V_{30Gy} [%]			
	VMAT	FFFVMAT6x	FFFVMAT10x	BECT+VMAT	VMAT	FFFVMAT6x	FFFVMAT10x	BECT+VMAT
1	9.7	11.9	12.7	6.4	5.1	6.6	7.8	0.9
2	11.0	12.8	12.5	3.5	7.2	8.1	7.4	0.5
3	5.5	10.0	8.7	5.9	1.9	5.5	3.4	1.4
4	9.2	11.3	11.2	1.5	1.8	4.5	3.4	0.0
5	12.2	14.6	14.1	3.3	9.1	10.9	10.5	0.2
6	11.5	12.1	10.7	10.8	7.8	7.3	6.2	4.4
7	8.7	10.1	9.0	10.3	3.8	4.3	4.0	5.1
8	10.1	9.8	11.6	4.8	4.6	5.4	6.6	1.6
9	9.9	11.0	11.4	3.1	3.8	5.7	6.8	0.6
10	0.2	0.8	1.0	-	0.0	0.2	0.2	-
Mean	8.8	10.4	10.3	5.5	4.5	5.9	5.6	1.6
σ	3.5	3.7	3.6	3.2	2.9	2.8	2.9	1.8
p-value	FFFVMAT6x	FFFVMAT10x	BECT+VMAT		FFFVMAT6x	FFFVMAT10x	BECT+VMAT	
	0.003	0.003	0.050		0.007	0.031	0.032	

Table 3.18 Selected heart evaluation metrics for VMAT, FFFVMAT6x, FFFVMAT10x, and BECT+VMAT. Abbreviations: NTCP = normal tissue complication probability.

Patient	Whole Heart NTCP [%]				Myocardium NTCP [%]			
	VMAT	FFFVMAT6x	FFFVMAT10x	BECT+VMAT	VMAT	FFFVMAT6x	FFFVMAT10x	BECT+VMAT
1	0.65	1.02	1.30	0.19	1.04	1.61	2.03	0.32
2	1.00	1.23	1.11	0.10	1.49	1.84	1.66	0.15
3	0.26	0.75	0.50	0.23	0.36	1.08	0.72	0.33
4	0.31	0.61	0.50	0.03	0.57	1.11	0.87	0.07
5	1.69	2.20	2.05	0.08	2.97	3.84	3.62	0.16
6	1.60	1.40	0.98	0.67	2.37	2.10	1.47	1.04
7	0.54	0.58	0.59	0.83	0.80	0.88	0.86	1.23
8	0.64	0.78	1.01	0.24	1.01	1.21	1.60	0.37
9	0.48	0.77	1.08	0.11	0.75	1.19	1.65	0.17
10	0.01	0.03	0.04	-	0.01	0.03	0.04	-
Mean	0.72	0.94	0.92	0.28	1.14	1.49	1.45	0.43
σ	0.56	0.58	0.55	0.28	0.91	1.00	0.96	0.42
p-value	FFFVMAT6x	FFFVMAT10x	BECT+VMAT		FFFVMAT6x	FFFVMAT10x	BECT+VMAT	
	0.013	0.114	0.047		0.011	0.099	0.054	

Table 3.19 Selected contralateral breast evaluation metrics for VMAT, FFFVMAT6x, FFFVMAT10x, and BECT+VMAT. Abbreviations: D_{mean} = mean dose; D_{max} = maximum dose; NS = no statistical significance; FFFVMAT6x p-value = VMAT vs. FFFVMAT6x; FFFVMAT10x p-value = VMAT vs. FFFVMAT10x; BECT+VMAT p-value = VMAT vs. BECT+VMAT.

Patient	D_{mean} [Gy]				D_{max} [Gy]			
	VMAT	FFFVMAT6x	FFFVMAT10x	BECT+VMAT	VMAT	FFFVMAT6x	FFFVMAT10x	BECT+VMAT
1	3.8	3.5	3.8	1.5	18.7	22.7	23.8	18.4
2	2.7	2.5	3.8	1.1	24.4	19.6	26.5	26.3
3	5.8	4.1	4.5	1.9	32.2	26.7	29.0	34.0
4	4.2	4.0	3.1	2.1	19.7	18.4	15.7	30.1
5	2.4	1.8	2.5	1.2	21.5	22.5	20.6	21.7
6	4.7	3.8	5.5	2.3	41.4	39.9	41.6	44.2
7	3.1	3.5	4.4	1.4	21.6	20.1	24.1	26.7
8	4.0	3.8	2.9	1.0	25.7	27.1	23.1	20.6
9	4.9	2.8	3.4	2.5	38.9	31.7	34.7	43.4
10	2.6	2.3	3.4	-	16.5	13.4	16.6	-
Mean	3.8	3.2	3.7	1.7	26.1	24.2	25.6	29.5
σ	1.1	0.8	0.9	0.6	8.6	7.5	7.9	9.4
p-value	FFFVMAT6x		FFFVMAT10x	BECT+VMAT	FFFVMAT6x		FFFVMAT10x	BECT+VMAT
	0.025		0.781	<0.001	NS		NS	NS

Table 3.20 Selected contralateral breast evaluation metrics for VMAT, FFFVMAT6x, FFFVMAT10x, and BECT+VMAT. Abbreviations: V_{5Gy} = volume that receives at least 5 Gy; SCCP = second cancer complication probability.

Patient	V_{5Gy} [%]				SCCP [%]			
	VMAT	FFFVMAT6x	FFFVMAT10x	BECT+VMAT	VMAT	FFFVMAT6x	FFFVMAT10x	BECT+VMAT
1	22.6	19.3	23.4	3.2	2.99	2.73	2.96	1.27
2	9.3	6.8	21.1	2.3	2.13	1.96	3.00	1.05
3	45.1	26.3	32.5	4.4	4.57	3.25	3.55	1.63
4	19.4	19.1	17.0	7.5	3.24	3.10	2.41	1.87
5	11.2	3.7	6.8	1.2	1.92	1.47	1.93	1.09
6	24.8	21.8	46.8	7.2	3.74	3.10	4.33	2.12
7	17.3	18.0	27.3	3.3	2.47	2.71	3.43	1.32
8	27.8	24.0	12.0	1.3	3.22	3.05	2.32	0.88
9	40.3	12.5	23.2	8.2	3.92	2.34	2.76	2.28
10	8.5	2.4	12.3	-	2.06	1.79	2.66	-
Mean	22.6	15.4	22.2	4.3	3.03	2.55	2.94	1.50
σ	12.4	8.5	11.6	2.7	0.88	0.63	0.69	0.50
p-value	FFFVMAT6x		FFFVMAT10x	BECT+VMAT	FFFVMAT6x		FFFVMAT10x	BECT+VMAT
	0.032		0.925	0.001	0.026		0.737	<0.001

Table 3.21 Selected skin (5mm shell) evaluation metrics for VMAT, FFFVMAT6x, FFFVMAT10x, and BECT+VMAT. Abbreviations: D_{mean} = mean dose; D_{max} = maximum dose; FFFVMAT6x p-value = VMAT vs. FFFVMAT6x; FFFVMAT10x p-value = VMAT vs. FFFVMAT10x; BECT+VMAT p-value = VMAT vs. BECT+VMAT.

Patient	D_{mean} [Gy]				D_{max} [Gy]			
	VMAT	FFFVMAT6x	FFFVMAT10x	BECT+VMAT	VMAT	FFFVMAT6x	FFFVMAT10x	BECT+VMAT
1	49.2	48.9	48.7	49.7	54.2	52.7	52.7	63.4
2	48.8	48.6	48.0	50.6	53.2	52.5	52.3	58.0
3	49.0	49.0	48.9	50.3	52.9	52.9	52.5	57.1
4	49.8	49.5	49.2	50.5	54.6	56.0	53.4	58.1
5	49.9	49.6	49.2	50.3	53.5	52.9	53.4	60.3
6	49.3	49.6	49.2	51.0	53.1	54.2	52.7	59.9
7	49.2	49.3	49.1	50.6	52.9	52.3	52.8	60.3
8	49.3	49.8	49.4	50.7	52.6	52.8	52.4	56.5
9	49.2	49.1	49.4	50.4	52.9	52.3	53.3	60.2
10	49.3	49.4	49.6	-	52.8	53.2	52.6	-
Mean	49.3	49.3	49.1	50.5	53.3	53.2	52.8	59.3
σ	0.3	0.4	0.5	0.4	0.7	1.1	0.4	2.1
p-value	FFFVMAT6x	FFFVMAT10x	BECT+VMAT		FFFVMAT6x	FFFVMAT10x	BECT+VMAT	
	0.838	0.100	<0.001		0.724	0.039	<0.001	

Table 3.22 Selected skin (5mm shell) evaluation metrics for VMAT, FFFVMAT6x, FFFVMAT10x, and BECT+VMAT. Abbreviations: D_{min} = minimum dose; TV-$V_{110\%}$ = percent volume receiving 110% of the prescription dose within treated volume; NS = no statistical significance.

Patient	D_{min} [Gy]				TV-$V_{110\%}$ [%]			
	VMAT	FFFVMAT6x	FFFVMAT10x	BECT+VMAT	VMAT	FFFVMAT6x	FFFVMAT10x	BECT+VMAT
1	3.8	3.9	3.7	0.0	0.00	0.00	0.00	4.01
2	0.3	4.3	4.6	0.0	0.00	0.00	0.00	5.89
3	19.2	18.8	18.3	11.4	0.00	0.00	0.00	1.57
4	35.3	36.4	38.6	36.6	0.00	0.12	0.00	0.50
5	35.4	33.8	31.4	19.6	0.00	0.00	0.00	5.20
6	35.4	35.8	29.4	7.5	0.00	0.00	0.00	4.26
7	32.0	34.2	31.9	23.4	0.00	0.00	0.00	4.20
8	22.1	22.0	21.8	25.0	0.00	0.00	0.00	2.63
9	13.9	14.1	13.8	28.1	0.00	0.00	0.00	4.46
10	28.7	30.0	29.4	-	0.00	0.00	0.00	-
Mean	22.6	23.3	22.3	16.8	0.00	0.01	0.00	3.64
σ	13.1	12.7	12.0	12.8	0.0	0.0	0.0	1.7
p-value	FFFVMAT6x	FFFVMAT10x	BECT+VMAT		FFFVMAT6x	FFFVMAT10x	BECT+VMAT	
	NS	NS	NS		0.343	NA*	<0.001	
* both groups contain only 0's, therefore variance cannot be calculated								

Table 3.23 Treatment time for VMAT, FFFVMAT6x, and FFFVMAT10x. Abbreviations: FFFVMAT6x p-value = VMAT vs. FFFVMAT6x; FFFVMAT10x p-value = VMAT vs. FFFVMAT10x; NS = no statistical significance.

fx	Arc 1 [min:sec]			Arc 2 [min:sec]			Total Treatment [min:sec]		
	VMAT	FFF VMAT 6x	FFF VMAT 10x	VMAT	FFF VMAT 6x	FFF VMAT 10x	VMAT	FFF VMAT 6x	FFF VMAT 10x
1	0:57	0:55	0:51	1:01	0:50	0:47	2:43	2:20	2:12
2	0:56	0:54	0:49	1:00	0:48	0:47	2:35	2:18	2:13
3	0:56	0:53	0:57	1:01	0:50	0:48	2:34	2:21	2:24
4	0:56	0:54	0:57	1:01	0:49	0:47	2:33	2:21	2:24
Mean	0:56	0:54	0:54	1:01	0:49	0:47	2:36	2:20	2:18
σ	0:00	0:01	0:04	0:01	0:01	0:01	0:05	0:01	0:07
p-value	FFFVMAT 6x	FFFVMAT 10x		FFFVMAT 6x	FFFVMAT 10x		FFFVMAT 6x	FFFVMAT 10x	
	NS	NS		<0.001	<0.001		0.001	0.004	

Table 3.24 Total number of monitor units for VMAT, FFFVMAT6x, and FFFVMAT10x. Abbreviations: FFFVMAT6x p-value = VMAT vs. FFFVMAT6x; FFFVMAT10x p-value = VMAT vs. FFFVMAT10x.

Patient	Arc 1			Arc 2			Total		
	VMAT	FFF VMAT 6x	FFF VMAT 10x	VMAT	FFF VMAT 6x	FFF VMAT 10x	VMAT	FFF VMAT 6x	FFF VMAT 10x
1	240	371	484	231	355	259	471	726	743
2	243	404	473	198	295	326	441	699	799
3	324	404	399	178	266	307	502	670	706
4	198	328	438	275	316	367	473	644	805
5	195	231	397	229	366	352	424	597	749
6	282	355	336	246	339	399	528	694	735
7	262	381	390	229	265	367	491	646	757
8	210	394	370	267	301	299	477	695	669
9	199	276	276	254	297	428	453	573	704
10	235	302	307	189	239	303	424	541	610
Mean	238.8	344.6	387	229.6	303.9	340.7	468.4	648.5	727.7
σ	41.8	59.0	67.7	32.7	41.0	51.3	33.7	60.7	58.7
p-value	FFFVMAT 6x	FFFVMAT 10x		FFFVMAT 6x	FFFVMAT 10x		FFFVMAT 6x	FFFVMAT 10x	
	<0.001	<0.001		<0.001	<0.001		<0.001	<0.001	

Chapter 4 Discussion

This study compared four advanced radiotherapy techniques for treating post-mastectomy breast cancer patients. VMAT, FFFVMAT6x, FFFVMAT10x, and BECT+VMAT plans were created retrospectively for ten left-sided post-mastectomy patients. The major goal of this study was to determine if BECT+VMAT and FFFVMAT (6x and 10x) can maintain equal or better dose coverage of the PTV than VMAT while reducing doses to OARs. In addition, it was important to predict the SCCP and NTCP associated with each technique and determine if any statistically significant difference can be ascertained between the techniques as compared to VMAT. The hypothesis of this study was that for a selected group of post-mastectomy breast cancer patients, BECT+VMAT and FFFVMAT (6x and 10x) could maintain equal or better dose coverage than VMAT while statistically significantly lowering ($p < 0.05$) predicted risks of side effects to the lungs, heart, and contralateral breast. The results of this study support that BECT+VMAT and FFFVMAT6x and FFFVMAT10x treatment plans can maintain equal or better dose coverage than VMAT even though BECT+VMAT treatment plans consistently contained hot spots. However, both FFFVMAT (6x and 10x) plans showed little improvement in reducing predicted risk of side effects with the exception of FFFVMAT6x reducing the SCCP of the contralateral breast over VMAT. Both FFFVMAT6x and FFFVMAT10x were able to significantly reduce the total treatment time over VMAT. BECT+VMAT was able to reduce the risk of side effects with statistical significance for the whole heart and contralateral breast compared to VMAT.

The key results for the specific aims of this work are presented in sections 4.1 and 4.2. The implications and significance of the results, strengths and limitations of this work, and possible future work will be discussed in sections 4.3 - 4.5.

4.1 Outcomes of Specific Aim One

Specific aim one compared treatment plans and predicted risks of side effects between BECT+VMAT and VMAT plans. This was achieved by creating comprehensive dose reconstructions, calculating tumor control probability, determine normal tissue complication probability for the whole

heart, myocardium, lungs, and calculating the second cancer risks for contralateral breast and lungs. Statistical significance was established for each compared dosimetric and radiobiological endpoint. BECT+VMAT treatment plans were created for nine of the ten patients select for this study. All ten patients had VMAT plans created. Six of the nine patients planned with BECT+VMAT and four of the ten patients planned with VMAT did not meet the plan acceptance criteria for the PTV goal of $V_{95\%} \geq$ 95%. However, all of the BECT+VMAT and VMAT treatment plans were deemed clinically acceptable by a radiation oncologist. All nine BECT+VMAT and all ten VMAT patients met the plan acceptance criteria that $V_{20Gy} < 20\%$ for the lungs and $V_{22.5Gy} < 20\%$ for the heart.

BECT+VMAT showed, with statistical significance, less conformity and less dose homogeneity compared to VMAT. No statistically significant difference was exhibited for TCP between BECT+VMAT and VMAT. All of the BECT+VMAT patients achieved nearly 100% TCP and six of the ten VMAT patients achieved nearly 100% TCP. This was expected because all plans were normalized to have 95% PTV volume receive 95% of the prescription dose (47.5 Gy).

BECT+VMAT was able to reduce, with statistical significance, $\bar{V}_{5Gy}$ for the lungs over VMAT. On the other hand, BECT+VMAT showed with statistical significance higher $\bar{V}_{20Gy}$ than VMAT. Simply stated, BECT+VMAT is able to reduced low doses to the lungs but increases high doses to the lungs as compared to VMAT. This is probably due to dose spilling of the electron beam to the ipsilateral lung. Since the electron beam dose falls off quickly in the low dose area, the contralateral lung has reduced dose. van der Laan *et al.* (2010) studied ten left-sided PMRT patients using a combined electron and photon IMRT planning technique and they found comparable mean lung doses as seen in this study. No statistically significant difference was seen between BECT+VMAT and VMAT for $\overline{NTCP}$ of the lungs. $\overline{NTCP}$ of the lungs with radiation pneumonitis grade two or higher as an endpoint was concluded to have a mean probability of approximately 2.7% for both techniques. In addition, no statistically significant difference was seen between BECT+VMAT and VMAT for $\overline{SCCP}$ of the lungs. $\overline{SCCP}$ of the lungs was concluded to have a mean probability of approximately 14.3% for both techniques.

BECT+VMAT was unable to reduce the mean dose to the heart as compared to VMAT with statistical significance. In a study conducted by van der Laan *et al.* (2010) looking at patients using a combined electron and photon IMRT technique, similar mean heart doses were observed. However, BECT+VMAT was able to reduce, with statistical significance, $\bar{V}_{5\text{Gy}}$ and $\bar{V}_{30\text{Gy}}$ for the heart over VMAT. This resulted in a statistically significant reduction in $\overline{NTCP}$ of the whole heart for BECT+VMAT plans compared to VMAT. The patient averaged predicted risk of cardiac mortality ($\overline{NTCP}$) for the whole heart was determined to be 0.72±0.56% for VMAT and 0.28±0.28% for BECT+VMAT. Furthermore, the patient averaged predicted risk of cardiac mortality ($\overline{NTCP}$) for the myocardium was determined to be 1.14±0.91% for VMAT and 0.43±0.42% for BECT+VMAT.

Significant reduction in patient average mean dose and $\bar{V}_{5\text{Gy}}$ of the contralateral breast was observed for BECT+VMAT compared to VMAT. The mean contralateral breast dose was in agreement to a similar study conducted by van der Laan *et al.* (2010). In addition, BECT+VMAT was able to reduce the contralateral breast $\overline{SCCP}$ by over 50%. $\overline{SCCP}$ values were 3.03±0.88% for VMAT and 1.50±0.50% for BECT+VMAT.

Skin erythema is expected for post-mastectomy chest wall patients since the skin is included in the PTV. Dose to the skin should be as close to prescription dose (50 Gy) as possible to sterilize any microscopic disease still present. Mean dose to the skin (5 mm shell) was statistically significantly higher (50.5 Gy) and just over prescription dose (50 Gy) for BECT+VMAT and was slightly lower (49.3 Gy) than the prescription dose for VMAT. Moist desquamation is also a concern with radiotherapy techniques for breast cancer and post-mastectomy patients. Perkins *et al.* (2001) studied a single PMRT patient who underwent a BECT technique and determined the patient had brisk erythema and moist desquamation but was able to complete treatment without interruption. Chen *et al.* (2010) has shown that TV-$V_{110\%}$ > 5.13% is an indicator of radiation induced skin toxicity that results in moist desquamation. $\overline{TV - V}_{110\%}$ for BECT+VMAT was significantly higher than VMAT but both techniques had mean values less than 5.13% so the patients did not show an increased risk of moist desquamation of the skin.

In summary, BECT+VMAT achieved comparable dose coverage of the PTV as compared to VMAT. In addition, BECT+VMAT significantly lowered risks for whole heart and contralateral breast compared to VMAT. However, BECT+VMAT showed comparable risks for the lungs and myocardium compared to VMAT. Patients with prior or current cardiopulmonary complications or those at an increased risk of cardiovascular disease may benefit from BECT+VMAT. Also, young women with an increased risk of radiation-induced cancer of the contralateral breast may benefit from BECT+VMAT.

4.2 Outcomes of Specific Aim Two

Specific aim two compared treatment plans and predicted risks of side effects between FFFVMAT (6x and 10x) and VMAT plans. This was achieved by creating comprehensive dose reconstructions, calculating tumor control probability, determine normal tissue complication probability for the whole heart, myocardium, lungs, and calculating the second cancer risks for contralateral breast and lungs. Statistical significance was established for each compared dosimetric and radiobiological endpoint. Treatment plans for VMAT, FFFVMAT6x, and FFFVMAT10x were created for all ten patients. Three of the ten patients planned with FFFVMAT6x, four of the ten patients planned with FFFVMAT10x, and four of the ten patients planned with VMAT did not meet the plan acceptance criteria for the PTV goal of $V_{95\%} \geq 95\%$. However, all of the FFFVMAT6x, FFFVMAT10x, and VMAT treatment plans were deemed clinically acceptable by a radiation oncologist. All ten FFFVMAT6x, FFFVMAT10x, and VMAT patients met the plan acceptance criteria that $V_{20Gy} < 20\%$ for the lungs and $V_{22.5Gy} < 20\%$ for the heart.

FFFVMAT6x and FFFVMAT10x showed, with no statistical significance, similar conformity and dose homogeneity compared to VMAT. No statistical significance was shown for TCP for either FFFVMAT technique over VMAT. Results from previous studies were in agreement with our outcomes for CI, DHI, and TCP for VMAT (Nichols *et al*., 2014, Wang *et al.*, 2015, Zhang *et al.,* 2015). Six of the ten FFFVMAT6x, nine of the ten FFFVMAT10x, and six of the ten VMAT patients achieved nearly 100% TCP. This was expected because all plans were normalized to have 95% PTV volume receive 95% of the prescription dose (47.5 Gy).

No statistical significance was seen in the mean lung dose for either FFFVMAT technique over VMAT. The mean lung dose reported in this work for VMAT was comparable to previously published research (Wang *et al.* 2015). In fact, both FFFVMAT techniques increased, with statistical significance, the $\bar{V}_{5\text{Gy}}$ and $\bar{V}_{20\text{Gy}}$ compared to VMAT. No statistically significant difference was seen between FFFVMAT6x and VMAT or FFFVMAT10x and VMAT for $\overline{NTCP}$ of the lungs. $\overline{NTCP}$ of the lungs with radiation pneumonitis grade two or higher as an endpoint was concluded to have a mean probability of approximately 3.0% for all techniques. Nichols *et al.* (2015) determined $\overline{NTCP}$ of the lungs to be 0.3 ± 0.1% based on 15 VMAT plans; significantly lower than calculated in this study. In addition, no statistically significant difference was seen between FFFVMAT6x and VMAT or FFFVMAT10x and VMAT for $\overline{SCCP}$ of the lungs. $\overline{SCCP}$ of the lungs was concluded to have a mean probability of approximately 13.8% for all techniques. Nichols *et al.* (2015) found the $\overline{SCCP}$ of the lungs to be approximately 5.3% for VMAT. Again, results that were lower than determined by this work.

No statistically significant change in mean heart dose was observed between FFFVMAT10x and VMAT. However, a statistically significant increase in mean heart dose was seen for FFFVMAT6x over VMAT with an increased value of 9.9±2.0 Gy vs. 9.0±1.5 Gy, respectively. Zhang *et al.* (2015) and Nichols *et al.* (2014) both determined a mean heart dose of around 13 Gy for 15 VMAT patients. In addition, $\bar{V}_{22.5\text{Gy}}$ and $\bar{V}_{30\text{Gy}}$ for the heart was significantly higher for FFFVMAT6x and FFFVMAT10x compared to VMAT. $\overline{NTCP}$ of the whole heart and myocardium for FFFVMAT6x vs. VMAT was increased with statistical significance. The patient averaged predicted risk of cardiac mortality ($\overline{NTCP}$) for the whole heart was determined to be 0.72±0.56% for VMAT and 0.94±0.58% for FFFVMAT6x. $\overline{NTCP}$ values for the whole heart reported here for VMAT are in agreement with values published in the literature (Nichols *et al.*, 2014, Wang *et al.*, 2015). The patient averaged predicted risk of cardiac mortality ($\overline{NTCP}$) for the myocardium was determined to be 1.14±0.91% for VMAT and 1.49±1.0% for FFFVMAT6x. No statistical significance was observed in $\overline{NTCP}$ of the whole heart and myocardium for

FFFVMAT10x plans compared to VMAT. The $\overline{NTCP}$ of the whole heart and myocardium values were approximately 0.8% and 1.3% for both techniques, respectively.

Significant reduction in patient average mean dose and $\overline{V}_{5Gy}$ of the contralateral breast was observed for FFFVMAT6x compared to VMAT. No significant difference was seen for FFFVMAT10x over VMAT. Nichols *et al.,* (2014), Wang *et al.*, (2015), and Zhang *et al.* (2015) reported the mean dose to the contralateral breast for VMAT as 1.5 Gy, 2.1 Gy, and 1.7 Gy, respectively. All of which were less than the mean dose of 3.8 Gy reported in this work. FFFVMAT6x was able to reduce the contralateral breast $\overline{SCCP}$. $\overline{SCCP}$ values were 3.03±0.88% for VMAT and 2.55±0.63% for FFFVMAT6x. However, FFFVMAT10x was unable to reduce the $\overline{SCCP}$ for the contralateral breast.

No statistically significant difference was seen for the mean skin dose between either FFFVMAT technique and VMAT. All techniques were slightly under prescription dose (50 Gy) with a patient averaged mean skin dose of 49.2 Gy. Finally, no significant difference was seen for $\overline{TV - V}_{110\%}$ for any VMAT technique and all had mean values less than 5.13% so the patients did not show an increased risk of moist desquamation of the skin.

In summary, FFFVMAT6x and FFFVMAT10x maintained equal dose coverage of the PTV compared to VMAT. In addition, FFFVMAT6x significantly lowered the predicted risk of side effects for the contralateral breast. However, FFFVMAT6x actually induced higher risks for the whole and myocardium but the absolute increase was very minor (~0.22% increase for whole heart and ~0.35% increase for myocardium, respectively). Furthermore, FFFVMAT techniques can significantly reduce total treatment times. Clinically, young women with increased risk of radiation-induced cancer of the contralateral breast may benefit from FFFVMAT6x.

4.3 Implications and Significance of the Results

Cardiac toxicity is a serious concern for women undergoing PMRT. Cardiac toxicity has been indicated as a primary reason for mortality among breast cancer survivors (Johansson *et al.*, 2002, Senkus-Konefka and Jassem, 2007). This work has show with statistical significance that BECT+VMAT

technique applied to left-sided PMRT chest wall patients can reduce NTCP for the whole heart. Patients with prior or current cardiopulmonary complications or those at an increased risk of cardiovascular disease (Weber *et al.*, 2006) may benefit from BECT+VMAT. It was also determined that BECT+VMAT can significantly reduce the SCCP for the contralateral breast. This is especially important for young patients. Studies have determined that premenopausal women under the age of 40 – 45 years old are at the highest risk for second cancers of the contralateral breast after radiation exposure and women over that age shown little or no risk of radiation-induced breast cancer (Boice *et al.,* 1992, Travis *et al.*, 2011). It is possible that younger patients requiring PMRT may further benefit from BECT+VMAT.

This work has determined that patients with more tissue between the distal PTV margin and the parietal pleura, thick tissue around the ribs and intercostal space, benefit the most from BECT+VMAT. This thick tissue has increased ability to attenuate the electron beam leading to decreased doses of the heart and lungs. In addition to further improve the BECT+VMAT technique it may be advantageous to pay closer attention to the PTV thickness in the lateral/posterior areas. When this region of the PTV is very thick the required electron energy must be increased to achieve optimal dose coverage. Higher electron energies result in larger distal dose fall-off regions, increasing lung and heart dose.

FFFVMAT6x was shown with statistical significance to reduce the contralateral breast SCCP. For the same reasons stated previously, FFFVMAT6x may be beneficial to younger patients who are at increased risk of radiation-induced cancer of the contralateral breast.

Furthermore, both FFFVMAT techniques were shown to significantly reduce treatment times for PMRT patients. This would implicate FFFVMAT plans could be advantageous for patients who need reduced treatment times. This could be people who are unable to remain on the treatment couch for longer periods due to discomfort. Reduced treatment times can also be beneficial for breath hold techniques. In addition, this work resulted in MU for VMAT in agreement with the literature (Wang *et al.*, 2015, Zhang *et al.*, 2015). This would indicate the VMAT plans of this work where of similar complexity as those created by other researchers.

4.4 Strengths and Limitations

This study was supported by many strengths: we compared novel advanced PMRT techniques, including VMAT, FFFVMAT (6x and 10x), and BECT+VMAT that were not investigated previously in the literature and realistic clinical patients were used. Planning was conducted using commissioned data for flattening filter free beams for energies 6 MV and 10 MV using a clinical TPS. We conducted detailed risk calculations that were used for comparing advanced techniques to the VMAT technique. Each plan was radiation oncologist approved and the entire dosimetry team assisted with questions and problems encountered when treatment planning. We calculated normal tissue complication probability and second cancer complication probability using recent dose response models. Not only was whole heart NTCP calculated, we went further by adding the myocardium contour and determining its NTCP based on Zhang *et al.* (2013) work further increasing the robustness of the NTCP outcomes for the heart. We included stray radiation dose in our second risk calculations by conducting out-of-field TLD dose measurements with an anthropomorphic phantom and corrected the DVHs used in calculating second risks, while most previous studies completely ignored stray radiation doses.

There were also a few limitations to this study. Only ten patients were included for the VMAT treatment plans and only nine patients were included for the BECT+VMAT treatment plans. Statistical significance and power could be improved by adding more patients to the population. In addition, BECT+VMAT is a very labor-intensive technique with respect to treatment planning and delivery. The planning process takes many intermediate steps with a significant amount of manual manipulations of the treatment planning software like transferring the electron dose distribution into the composite photon plan. In addition, the technique requires using a the third party .decimal p.d (.decimal, Inc., Sanford, FL) software. The machineable wax bolus also needs to be created off-site and upon receiving needs to have addition quality assurance conducted. BECT+VMAT also requires the manufacture of large cerrobend blocks that take time to create and are cumbersome to use by radiation therapist.

4.5 Future Work

Potential future work for this study could be increasing the number of patients. This would increase the statistical power of this study. Adding more left-sided PMRT patients, including right-sided PMRT patients, and including patients who have immediate breast reconstruction before PMRT can provide a clearer picture of who may benefit the most from advanced PMRT techniques and give a better understanding of when a certain technique may be more beneficial over another. Including patients who have metallic tissue expanders that may perturb the dose distributions could have a significant impact on the feasibility of the BECT+VMAT since the high-Z material can negatively affect the electron beam.

Another interesting future work would be adding intensity modulated electron therapy (IMET) in this study. This technique could potentially reduce the magnitude of any hot and cold spots. This could also remove the need for VMAT for the latter technique. IMET could potentially lead to more conformal and homogenous dose distributions to the PTV and reduce the low dose bath to OARs.

In addition, it would be interesting to study the effect of adding breath hold technique. Patient breath holding can increase the distance between the chest wall PTV and the heart further leading to decreased heart dose.

Another future work would be to measure the total treatment time for all of the VMAT plans created for this project. This would increase the confidence that FFFVMAT can significantly reduce treatment time over VMAT.

Chapter 5 Conclusion

The results of this study have effectively shown our hypothesis was supported insofar as BECT+VMAT maintained equal or better dose coverage than VMAT. The results also support the hypothesis that BECT+VMAT can statistically significantly lower the predicted risk of side effects for the heart and contralateral breast. However, the hypothesis that BECT+VMAT can significantly reduce the predicted risk of side effects to the lungs was not supported.

In addition, the results of this study have shown our hypothesis was supported that FFFVMAT6x can maintain equal or better dose coverage than VMAT. The results also support the hypothesis that FFFVMAT6x can statistically significantly lower the predicted risk of side effects for the contralateral breast. However, the hypothesis that FFFVMAT6x can significantly reduces the predicted risk of side effects to the lungs and heart was not supported.

Finally, the results of this study have shown our hypothesis was supported that FFFVMAT10x can maintain equal or better dose coverage than VMAT. However, the hypothesis that FFFVMAT10x can significantly reduces the predicted risk of side effects to the lungs, heart, and contralateral breast was not supported. Our study has also shown that FFFVMAT techniques can significantly reduce total treatment times.

This work has shown that BECT+VMAT produces clinically acceptable plans while reducing OAR doses. Both FFFVMAT techniques are comparable to VMAT with FFFVMAT6x having slight improvements. Even though all VMAT techniques produce more homogenous and conformal dose distributions, BECT+VMAT is a viable option for treating post-mastectomy patients possibly leading to reduced risks of normal tissue complications.

References

(EBCTCG) Eartly Breast Cancer Trialist Collaborative Group 2005 Effects of radiotherapy and of differences in the extent of surgery for early breast cancer on local recurrence and 15-year survival: an overview of the randomised trials *The Lancet* **366** 2087-106.

(RTOG) Radiation Therapy Oncology Group 2015 Breast cancer atlas for radiation therapy planning: Consensus definitions. http://www.rtog.org/CoreLab/ContouringAtlases/BreastCancerAtlas.aspx.

Abo-Madyan Y, Aziz, M. H., Aly, M., Schneider, F., Sperk, E., Clausen, S., Giordano, F. A., Herskind, C., Steil, V., Wenz, F., Glatting, G. 2014 Second cancer risk after 3D-CRT, IMRT and VMAT for breast cancer *Radiotherapy and Oncology* **110** 471-6.

Almberg S S, Lindmo, T., Frengen, J. 2011 Superficial doses in breast cancer radiotherapy using conventional and IMRT techniques: A film-based phantom study *Radiotherapy and Oncology* 259-64.

Ares C A, Khan, S., MacArtain, A. M., Heuberger, J., Goitein, G., Gruber, G., Lutters, G., Hug, E. B., Bodis, S., Lomax, A. J. 2010 Postoperative proton radiotherapy for localized and locoregional breast cancer: Potential for clinically relevant improvements? *International Journal of Radiation Oncolocy Biology Physics* **76** 685-97.

Boice J D, Jr., Harvey E. B., Blettner M., Stovall M., Flannery J. T. 1992 Cancer in the contralateral breast after radiotherapy for breast cancer *N Engl J Med* **326** 781-785.

Bonadonna G, & Valagussa, P. 1997 Conventinal adjuvant chemotherapy *Textbook of Breast Cancer: A Clinical Guide to Therapy* ed G. Bonadonna, G. N. Hortobagyi, A. M. Gianni (London: Dunitz) pp 113, 159-60.

Brenner D J 1993 Dose, volume, and tumor-control predictions in radiotherapy *Int J Radiat Oncol Biol Phys* **26** 171-9.

Cashmore J 2008 The characterization of unflattened photon beams from a 6 MV linear accelerator *Physics in Medicine and Biology* **53** 1933-46.

Chen M, Chen, W., Lai, C., Hung, C., Liu, K., Cheng, Y. 2010 Predictive factors of radiation-induced skin toxicity in breast cancer patients *BMC Cancer* 10:508.

Donovan E M, James, H., Bonora, M., Yarnold, J. R., Evans, P. M. 2012 Second cancer incidence risk estimates using BEIR VII models for standard and complex external beam radiotherapy for early breast cancer *Medical Physics* **39** 5814-24.

Fischbach M, Halg, R. A., Hartmann, M., Besserer, J., Gruber, G., Schneider, U. 2013 Measurement of skin and target dose in post-mastectomy radiotherapy using 4 and 6 MV photon beams *Radiation Oncology* 1-5.

Gagliardi G, Lax, I., Rutqvist, E. 2001 Partial irradiation of the heart *Seminars in Radiation Oncology* **11** 224-33.

Gagliardi G, Lax, I., Soderstrom, S., Gyenes, G., Rutqvist, L. E. 1998 Prediction of excess risk of long-term cardiac mortality after radiotherapy of stage I breast cancer *Radiotherapy and Oncology* **46** 63-71.

Georg D, Knoos, T., & McClean, B. 2011 Current status and future perspective of flattening filter free photon beams *Medical Physics* **38** 1280-93.

Guo B, & Yuan, Y. 2015. A comparative review of methods for comparing means using partially paired data. *Statistical Methods in Medical Research*, doi: 10.1177/0962280215577111.

Harris J R, & Morrow, M. 1996 Local management of invasive breast cancer *Diseases of The Breast* ed J. R. Harris, M. E. Lippman, M. Morrow, S. Hellman (Philadelphia: Lippincott-Raven) pp 487-600.

Hernandez M 2014 A treatment planning comparison of volumetric modulated arc therapy and proton therapy for a sample of breast cancer patients treated with post-mastectomy radiotherapy: A thesis. In: *Physics and Astronomy,* (Baton Rouge, LA: Louisiana State Univeristy).

Hogstrom K R, Antolak J. A., Kudchadker R. J., Ma C.-M. C., Leavitt D. D. Modulated electron therapy. In: J Palta and R. Mackie (eds). Intensity Modulated Radiation Therapy, The State of the Art: Proceedings of the 2003 AAPM Summer School, pp. 749-786, Madison: Medical Physics Publishing.

Howell R M, Scarboro, S. B., Taddei, P. J., Krishnan, S., Kry, S. F., Newhauser, W. D. 2010 Methodology for determining doses to in-field, out-of-field and partially in-field organs for late effects studies in photon radiotherapy *Physics in Medicine and Biology* **55** 7009-23.

Jagetic L J, & Newhauser W. D. 2015 A simple and fast physics-based analytical method to calculate therapeutic and stray doses from external beam, magavoltage x-ray therapy *Physics in Medicine and Biology* **60** 4753-75.

Johansson J, Isacsson U., Lindman H., Montelius A., Glimelius B. 2002 Node-positive left-sided breast cancer patients after breast-conserving surgery: potential outcomes of radiotherapy modalities and techniques *Radiother Oncol* **65** 89-98.

Kallman P, Agren A., Brahme A. 1992 Tumour and normal tissue responses to fractionated non-uniform dose delivery *Int J Radiat Biol* **62** 249-62.

Kavanaugh J A, Hogstrom, K. R., Chu, C., Carver, R. A., Fontenot, J. P., Henkelmann, G. 2013 Delivery confirmation of bolus electron conformal therapy combined with intensity modulated x-ray therapy *Medical Physics* **40** 021724-1 - 121724-14.

Lang S, Shrestha, B., Graydon, S., Cavelaars, F., Linsenmeier, C., Hrbacek, J., Klock, S., Studer, G., Riesterer, O. 2013 Clinical application of flattening filter free beams for extracranial stereotactic radiotherapy *Radiotherapy and Oncology* 255-9.

Lichter A S 1998 Breast cancer *Textbook of Radiation Oncology* ed S. A. Leibel, T. L. Phillips (Philadelphia: Saunders) pp 1037.

Levitt S H, & Perez, C. A. 1987 *Principles and Practice of Radiation Oncology* ed C. A. Perez, L. W. Brady, A. Becker (Philadelphia: Lippincott) pp 782-84.

Low D A, G. Starkschall, N. E. Sherman, S. W. Bujnowski, J. R. Ewton & K. R. Hogstrom 1995 Computer-aided design and fabrication of an electron bolus for treatment of the paraspinal muscles I*nternational Journal of Radiation Oncology Biology and Physics* **33** 1127-38.

Ma J, Li, J., Xie, J., Chen, J., Zhu, C., Cai, G., Zhang, Z., Guo, X., Chen, J. 2013 Post mastectomy linac IMRT irradiation of chest wall and regional nodes: dosimetry data and acute toxicities *Radiation Oncology* **8:81** 1-10.

Mackie T R, Olivera, G. H., Kapatoes, J. M., Ruchala, K. J., Balog, J. P., Tome, W. A., Hui, S., Kissick, M., Wu, C., Jeraj, R., Reckwerdt, P. J., Harari, P., Ritter, M., Forrest, L., Welsh, J. S., Mehta, M. P. Helical Tomotherapy. 247-84.

Marks L B, Yorke, E. D., Jackson, A., Ten Haken, R. K., Constine , L. S., Eisbruch, A., et al. 2010 Use of normal tissue complication probability models in the clinic *International Journal of Radiation Oncology Biology Physics* **76** S10-S9.

Mu X, Ologsson, L., Karlsson, M., Sjogren, R., Zackrisson, B. 2004 Can Photon IMRT be Improved by Combination with Mixed Electron and Photon Techniques? *Acta Oncologica* **43** 727-35.

Nichols G P 2012 A treatment planning comparison of dual-arc VMAT vs. helical tomotherapy for post-mastectomy radiotherapy. In: *Physics and Astronomy,* (Baton Rouge Louisiana State University) 110.

Nichols G P, Fontenot, J. D., Gibbons, J. P., Sanders, M. E. 2014 Evaluation of volumetric modulated arc therapy for postmastectomy treatment *Radiation Oncology* **9:66** 1-8.

Overgaard M, Hansen, P. S., Overgaard, J., Rose, C., Andersson, M., Bach, F., Kjaer, M., Gadeberg, C. C., Mouridsen, H. T., Jensen, M., Zedeler, K. 1997 Postoperative radiotherapy in high-risk permenopausal women with breast cancer who receive adjuvant chemotherapy *The New England Journal of Medicine* **337** 949-55.

Peirce L J, Butler, J. B., Martel, M. K., Normolle, D. P., Koelling, T., Marsh, R. B., Lichter, A. S., Fraass, B. A. 2002 Postamstectomy Radiotherapy of the Chest Wall: Dosimetric Comparison of Common Techniques *International Journal of Radiation Oncolocy Biology Physics* **52** 1220-30.

Perkins G H, McNeese, M. D., Antolak, J. A., Buchholz, T. A., Strom, E. A., Hogstrom, K. R. 2001 A custom three-dimensional electron bolus technique for optimization of postmastectomy irradiation *International Journal of Radiation Oncolocy Biology Physics* **51** 1142-51.

Rosca F 2012 A hybrid electron and photon IMRT planning technique that lowers normal tissue integral patient dose using standard hardware *Medical Physics* **39** 2964-71.

Rudat V, Nour, A., Alaradi, A. A., Mohamed, A., & Altuwaijri, S. 2014 In vivo surface dose measurement using GafChromic film dosimetry in breast cancer radiotherapy: comparison of 7-field IMRT, tangential IMRT and tangential 3D-CRT *Radiation Oncology* **9** 1-9.

Schneider U, Kaser-Hotz 2005 A simple dose-response relationship for modeling secondary cancer incidence after radiotherapy *Z Med Phys* **15** 31-7.

Senkus-Konefka E, & Jassem J. 2007 Cardiovascular effects of breast cancer radiotherapy *Cancer Treat Rev* **33** 578-93.

Seppenwoolde Y, Lebesque, J. V., De Jaeger, K., Belderbos, J. S. A., Boersma, L. J., Schilstra, C., Henning, G. T., Hayman, J. A., Martel, M. K., Ten Haken, R. K. 2003 Comparing different NTCP models that predict the incidence of radiation pneumonitis *International Journal of Radiation Oncolocy Biology Physics* **55** 724-35.

Siegel R L, Miller, K. D., Jemal, A. J. 2015 Cancer Statistics, 2015 *CA: A Cancer Journal for Clinicians* **65** 5-29.

Sorensen B S, Vestergaard, A., Overgaard, J., Praestegaard, L. H. 2011 Dependence of cell survival on instantaneous dose rate of a linear accelerator *Radiotherapy and Oncology* 223-5.

Spruijt K H, Dahele, M., Cuijpers, J. P., Jeulink, M., Rietveld, D., Slotman, B. J., et al. 2013 Flattening filter free vs flattened beams for breast irradiation *International Journal of Radiation Oncolocy Biology Physics* **8** 506-13.

Taddei P J, Jalbout, W., Howell, R. M., Khater, N., Geara, F., Homann, K., et al. 2013 Analytical model for out-of-field dose in photon craniospinal irradiation *Phisics in Medicine and Biology* **58** 7463-79.

Travis L B, Hill D. A., Dores G. M., Gospodarowicz M., van Leeuwen F. E., Holowaty E., Glimelius B., Andersson M., Wiklund T., Lynch C. F., Van't Veer M. B., Glimelius I., Storm H., Pukkala E., Stovall M., Curtis R., Boice J. D., Jr., Gilbert E. 2003 Breast cancer following radiotherapy and chemotherapy among young women with Hodgkin disease *JAMA* **290** 465-75.

van der Laan H P, Korevaar, E. W., Dolsma, W. V., Maduro, J. H., Langendijk, J. A. 2010 Minimising contralateral breast dose in post-mastectomy intensity-modulated radiotherapy by incorporating conformal electron irradiation *Radiotherapy and Oncology* **94** 235-40.

Van't Riet A, Mak A. C., Moerland M. A., Elders L. H. 1997 A conformation number to quantify the degree of conformality in brachytherapy and external beam irradiation: Application to the prostate *Int J Radiat Oncol Biol Phys* **37** 731–6.

Wang J, Li, X., Deng, Q., Xia, B., Wu, S., Liu, J., Ma, S. 2015 Postoperative radiotherapy following mastectomy for patients with left-sided breast cancer: A comparative dosimetric study *Medical Dosimetry* **40** 190-194.

Webb S, Nahum, A. E. 1993 A model for calculating tumour control probablility in radiotherapy including the effects of inhomogeneous distributions of dose and clonogenic cell density *Phisics in Medicine and Biology* **38** 653-66.

Weber D C, Ares C., Lomax A. J., Kurtz J. M. 2006 Radiation therapy planning with photons and protons for early and advanced breast cancer: an overview *Radiation Oncology* **1** 22.

Wood W C, Muss, H. B., Solin, L. J., Olopade, O. I. 2005 Malignant tumors of the breast *Cancer, Principles & Practice of Oncology* 7th edition ed V. T. Devita Jr., S. Hellman, S. A. Rosenberg (Philadelphia, PA: Lippincott Williams & Wilkins) pp 1435-62.

Wu Q, Mohan R., Morris M., Lauve A., Schmidt-Ullrich R. 2003 Simultaneous integrated boost intensity-modulated radiotherapy for locally advanced head-and-neck squamous cell carcinomas. I: dosimetric results *Int J Radiat Oncol Biol Phys* **56** 573-85.

Zhang Q, Yu, X. L., Hu, W. G., Chen, J. Y., Wang, J. Z., Ye, J. S., Guo, X. M. 2015 Dosimetric comparison for volumetric modulated arc therapy and intensity- modulated radiotherapy on the left-sided chest wall and internal mammary nodes irradiation in treating post-mastectomy breast cancer *Radiology and Oncology* **49** 91-8.

Zhang R, Howell, R. M., Homann, K., Giebeler, A., Taddei, P. J., Mahajan, A., et al. 2013 Predicted risks of radiogenic cardiac toxicity in two pediatric patients undergoing photon or proton radiotherapy *Radiation Oncology* **8** 1-10.

Zwahlen D R, Lang, S., Hrbacek, J., Glansmann, C., Kloeck, S., Najafi, Y., Streller, T., Studer, G., Zaugg, K., Luefolf, U. M. 2012 The Use of Photon Beams of a Flattening Filter-free Linear Accelerator for Hypofractionated Volumetric Modulated Arc Therapy in Localized Prostate Cancer *International Journal of Radiation Oncolocy Biology Physics* **83** 1655-60.

Appendix A: Isodose Distributions and Dose Volume Histograms

Isodose distributions along with dose volume histograms for each patient within the sample population are displayed within this section. Color coding is consistent with methods listed in Table 3.1.

Patient CW1

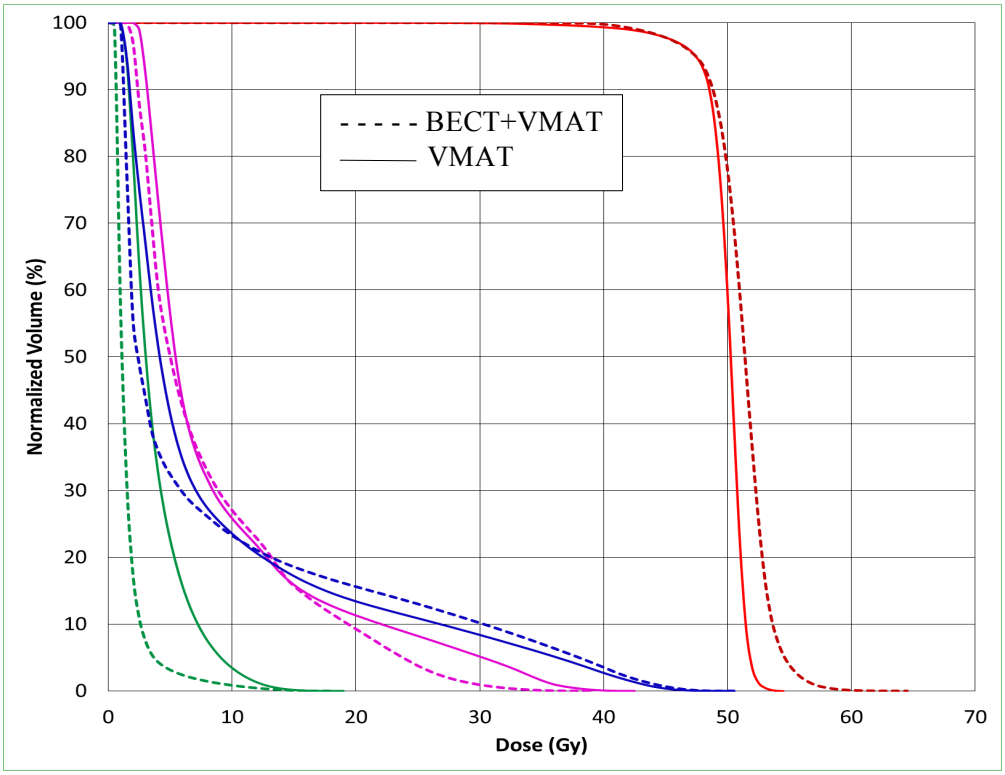

Figure A.1 DVH for patient CW1 comparing PTV (red), lungs (blue), heart (magenta), and breast (green) for BECT+VMAT (dashed line) and VMAT (solid line).

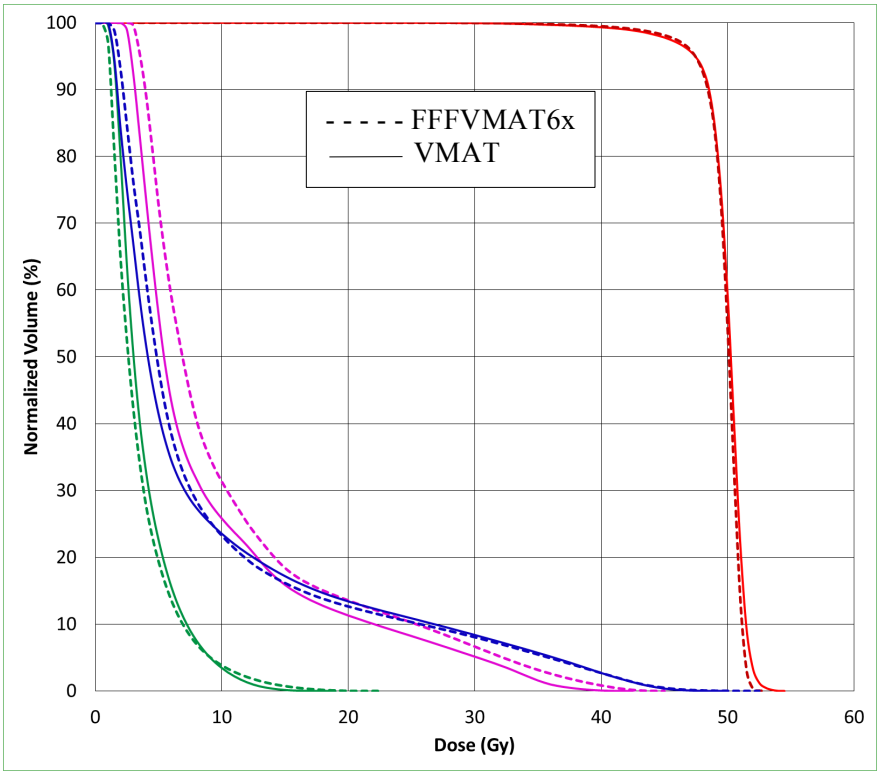

Figure A.2 DVH for patient CW1 comparing PTV (red), lungs (blue), heart (magenta), and breast (green) for FFFVMAT6x (dashed line) and VMAT (solid line).

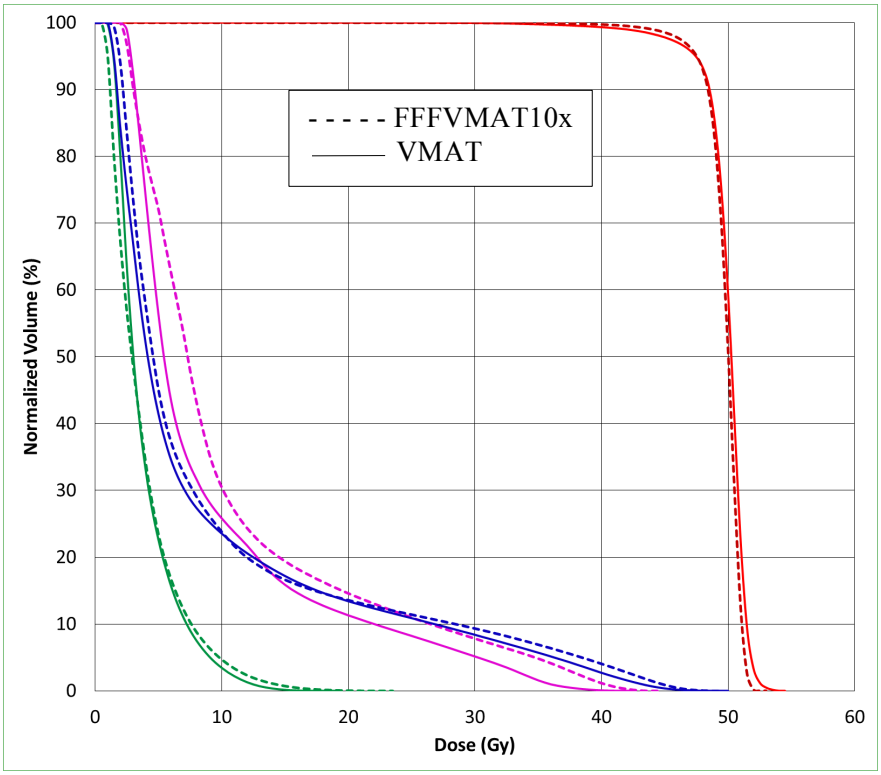

Figure A.3 DVH for patient CW1 comparing PTV (red), lungs (blue), heart (magenta), and breast (green) for FFFVMAT10x (dashed line) and VMAT (solid line).

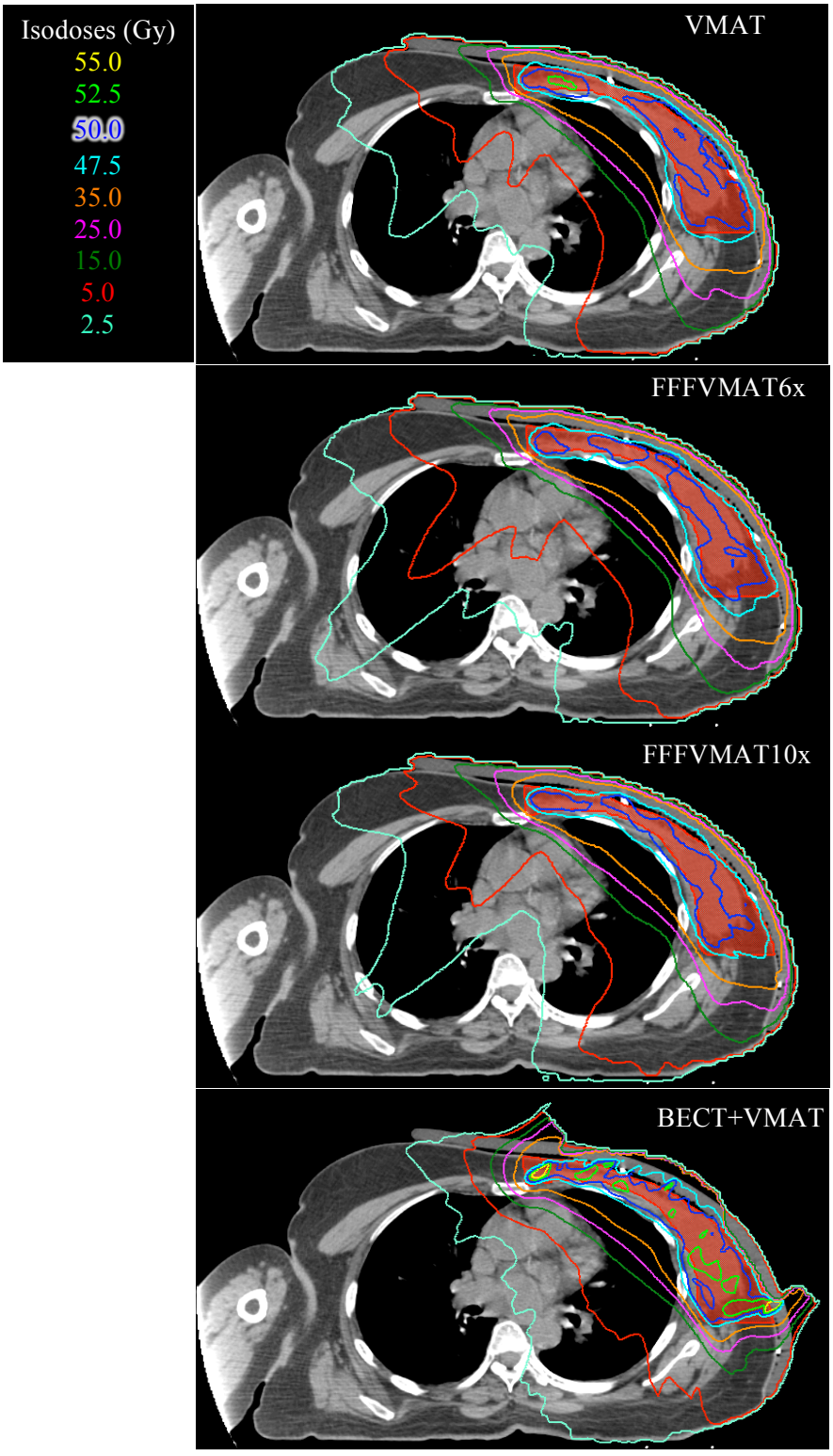

Figure A.4 Isodose distribution for patient CW1 for VMAT (top), FFFVMAT6x (top middle), FFFVMAT10x (bottom middle), and BECT+VMAT (bottom) treatment plans in axial slice on VMAT beam isocenter.

Patient CW2

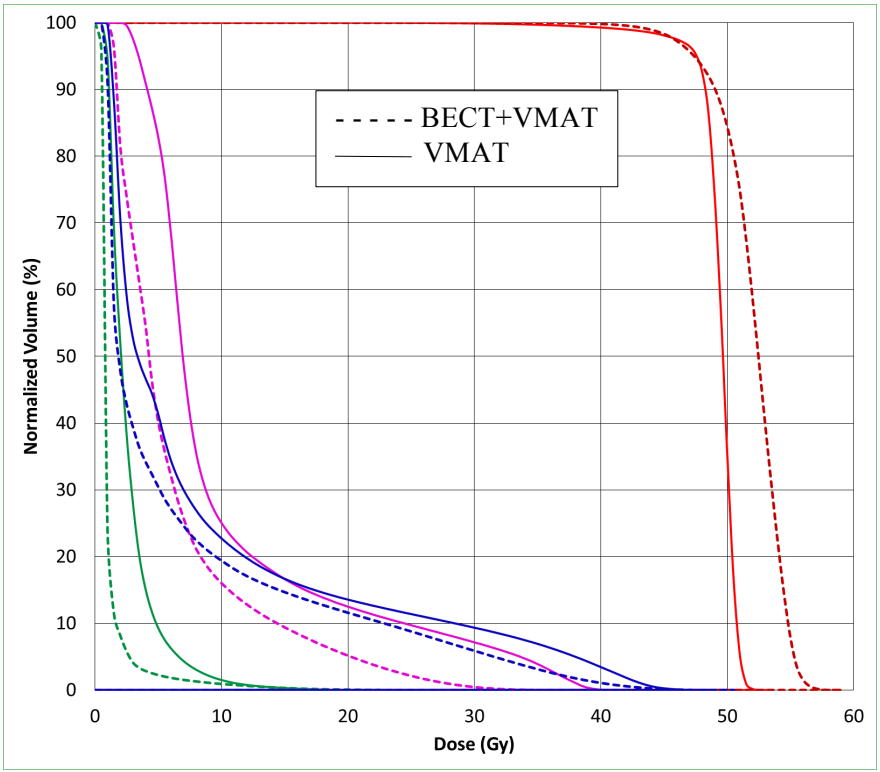

Figure A.5 DVH for patient CW2 comparing PTV (red), lungs (blue), heart (magenta), and breast (green) for BECT+VMAT (dashed line) and VMAT (solid line).

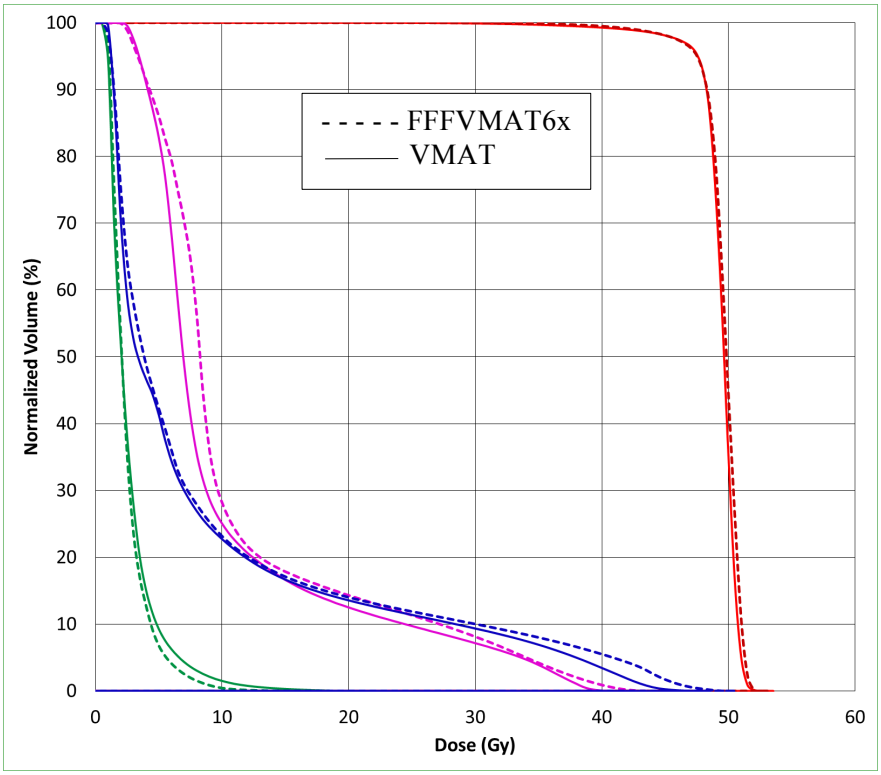

Figure A.6 DVH for patient CW2 comparing PTV (red), lungs (blue), heart (magenta), and breast (green) for FFFVMAT6x (dashed line) and VMAT (solid line).

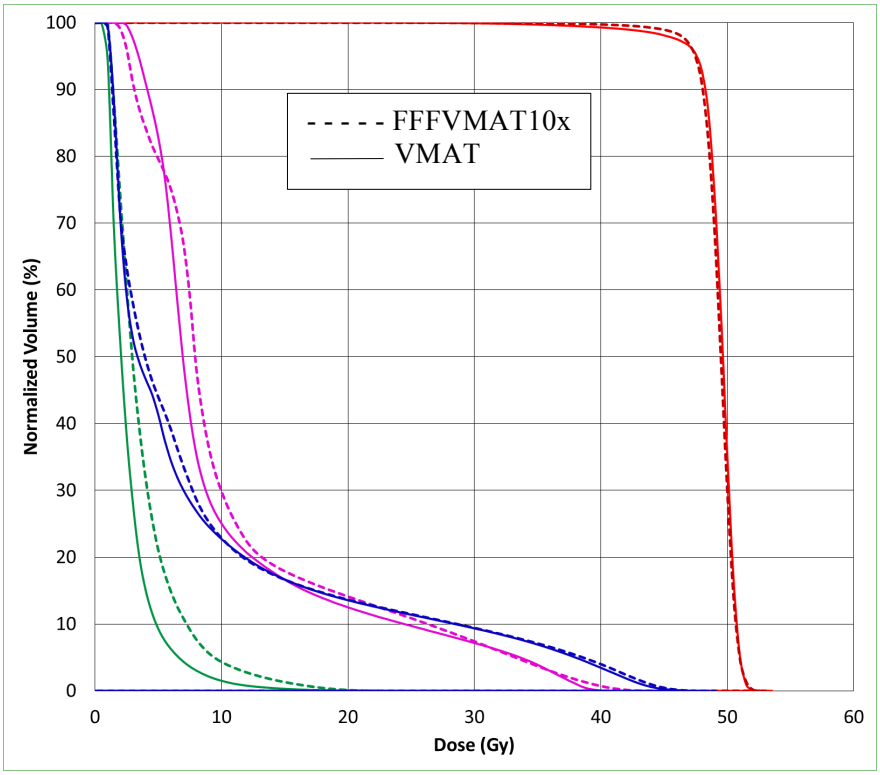

Figure A.7 DVH for patient CW2 comparing PTV (red), lungs (blue), heart (magenta), and breast (green) for FFFVMAT10x (dashed line) and VMAT (solid line).

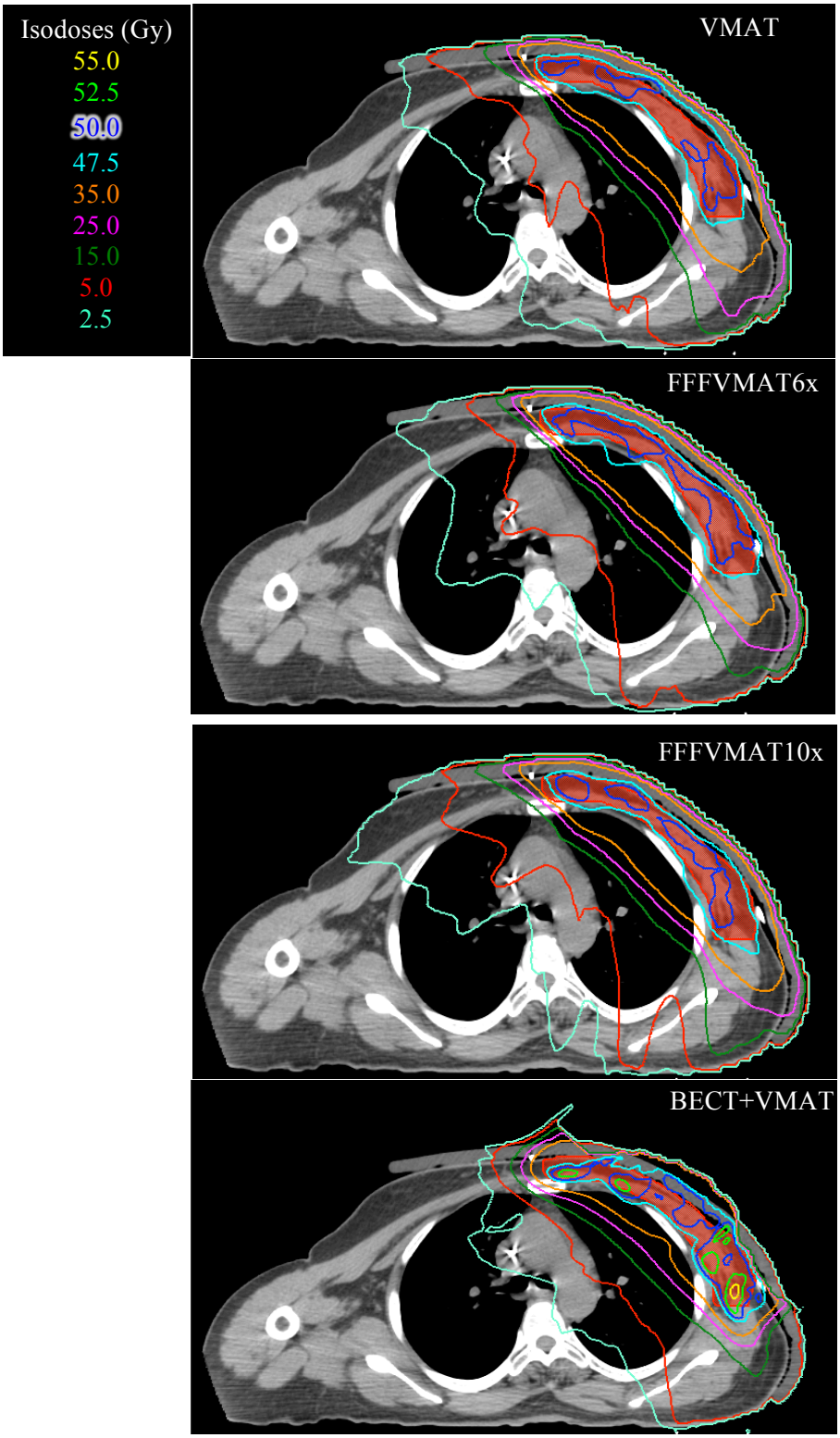

Figure A.8 Isodose distribution for patient CW2 for VMAT (top), FFFVMAT6x (top middle), FFFVMAT10x (bottom middle), and BECT+VMAT (bottom) treatment plans in axial slice on VMAT beam isocenter.

Patient CW3

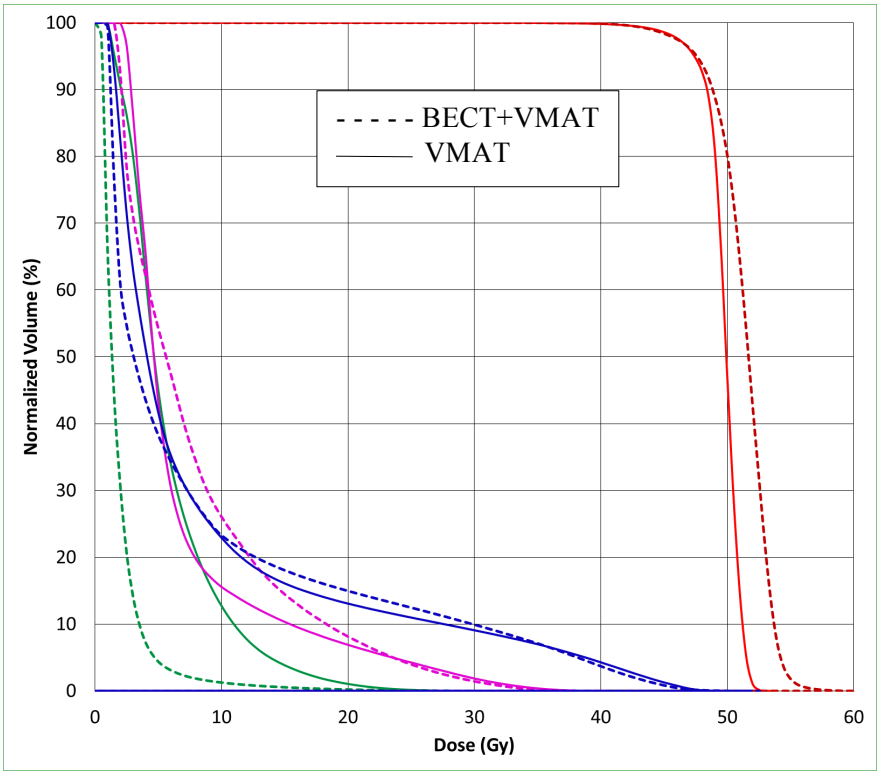

Figure A.9 DVH for patient CW3 comparing PTV (red), lungs (blue), heart (magenta), and breast (green) for BECT+VMAT (dashed line) and VMAT (solid line).

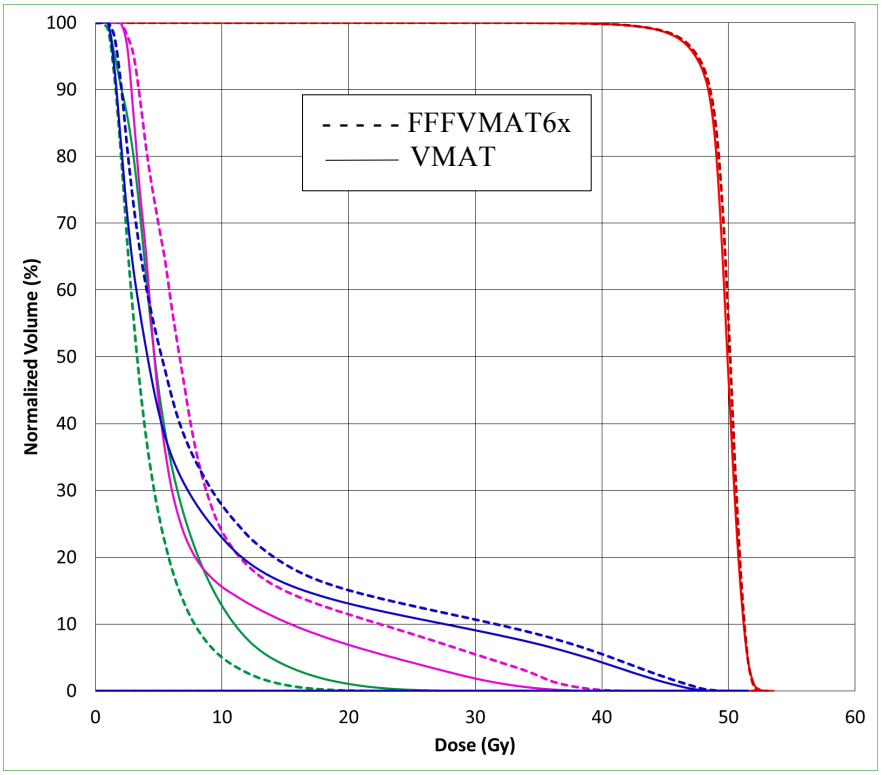

Figure A.10 DVH for patient CW3 comparing PTV (red), lungs (blue), heart (magenta), and breast (green) for FFFVMAT6x (dashed line) and VMAT (solid line).

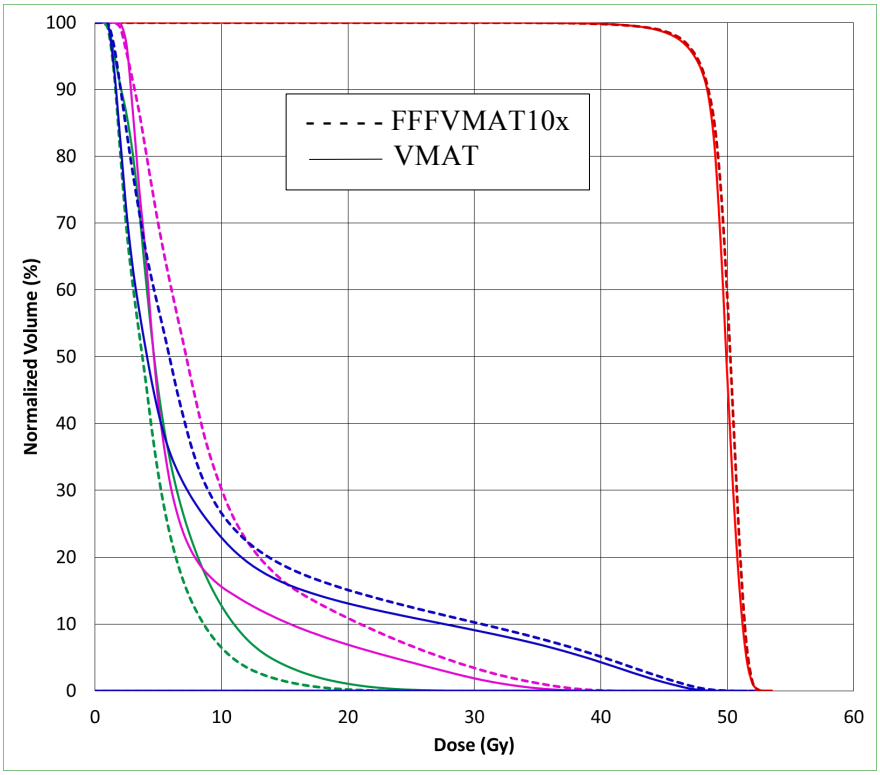

Figure A.11 DVH for patient CW3 comparing PTV (red), lungs (blue), heart (magenta), and breast (green) for FFFVMAT10x (dashed line) and VMAT (solid line).

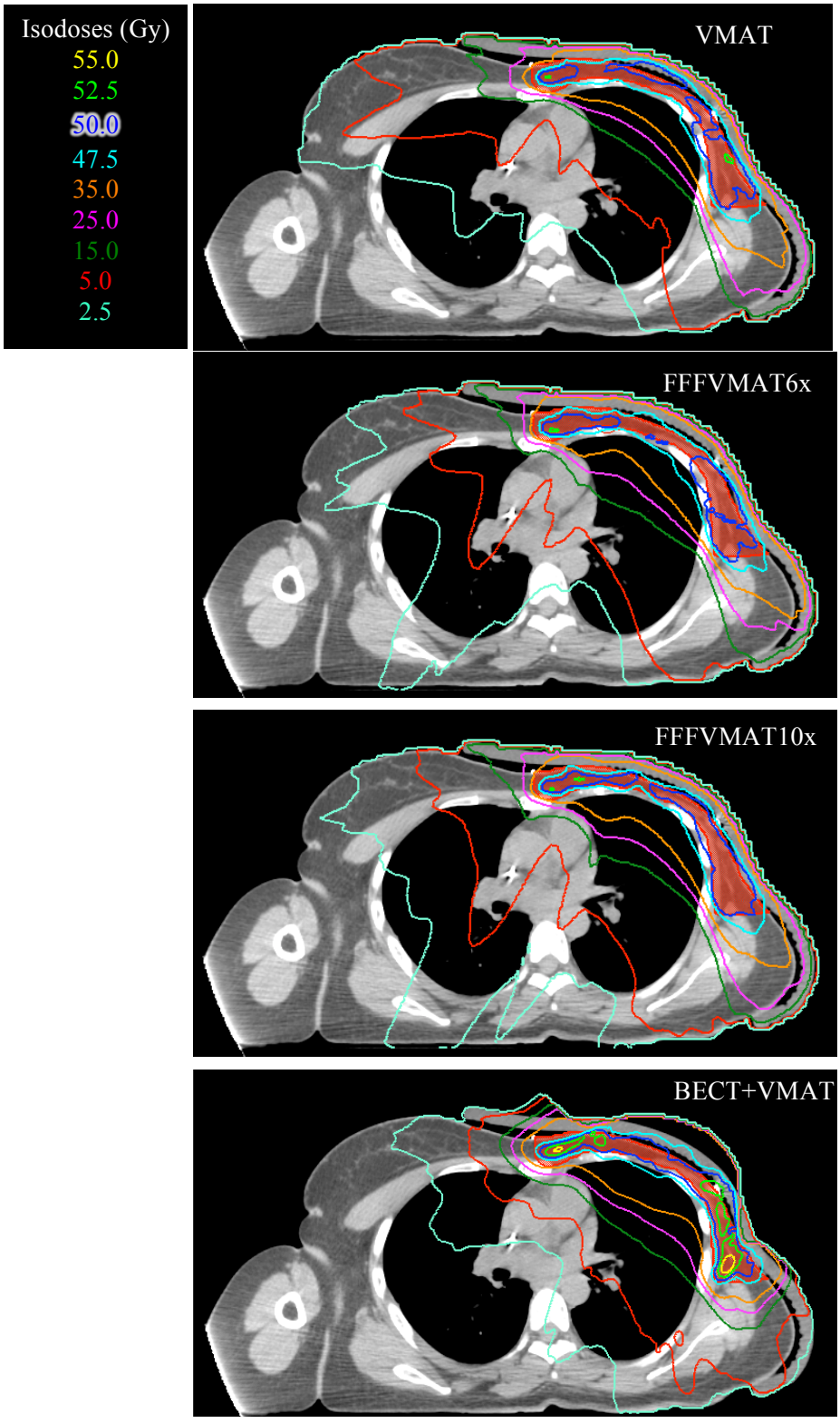

Figure A.12 Isodose distribution for patient CW3 for VMAT (top), FFFVMAT6x (top middle), FFFVMAT10x (bottom middle), and BECT+VMAT (bottom) treatment plans in axial slice on VMAT beam isocenter.

Patient CW5

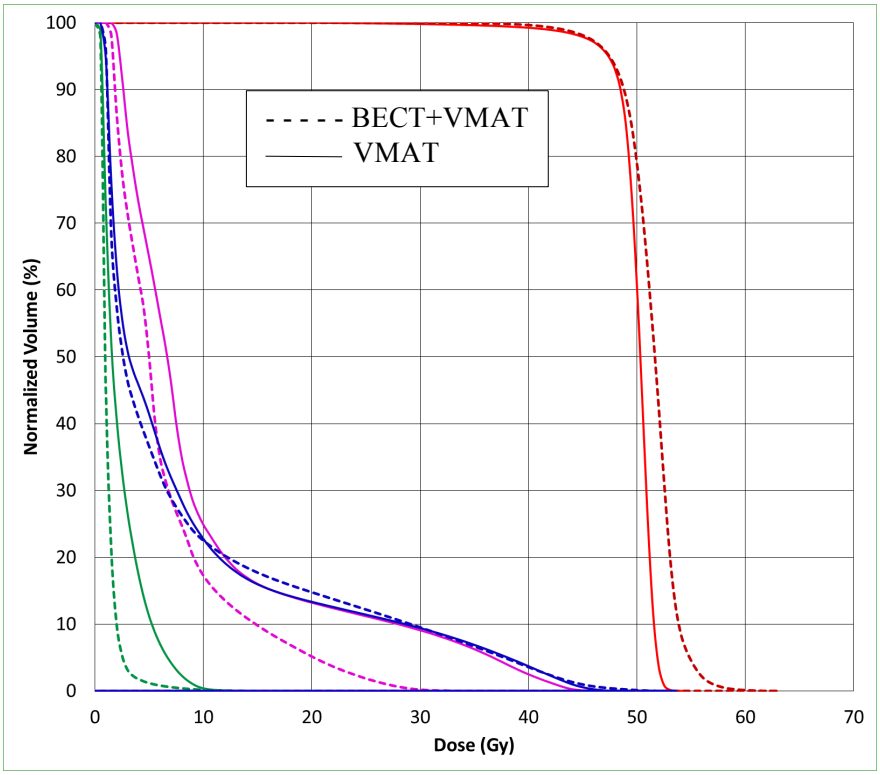

Figure A.13 DVH for patient CW5 comparing PTV (red), lungs (blue), heart (magenta), and breast (green) for BECT+VMAT (dashed line) and VMAT (solid line).

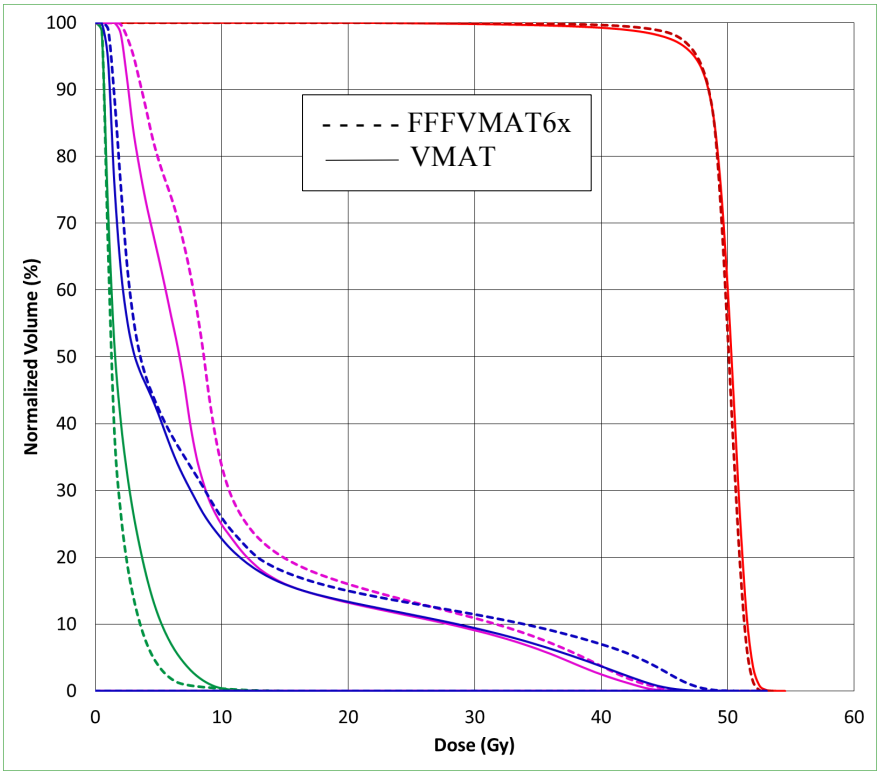

Figure A.14 DVH for patient CW5 comparing PTV (red), lungs (blue), heart (magenta), and breast (green) for FFFVMAT6x (dashed line) and VMAT (solid line).

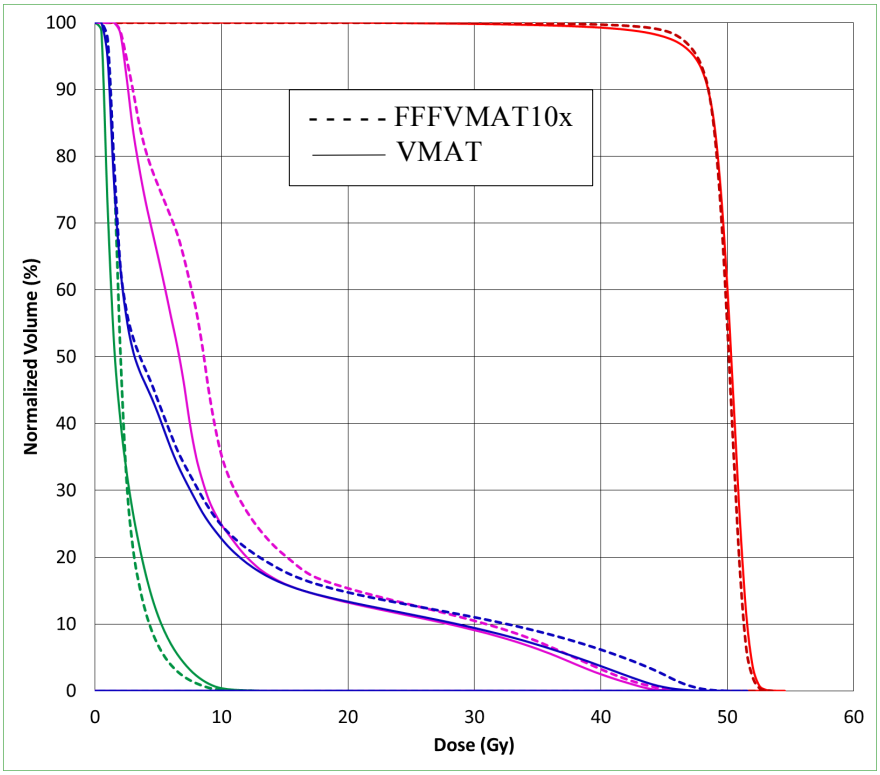

Figure A.15 DVH for patient CW5 comparing PTV (red), lungs (blue), heart (magenta), and breast (green) for FFFVMAT10x (dashed line) and VMAT (solid line).

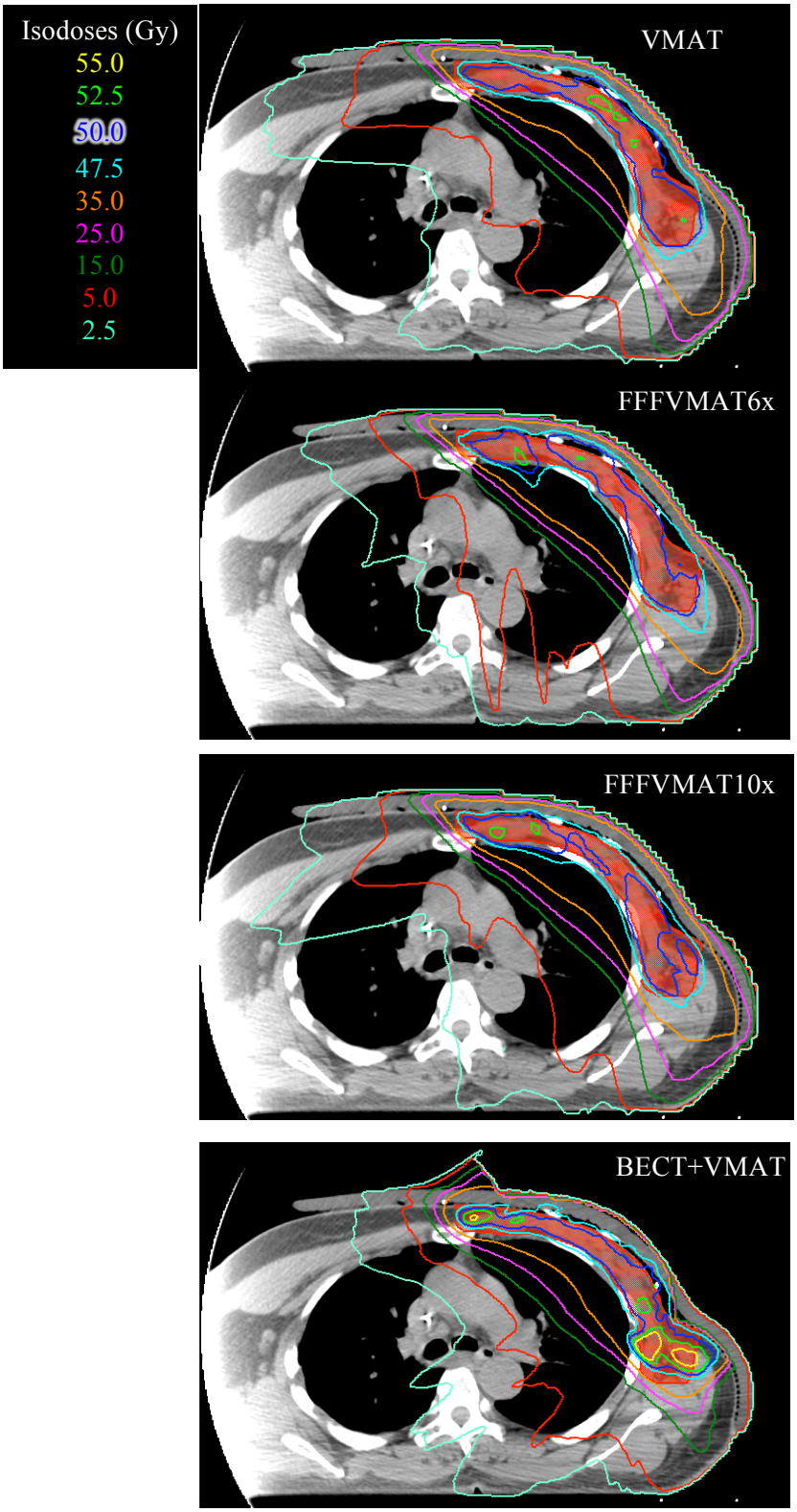

Figure A.16 Isodose distribution for patient CW5 for VMAT (top), FFFVMAT6x (top middle), FFFVMAT10x (bottom middle), and BECT+VMAT (bottom) treatment plans in axial slice on VMAT beam isocenter.

Patient CW6

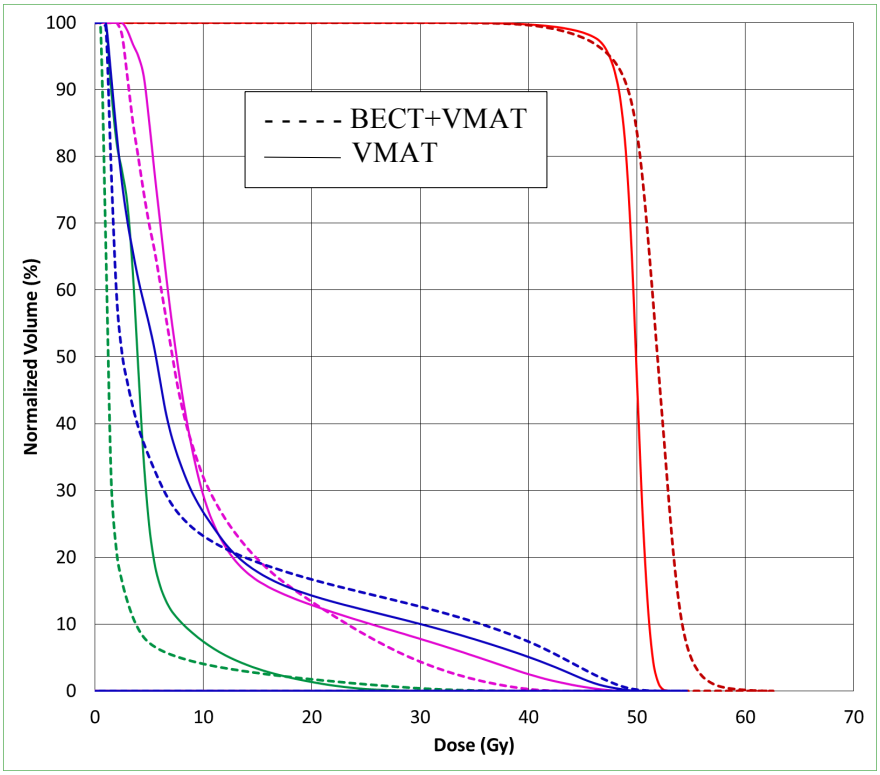

Figure A.17 DVH for patient CW6 comparing PTV (red), lungs (blue), heart (magenta), and breast (green) for BECT+VMAT (dashed line) and VMAT (solid line).

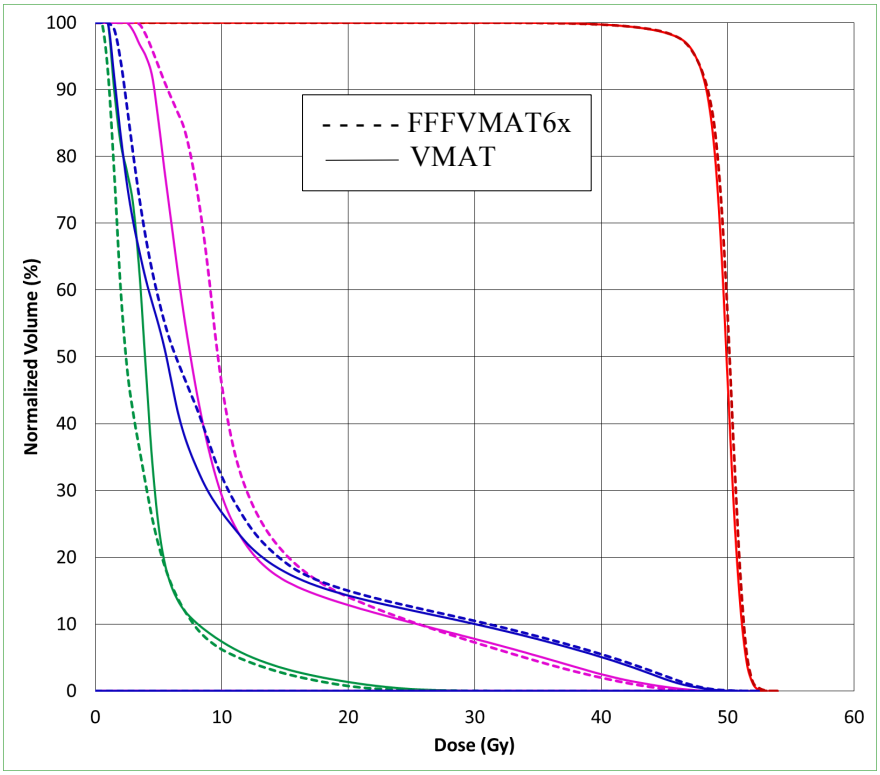

Figure A.18 DVH for patient CW6 comparing PTV (red), lungs (blue), heart (magenta), and breast (green) for FFFVMAT6x (dashed line) and VMAT (solid line).

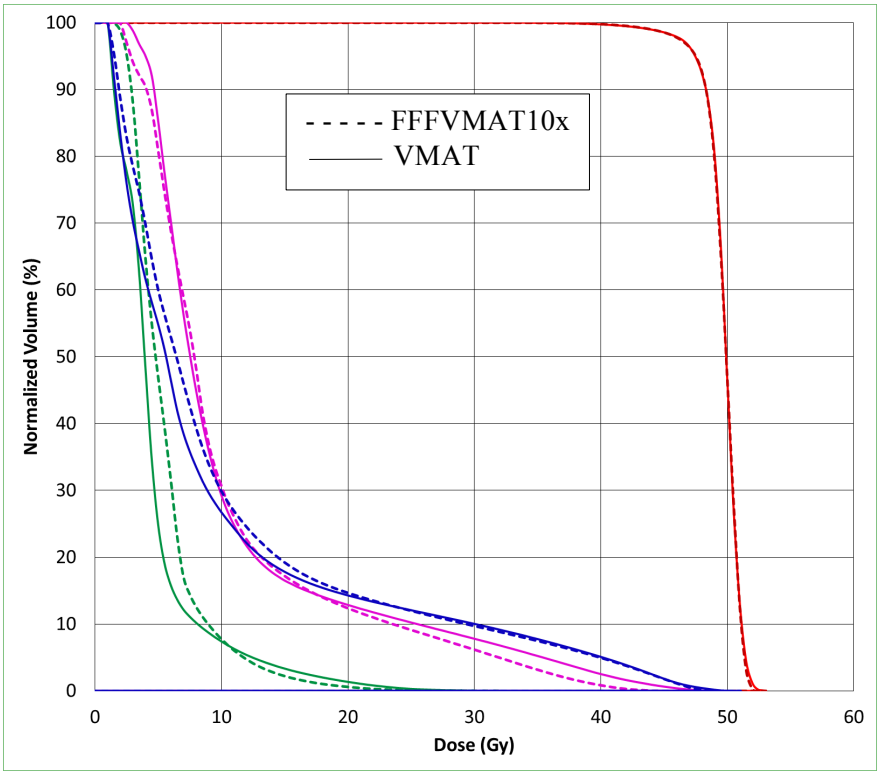

Figure A.19 DVH for patient CW6 comparing PTV (red), lungs (blue), heart (magenta), and breast (green) for FFFVMAT10x (dashed line) and VMAT (solid line).

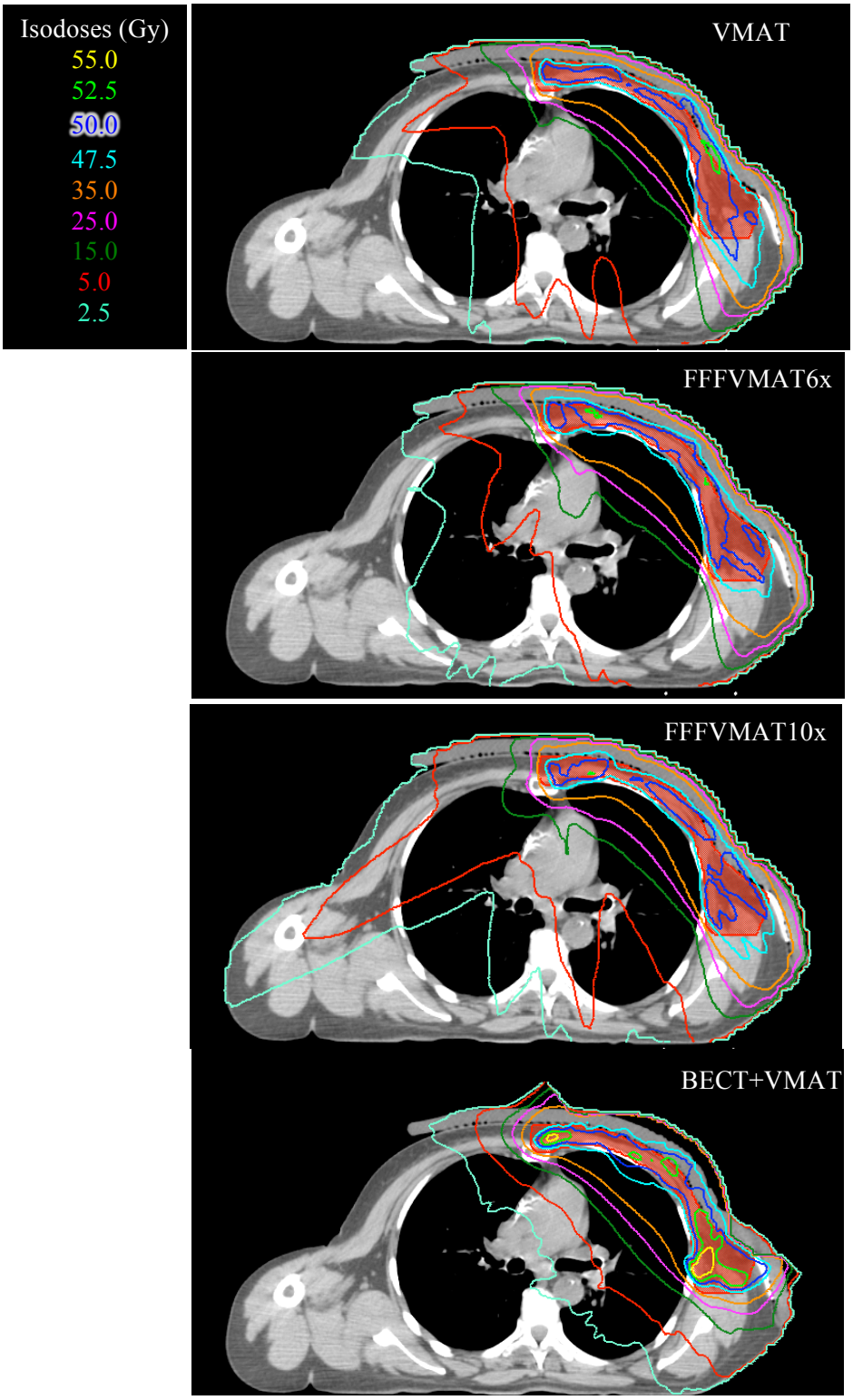

Figure A.20 Isodose distribution for patient CW6 for VMAT (top), FFFVMAT6x (top middle), FFFVMAT10x (bottom middle), and BECT+VMAT (bottom) treatment plans in axial slice on VMAT beam isocenter.

Patient CW7

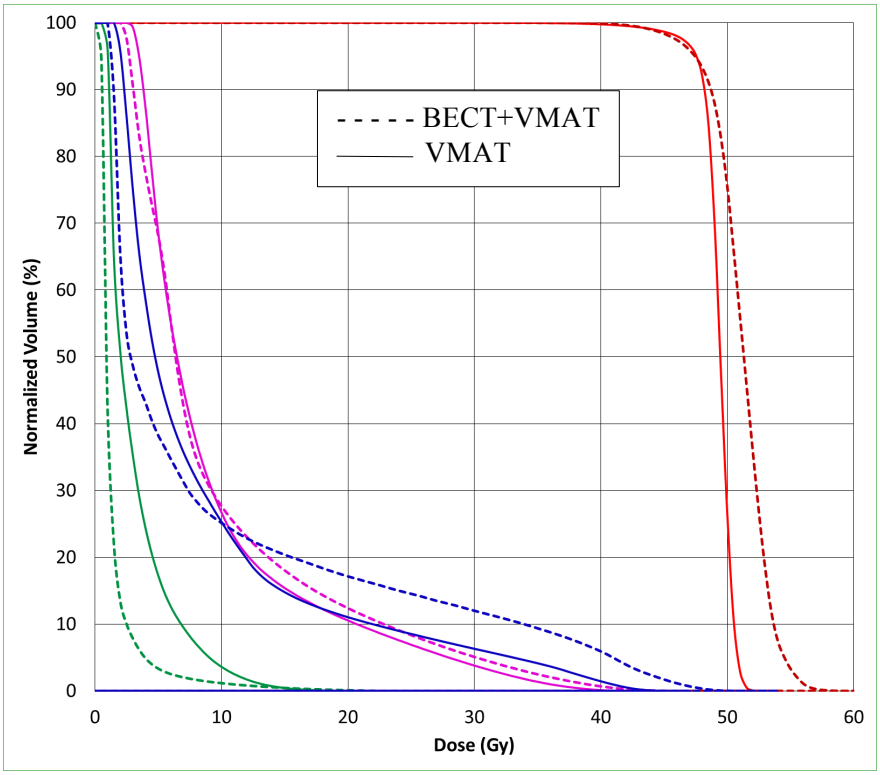

Figure A.21 DVH for patient CW7 comparing PTV (red), lungs (blue), heart (magenta), and breast (green) for BECT+VMAT (dashed line) and VMAT (solid line).

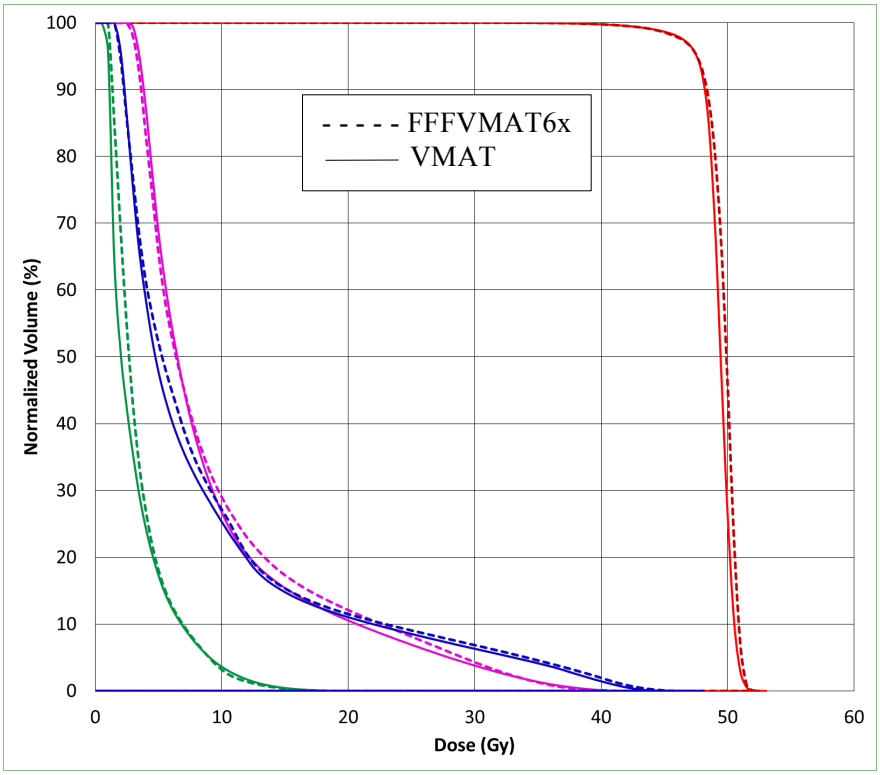

Figure A.22 DVH for patient CW7 comparing PTV (red), lungs (blue), heart (magenta), and breast (green) for FFFVMAT6x (dashed line) and VMAT (solid line).

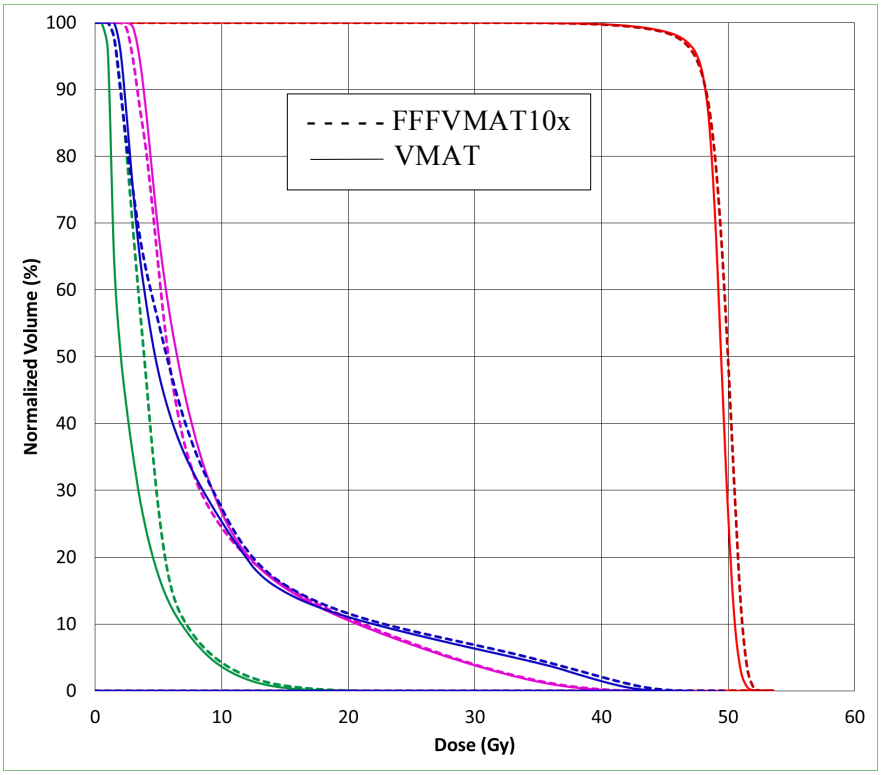

Figure A.23 DVH for patient CW7 comparing PTV (red), lungs (blue), heart (magenta), and breast (green) for FFFVMAT10x (dashed line) and VMAT (solid line).

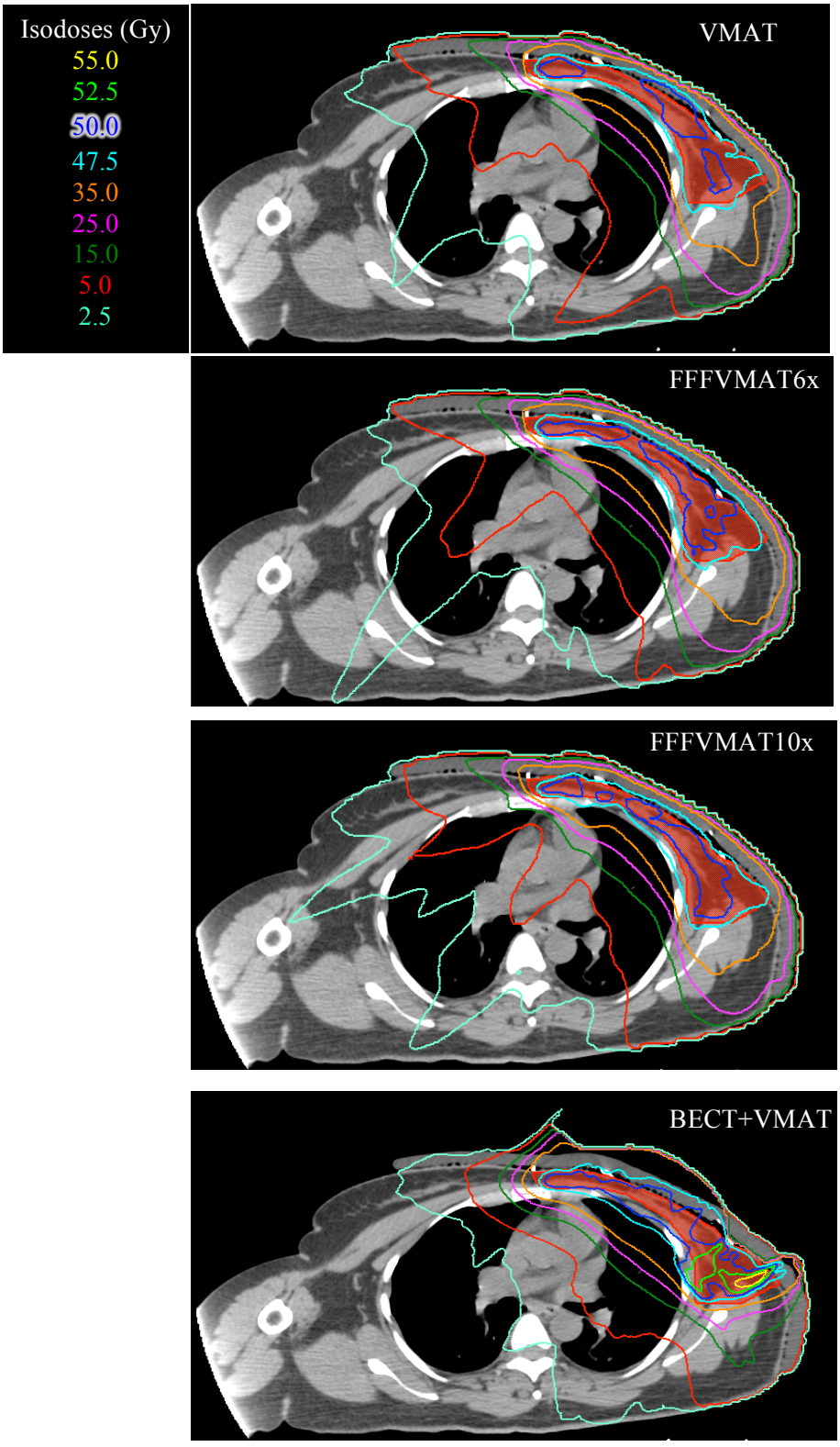

Figure A.24 Isodose distribution for patient CW7 for VMAT (top), FFFVMAT6x (top middle), FFFVMAT10x (bottom middle), and BECT+VMAT (bottom) treatment plans in axial slice on VMAT beam isocenter.

Patient CW8

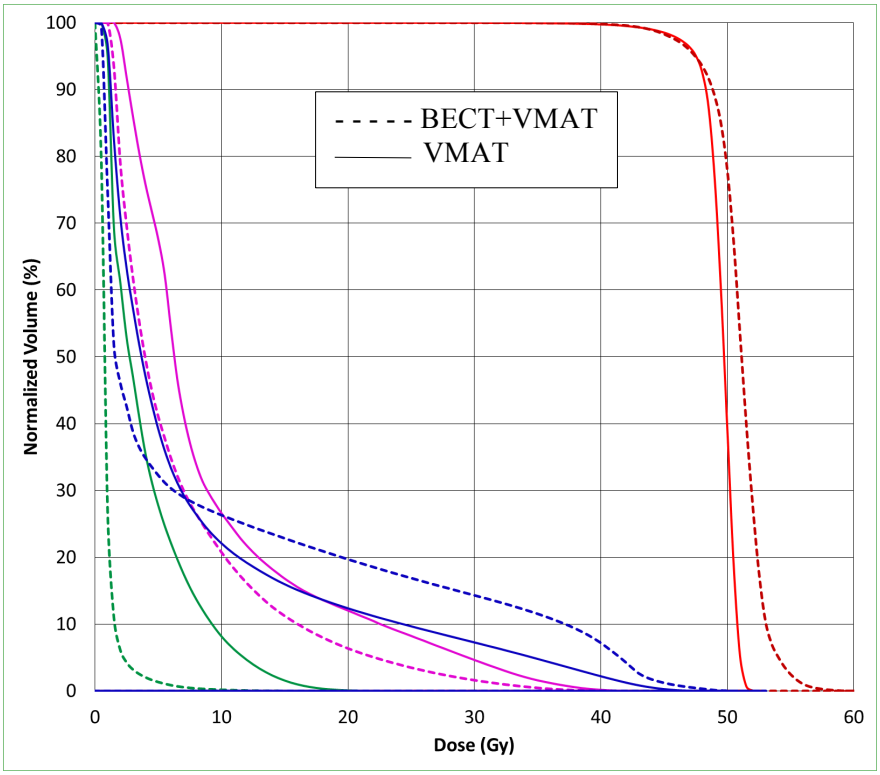

Figure A.25 DVH for patient CW8 comparing PTV (red), lungs (blue), heart (magenta), and breast (green) for BECT+VMAT (dashed line) and VMAT (solid line).

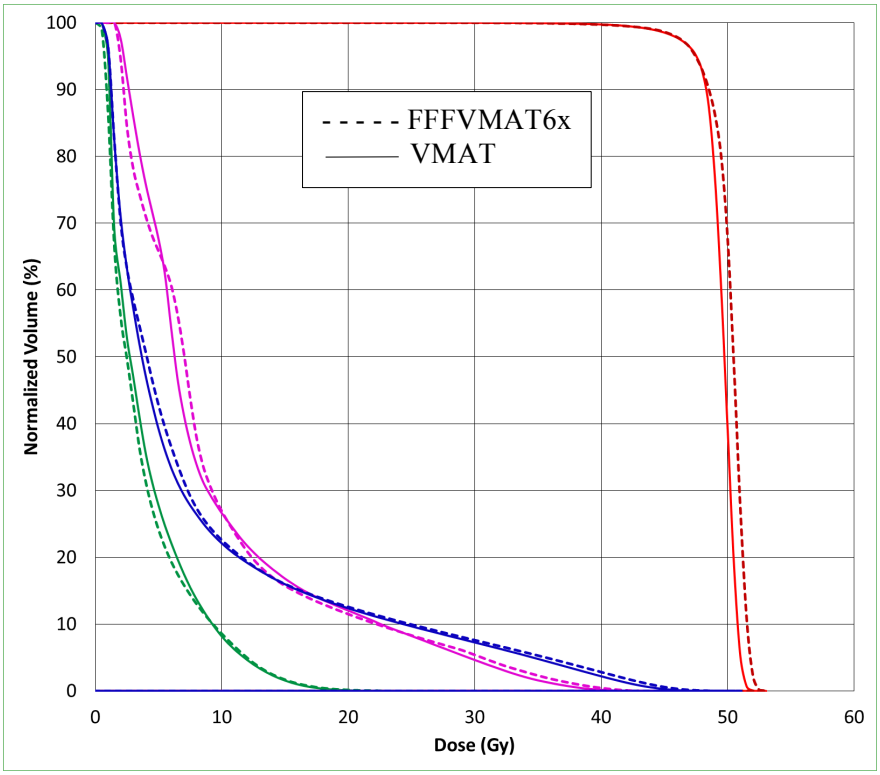

Figure A.26 DVH for patient CW8 comparing PTV (red), lungs (blue), heart (magenta), and breast (green) for FFFVMAT6x (dashed line) and VMAT (solid line).

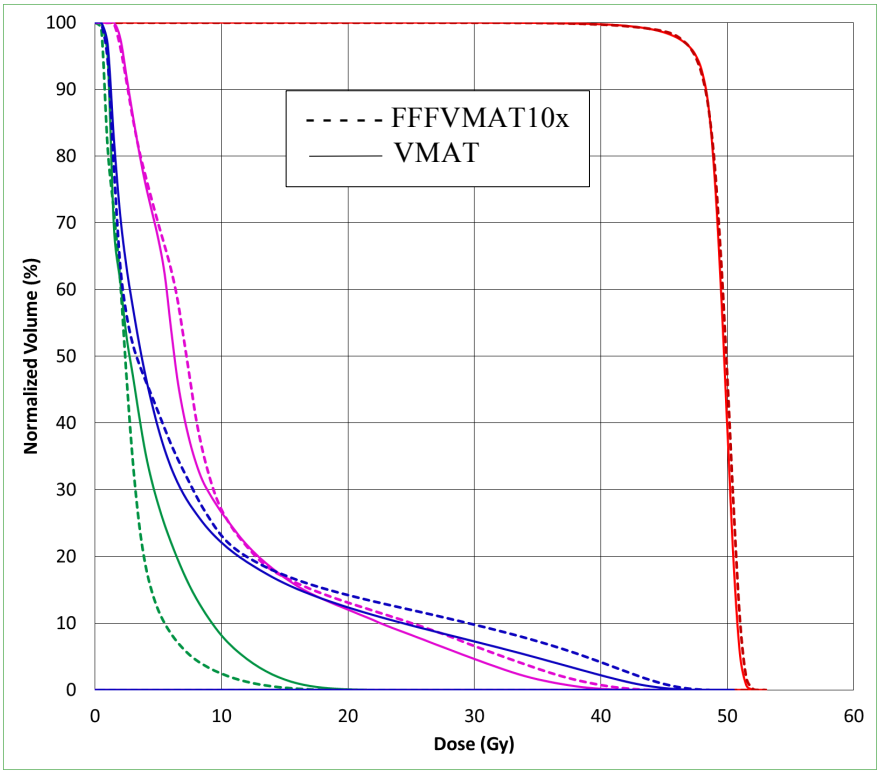

Figure A.27 DVH for patient CW8 comparing PTV (red), lungs (blue), heart (magenta), and breast (green) for FFFVMAT10x (dashed line) and VMAT (solid line).

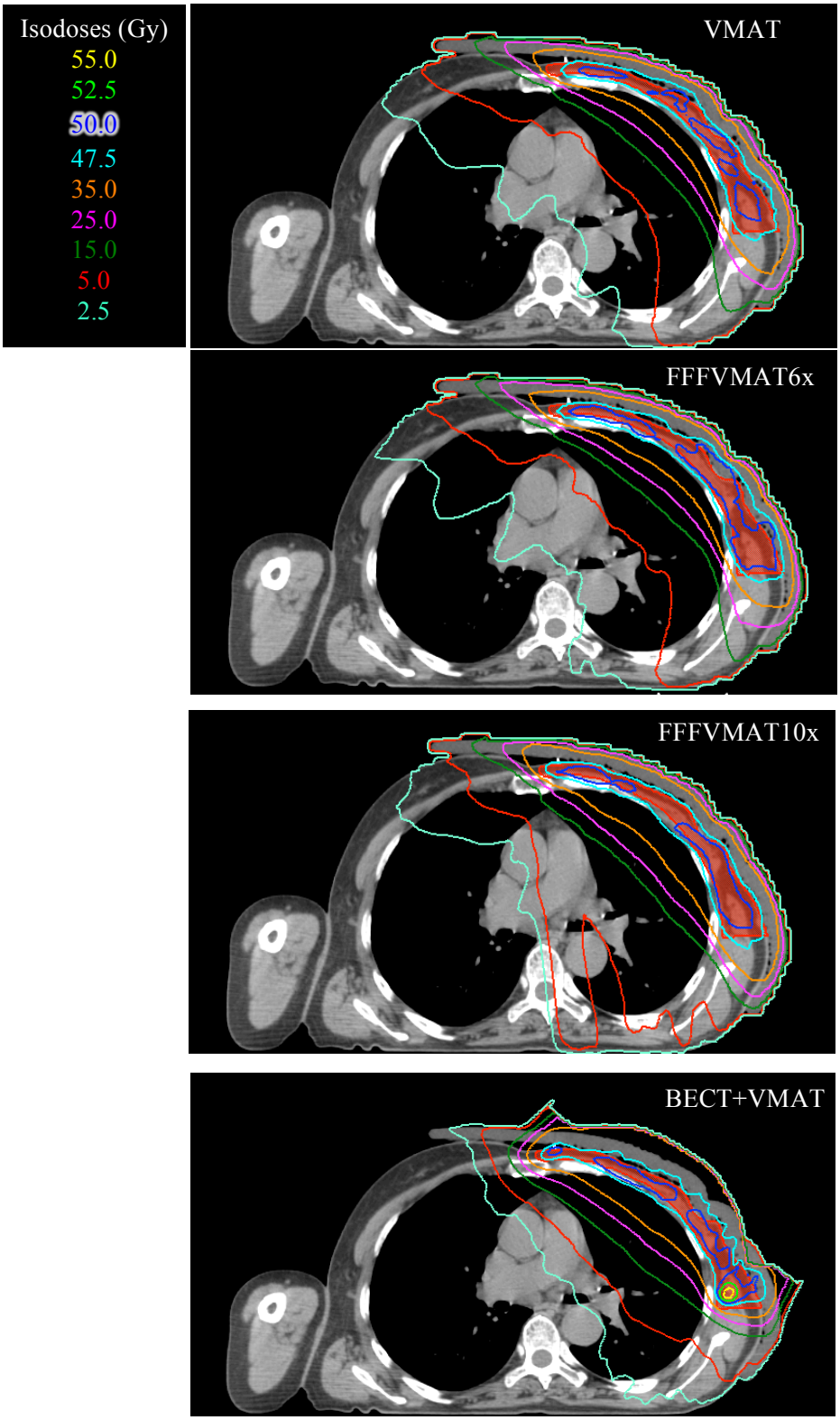

Figure A.28 Isodose distribution for patient CW8 for VMAT (top), FFFVMAT6x (top middle), FFFVMAT10x (bottom middle), and BECT+VMAT (bottom) treatment plans in axial slice on VMAT beam isocenter.

Patient CW9

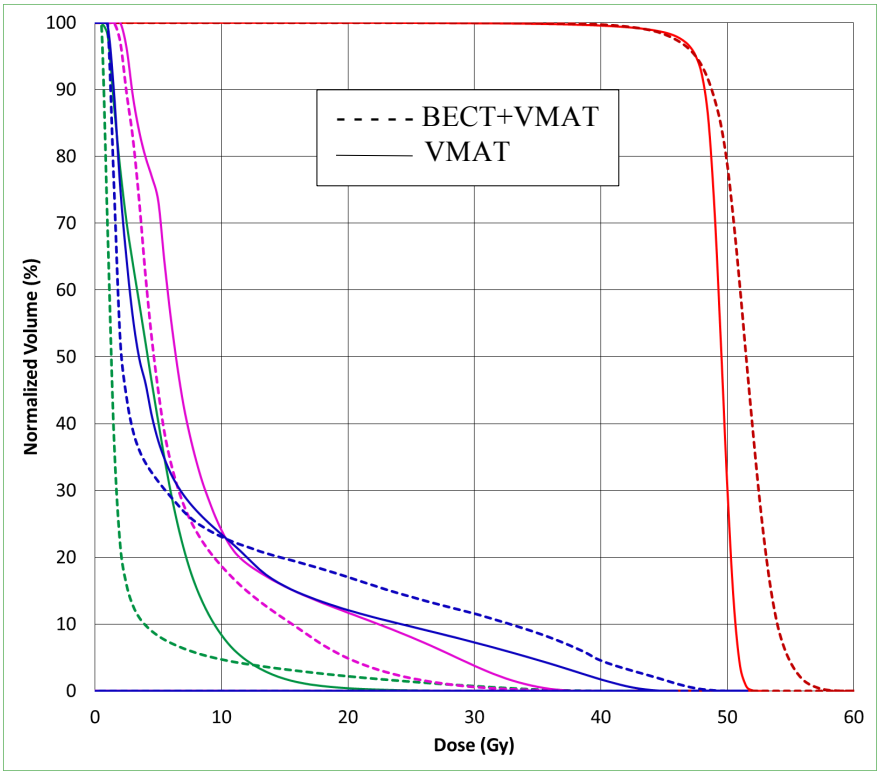

Figure A.29 DVH for patient CW9 comparing PTV (red), lungs (blue), heart (magenta), and breast (green) for BECT+VMAT (dashed line) and VMAT (solid line).

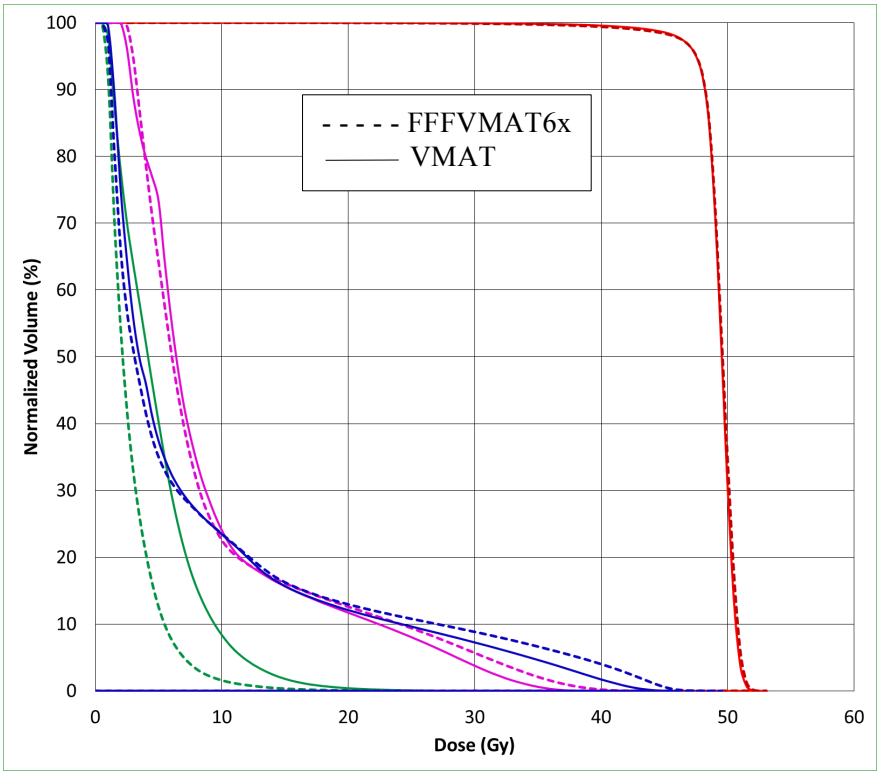

Figure A.30 DVH for patient CW9 comparing PTV (red), lungs (blue), heart (magenta), and breast (green) for FFFVMAT6x (dashed line) and VMAT (solid line).

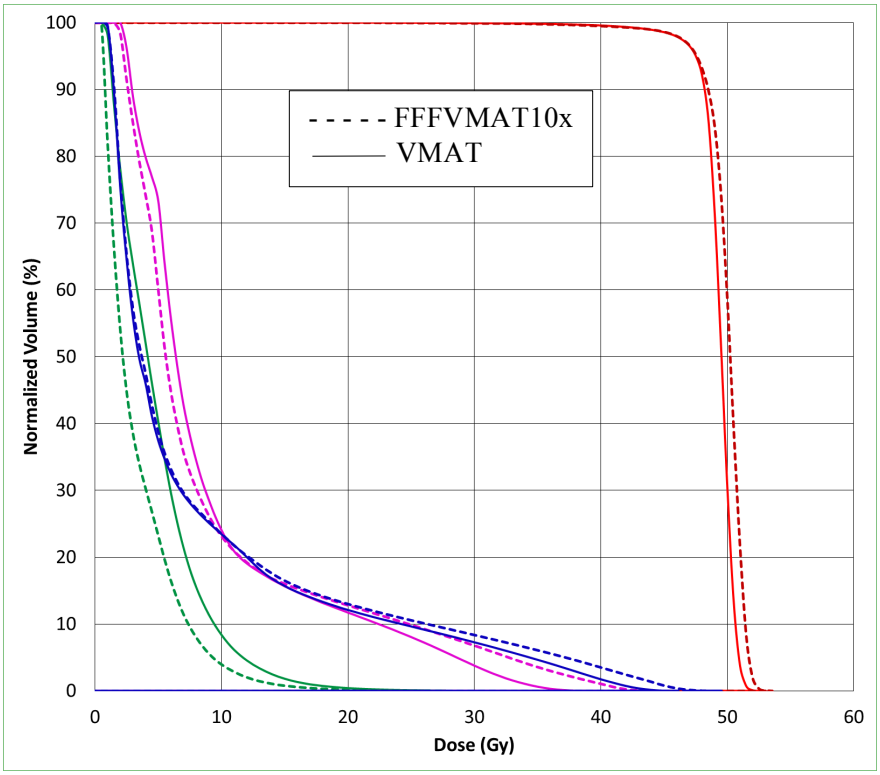

Figure A.31 DVH for patient CW9 comparing PTV (red), lungs (blue), heart (magenta), and breast (green) for FFFVMAT10x (dashed line) and VMAT (solid line).

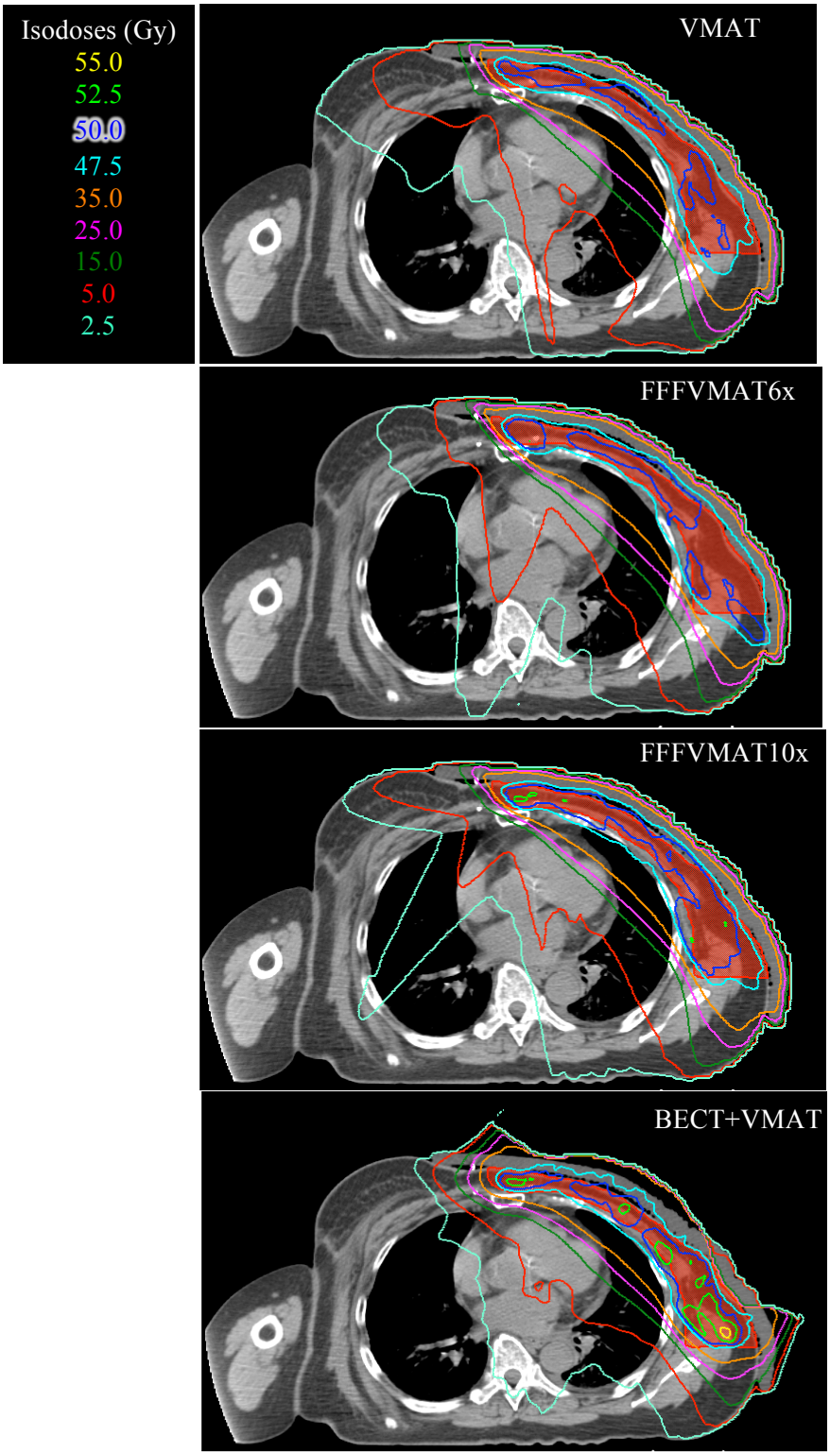

Figure A.32 Isodose distribution for patient CW9 for VMAT (top), FFFVMAT6x (top middle), FFFVMAT10x (bottom middle), and BECT+VMAT (bottom) treatment plans in axial slice on VMAT beam isocenter.

Patient CW10

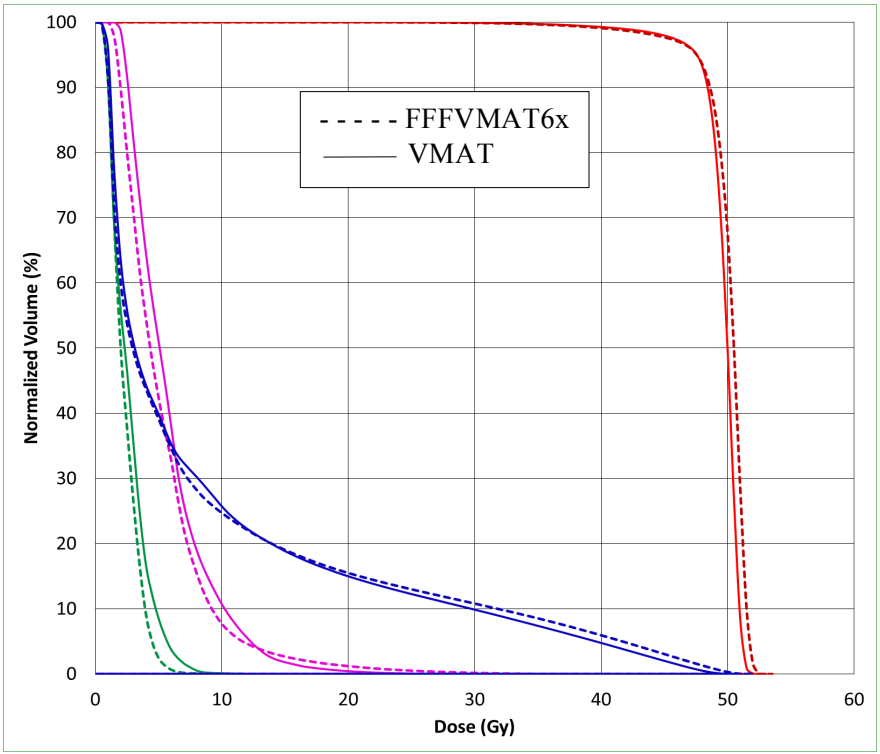

Figure A.33 DVH for patient CW10 comparing PTV (red), lungs (blue), heart (magenta), and breast (green) for FFFVMAT6x (dashed line) and VMAT (solid line).

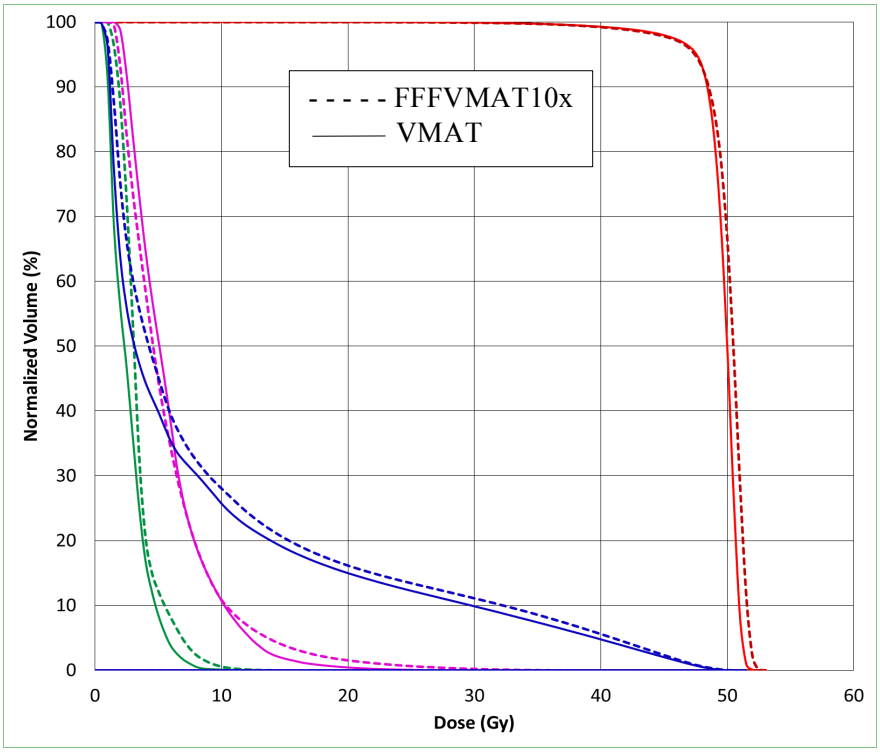

Figure A.34 DVH for patient CW10 comparing PTV (red), lungs (blue), heart (magenta), and breast (green) for FFFVMAT10x (dashed line) and VMAT (solid line).

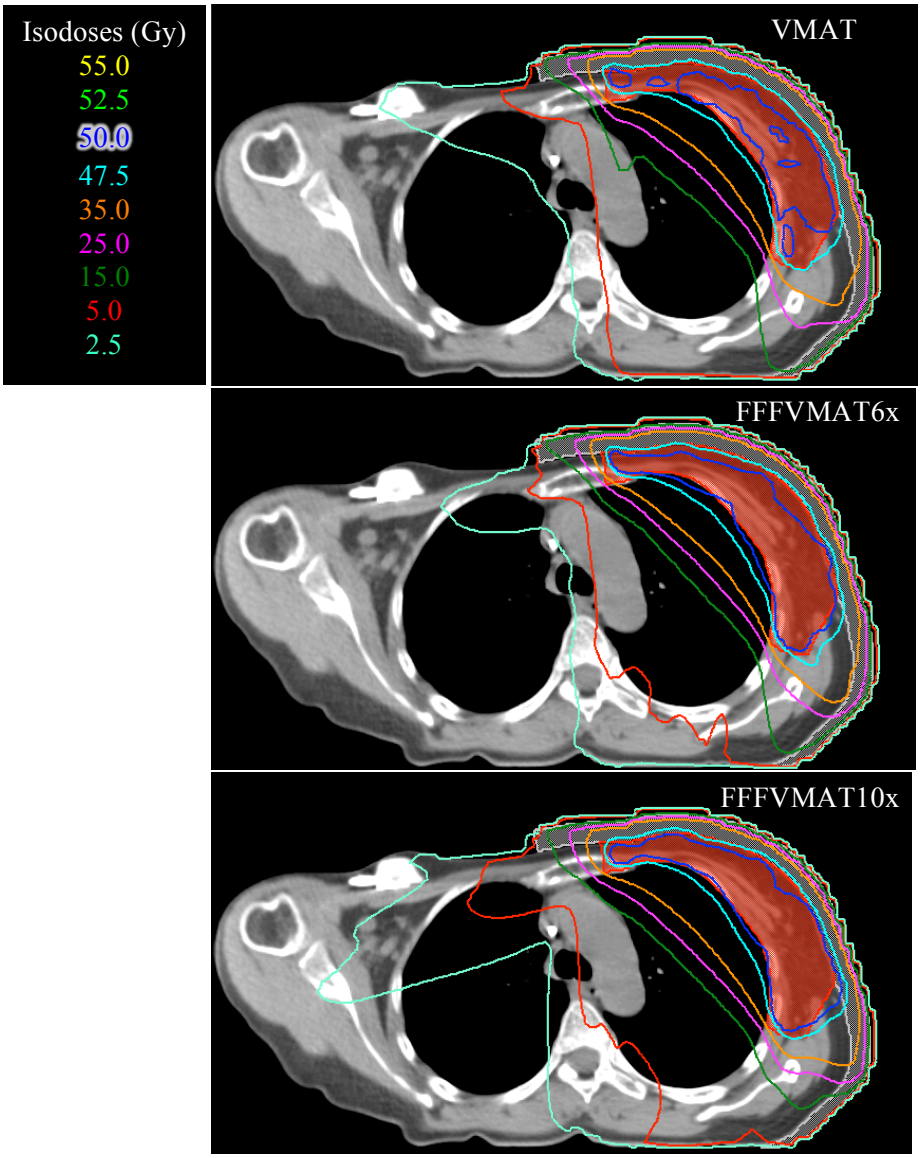

Figure A.35 Isodose distribution for patient CW10 for VMAT (top), FFFVMAT6x (middle), and FFFVMAT10x (bottom) treatment plans in axial slice on VMAT beam isocenter.

Appendix B: List of Abbreviations

AX: Axillary

BECT: Bolus Electron Conformal Therapy

BECT+VMAT: Bolus Electron Conformal Therapy with Volumetric Modulated Arc Therapy

BEV: Beams Eye View

CI: Conformity Index

DHI: Dose Homogeneity Index

FFFVMAT6x: Flattening Filter Free Volumetric Arc Therapy 6 MV

FFFVMAT10x: Flattening Filter Free Volumetric Arc Therapy 10 MV

fx: Fraction

Gy: Gray

IMET: Intensity Modulated Electron Therapy

IMN: Internal Mammary chain lymph Nodes

IMRT: Intensity Modulated Radiation Therapy

IMXT: Intensity Modulated X-ray Therapy

MU: Monitor Units

NS: No Statistical Significance

NTCP: Normal Tissue Complication Probability

OARs: Organs at Risk

PMRT: Post-Mastectomy Radiotherapy

PTV: Planning Target Volume

ROI: Region Of Interest

RTOG: Radiation Therapy Oncology Group

Rx: Prescription

SC: Superclavicular

SCCP: Second Cancer Complication Probability

VMAT: Standard Volumetric Arc Therapy

TCP: Tumor Control Probability

TPS: Treatment Planning System

VMAT: Volumetric Modulated Arc Therapy

Appendix C: IRB Approval Form

ACTION ON EXEMPTION APPROVAL REQUEST

Institutional Review Board
Dr. Dennis Landin, Chair
130 David Boyd Hall
Baton Rouge, LA 70803
P: 225.578.8692
F: 225.578.5983
irb@lsu.edu | lsu.edu/irb

TO: Rui Zhang
Physics and Astronomy

FROM: Dennis Landin
Chair, Institutional Review Board

DATE: December 21, 2015

RE: **IRB#** E9650

TITLE: Comprehensive evaluation of efficacy and cost-effectiveness of modern postmastectomy radiotherapies

New Protocol/Modification/Continuation: New Protocol

Review Date: 11/9/2015

Approved X **Disapproved**_____

Approval Date: 12/21/2015 **Approval Expiration Date:** 12/20/2018

Exemption Category/Paragraph: 4a

Signed Consent Waived?: N/A

Re-review frequency: (three years unless otherwise stated)

LSU Proposal Number (if applicable):

Protocol Matches Scope of Work in Grant proposal: (if applicable)

By: Dennis Landin, Chairman 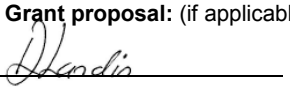

PRINCIPAL INVESTIGATOR: PLEASE READ THE FOLLOWING –
Continuing approval is CONDITIONAL on:

1. Adherence to the approved protocol, familiarity with, and adherence to the ethical standards of the Belmont Report, and LSU's Assurance of Compliance with DHHS regulations for the protection of human subjects*
2. Prior approval of a change in protocol, including revision of the consent documents or an increase in the number of subjects over that approved.
3. Obtaining renewed approval (or submittal of a termination report), prior to the approval expiration date, upon request by the IRB office (irrespective of when the project actually begins); notification of project termination.
4. Retention of documentation of informed consent and study records for at least 3 years after the study ends.
5. Continuing attention to the physical and psychological well-being and informed consent of the individual participants, including notification of new information that might affect consent.
6. A prompt report to the IRB of any adverse event affecting a participant potentially arising from the study.
7. Notification of the IRB of a serious compliance failure.
8. **SPECIAL NOTE:**

**All investigators and support staff have access to copies of the Belmont Report, LSU's Assurance with DHHS, DHHS (45 CFR 46) and FDA regulations governing use of human subjects, and other relevant documents in print in this office or on our World Wide Web site at http://www.lsu.edu/irb*

Vita

David was born in Rogers, Arkansas, in September 1983. In 2006, David attended Crowder College in Neosho, Missouri. In 2009 he went on to attend Pittsburg State University in Pittsburg, Kansas, where he received a Bachelor of Science degree in Biology with a minor in Chemistry as well as a Bachelor of Science degree in Physics with a minor in Mathematics.

After graduating with honors in 2013, David and his wife, Andrea moved to Baton Rouge, Louisiana to pursue a graduate position within the medical physics program at Louisiana State University. While attending Louisiana State University he became the proud father of his beautiful daughter, Anastasia. David will begin the medical physics residency training program at CARTI, Inc. in Little Rock, Arkansas starting in July of 2016.